Charles University
Faculty of Science

Study programme: Biology
Branch of study: Immunology

Bc. Iva Benešová

Microbiota as a modulator of carcinogenesis

Vliv mikrobiomu na karcinogenezi

Diploma thesis

Supervisor: MUDr. Miloslav Kverka, Ph.D.

Prague, 2021

Prohlášení:

Prohlašuji, že jsem závěrečnou práci zpracovala samostatně a že jsem uvedla všechny použité informační zdroje a literaturu. Tato práce ani její podstatná část nebyla předložena k získání jiného nebo stejného akademického titulu.

V Praze, 5. 8. 2021

Podpis:

Acknowledgement

I want to thank my supervisor for his time, precious advice and suggestions while writing this master thesis and his trust in me during experiment design, performance, and analysis. He fully supported me, and only thanks to him I could have learned a wide variety of methods, troubleshooting, critical thinking, and other essential skills necessary for the early career student. Next, I would like to thank the whole group of the laboratory of cellular and molecular immunology at the Institute of Microbiology of the CAS v.v.i for all their support, friendly working environment and help with my demanding experiments. Last but not least, I want to thank my whole family and boyfriend for their support during work in the laboratory and writing this master thesis.

This work has been supported by the Ministry of Health of the Czech Republic (NV19-03-00179).

Abstract

Many studies show the ability of gut microbes to modulate the anti-tumour immune response by direct triggering the immune cells or by bacterial metabolites. Interestingly bacteria may even migrate to the tumour tissue and orchestrate the immune response on site. These anti-tumour effects can be improved by the administration of immune checkpoint inhibitors (ICI). Notably, some microbial effects occur only in the presence of ICI. On the contrary, microbiota may also promote tumour growth and negatively impact the effects of ICI therapy.

We have disrupted the gut microbiota homeostasis by antibiotics (ATB) to study the effects of gut microbiota on the ICI. This disturbance led surprisingly to reduced tumour growth and enhanced pro-inflammatory immune response not only in the gut but also within the tumour tissue, where especially IFN-γ orchestrated the anti-tumour immune response.

Importantly the anti-tumour immune response could be transferred through colonisation of germ-free mice by ATB-changed gut microbiota if concomitantly anti-programmed cell death protein 1 (αPD-1) monoclonal antibody was administrated. These mice had elevated levels of segmented filamentous bacteria (SFB), which induced systemic immune response with increased expression of IL-17 and elevated amounts of Th 17 cells, resulting in decreased tumour growth. In conclusion, this master thesis indicates the potential of gut microbiota to modulate the anti-tumour immune response and even the responsiveness to ICI.

Key words: gut microbiota, tumour, immune checkpoint inhibitors, anti-PD-1, anti-tumour immune response, colonisation, microbiota transfer, antibiotics

Abstrakt

Mnoho studií prokázalo schopnost střevní mikrobioty ovlivňovat protinádorovou imunitní odpověď, buď přímou interakcí s imunitními buňkami, nebo skrz bakteriální metabolity. Některé bakterie dokonce mohou migrovat do nádorů a zde ovlivňovat imunitní odpověd. Podání imunitních checkpoint inhibitorů (ICI) může zlepšit protinádorovou imunitní odpověď. Některé účinky mikrobioty jsou dosaženy pouze v přítomnosti ICI. Na druhou stranu, mikrobiota může indukovat růst nádorů a negativně ovlivnit účinky ICI.

Pro studium vlivu střevní mikrobioty na ICI terapii jsme narušili střevní homeostázi podáním antibiotik (ATB). To vedlo ke sníženému růstu nádorů a zvýšené prozánětlivé imunitní odpovědi nejen ve střevech ale i v nádorech, kde především IFN-γ indukoval účinnou imunitní odpověď.

Tato efektivní protinádorová imunitní odpověď byla přenesena kolonizací bezmikrobních myší mikrobiotou od myší s podanými ATB, pokud byla současně podána αPD-1 monoklonální protilátka. Kolonizované myši měly zvýšené množství segmentovaných filamentózních bakterií (SFB), což vedlo ke zvýšeným hladinám IL-17 a Th17 a ve výsledku ke sníženému růstu nádorů. Souhrnně tato diplomová práce ukazuje schopnosti střevní mikrobioty ovlivňovat protinádorovou imunitní odpověď a dokonce i odpovídavost na léčbu ICI.

Klíčová slova: střevní mikrobiota, nádor, imunitní checkpoint inhibitory, anti-PD-1, protinádorová imunita, kolonizace, mikrobiální transfer, antibiotika

Table of contents

List of abbreviations

αCTLA-4	anti-cytotoxic T lymphocyte-antigen 4
αIL-10R	anti-interleukin 10 receptor
αPD-1	anti-programmed cell death protein 1
ag	antigen
APC	antigen presenting cell
ATB	antibiotics
CD	cluster of differentiation
CFU	colony forming units
CRC	colorectal cancer
CS	caesarean section
CTLA-4	cytotoxic T lymphocyte-antigen 4
CTL	cytotoxic T lymphocytes
CTX	cyclophosphamide
DC	dendritic cells
ELISA	enzyme-linked immunosorbent assay
FOXP3	Forkhead Box P3
FMT	faecal microbiota transplantation
GF	germ-free
IBD	inflammatory bowel disease
ICI	immune checkpoint inhibitor
ICOS	inducible costimulator
IFN-γ	interferon-gamma
Ig	immunoglobulin
IL	interleukin

ILC	innate lymphoid cells
IS	immune system
JAX	Jackson Laboratory
LDC	lysine decarboxylase
LTS	long term survivors
M1	type 1 macrophages
M2	type 2 macrophages
mAb	monoclonal antibody
MDSC	myeloid-derived suppressor cells
Mϕ	macrophages
MLN	mesenteric lymph nodes
MM	metastatic melanoma
MHC	major histocompatibility complex
NK	natural killer
NKT	natural killer T
NR	non-responders
NSCLC	non-small cell lung cancer
ODN	oligodeoxynucleotides
PD-1	programmed cell death protein 1
PD-L1	programmed death-ligand 1
PD-L2	programmed death-ligand 2
PP	Peyer´s patches
R	responders
RNS	reactive nitrogen species
RORγt	retinoic-acid-receptor-related orphan receptor gamma
ROS	reactive oxygen species

rRNA	ribosomal RNA
SFB	segmented filamentous bacteria
SHP2	Src homology region 2 domain-containing phosphatase-2
STS	short term survivors
TAC	Taconic Farm
T-bet	T-box expressed in T cells
TBI	total body irradiation
TCR	T cell receptor
TGF-β	transforming growth factor-beta
Th	T helper
TNF-α	tumour necrosis factor-alpha
Treg	regulatory T cells
PRR	pattern recognition receptor
RCC	renal cell carcinoma
RT-qPCR	quantitative reverse transcription polymerase chain reaction

1 Introduction

In our gut reside approximately 10^{14} microbes that can affect physiological functions and mental state, and therefore they influence overall human health. However, the importance of microbiota has been overlooked until recently. It is no wonder that gut microbiota is sometimes called a new organ due to its specific biochemical interactions and systemic integration throughout the body. The gut microbiota composition varies among individuals, and gut colonisation starts in the early stages of life. Concurrently host lifestyle, such as diet or stress and importantly antibiotics (ATB) administration, can change the gut microbiota composition. Therefore, the constantly changing gut microbiota must be under continual supervision of the immune system (IS) to prevent pathogenic infections and bacterial invasions into sterile parts of the body.

On the other hand, gut microbiota can modulate the immune responses, which are not only gut-restricted. Many studies show the ability of gut microbes to modulate the anti-tumour immune response by triggering the immune cells in the gut through direct interactions, such as bacterial translocation or molecular mimicry. Moreover, bacterial metabolites may act *in situ* or remotely. Interestingly certain bacteria may even migrate to the tumour tissue and orchestrate the immune response on site. These anti-tumour effects can be improved by the administration of immune checkpoint inhibitors (ICI). Notably, some microbial effects on the anti-tumour immunity occur only in the presence of ICI. On the contrary, microbiota may also promote tumour growth and negatively impact the effects of ICI therapy.

Nowadays, many microbes are associated with responsiveness or unresponsiveness to certain ICI therapy; however, the mechanism of action and description of immune changes and effector molecules in various parts of the body that may connect the gut and tumour are often missing. Therefore, this master thesis focuses on the elucidation of microbiota-caused immune changes in the gut, spleen and tumour of anti-programmed cell death protein 1 (αPD-1) treated mice. A better understanding of microbiota-driven effects on the anti-tumour immune response with concomitant αPD-1 monoclonal antibody (mAb) would improve the selection of suitable patients for this therapy and would ameliorate the treatment results. Additionally, the knowledge can be used to understand the mechanism behind responsiveness and unresponsiveness to ICI therapy among patients and for the selection of suitable donors for faecal microbiota transplantation (FMT).

2 Literature review

2.1 Human microbiota

The Human microbiota is determined as a composition of archaea, bacteria, fungi, and viruses in the human body. Term microbiota is generally used for microorganisms, while microbiome refers to the set of microbial genes. However, both terms are sometimes used as synonyms (Fernández et al., 2018). Nowadays accepted ratio of all human cells to bacterial is 1:1.3 (Sender et al., 2016). Bacteria are most abundant in the gut, predominantly in the colon, where 10^{13-14} of microorganisms are estimated (Turnbaugh et al., 2007), followed by the skin with 10^{12} microorganisms (Sender et al., 2016). Human Microbiome Project revealed the individuality of human microbiota composition, which begins to form during delivery, depends on the environment, and may quickly change or persist over time (Proctor et al., 2019). Additionally, multiple factors, such as host lifestyle, contribute to the variability of the human microbiome (Turnbaugh et al., 2007).

Not only gut, skin or sex organs are colonised by microbiota (Gilbert et al., 2018), but also oral and nasal cavity (Dashper et al., 2019; Lal et al., 2017). Additionally, in cancer patients, even tumour microbiome was observed (Nejman et al., 2020). Most of the microbiota is harmless or even beneficial for us. It protects us against pathogens and contributes to normal physiological functions. To better understand the host-microbiota interactions, the microbiota should be considered a community, not an individual organism. Ecological principles are being used to clarify interactions among microbes and between their host (Lozupone et al., 2012).

2.2 Gut microbiota

The unique environment in the gut, constant temperature, an abundance of substrates and anaerobic conditions form an original niche in the gut, where approximately 10^{14} of microbes reside (Qin et al., 2010). Faecal samples of 124 Europeans contain 3.3 million non-redundant microbial genes, approximately 150 times more than the number of human genes (Qin et al., 2010). The microbiota composition and density differ markedly in each compartment (**Fig. 1**). The amounts of microbes rise from the small intestine (10^{4}-10^{8} colony forming units (CFU)/ml) to the large intestine (10^{10}-10^{12} CFU/ml) (Cresci & Bawden, 2015).

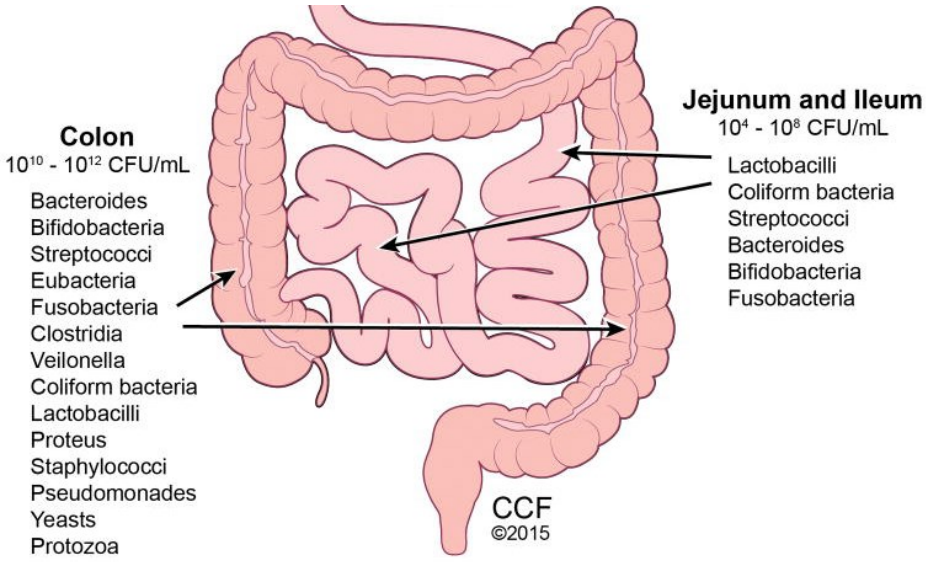

Figure 1 Composition and quantity of microbiota in the various parts of gut. The amount of microbiota increases from the small intestine to the large. The microbiota composition is specific for each department. Picture from Cresci & Bawden, 2015.CFU = colony forming units

2.2.1 Colonisation and variability of gut microbiota

Meconium, the first stool of neonate, already contains bacteria, predominantly *Enterococcus* and *Staphylococcus* (Jiménez et al., 2008). This suggests that early microbial stimulation may trigger IS development already during fetal life. The first 1000 days, from delivery to 2nd year of life, are crucial for shaping and establishment of gut microbiota composition. The most critical factors are the mode of delivery, type of feeding and ATB treatment (Butel et al., 2018).

Vaginally delivered neonates resemble the vaginal microbiota of their mother (Bäckhed et al., 2015). While the microbiota of neonates born by caesarean section (CS) is more variable and mostly correspond to their mother's skin microbiota, that lack or display lower amounts of *Bacteroides* (Dominguez-Bello et al., 2010). Decreased abundance of this genus is associated with impropriate development of IS and allergies. After the delivery, children are exposed to various microbes in the environment, for example, through food and physical contact. All of this enhances the variability among individuals; however, the bacterial diversity remains still low (Butel et al., 2018; Neuman et al., 2018).

Brest milk is non-sterile, and it contains, besides other bacterial species, beneficial *Bifidobacteria* (Lugli et al., 2020) that strengthen gut mucosa protection against pathogens and increase immunoglobulin (Ig) A secretion (Cresci & Bawden, 2015; Schroeder et al.,

2018). Human milk contains oligosaccharides that are not hydrolysable by human digestive enzymes, but *Bifidobacteria* can metabolise them (James et al., 2016; Lawson et al., 2019). As a result, infants fed by breast milk have higher amounts of *Bifidobacteria* (J. Ma et al., 2020).

The microbial diversity increases with the transition from breastfeeding or formula feeding to solid food. Until that, predominate microbiota that is capable of milk utilisation. After diet switch, prevail bacteria capable of digesting the new form of diet (Ku & Lee, 2020). This shows that diet is a key factor in the formation of the adult-type gut microbiome.

Filippo et al. (2010) took diet as a source of gut microbiota variability into consideration. In this study microbiome of European children that consume a Western-type diet (high animal protein, simple sugars, starch, fat and low fibre) was compared to the microbiome of children from a rural area in Burkina Faso. Their diet is low on animal protein and fat, high on fibre and plant polysaccharides. Higher microbial diversity was observed in children from Burkina Faso. For example, their microbiome included unique bacteria from *Prevotella* and *Xylanibacter* genus that can hydrolyse cellulose and xylan. Other differences in bacterial composition were also observed; *Actinobacteria* and *Bacteroidetes* were more abundant in children from Burkina Faso (10% versus 6.7% and 57.7% versus 22.4% respectively), while *Firmicutes* and *Proteobacteria* were decreased (27.3% versus 63.7% and 0.8% versus 6.7% respectively). After this study, many others followed and confirmed the influence of diet on the microbiota variability and revealed a link between specific dietary patterns and the presence of particular microbiota (Conteh & Huang, 2020; Filippis et al., 2016).

Moreover, a relationship between diet, gut microbiota and predispositions to obesity (Kong et al., 2019) and type 2 diabetes has been observed since gut microbiota modulates energy balance as well (Cano et al., 2012). Additionally, a link between diet and gut microbiota was revealed in the development of cancer (Münch et al., 2019) and inflammatory bowel diseases (IBD) (Burisch et al., 2014). In conclusion, a varied and complex diet contribute to a more diversified microbiome and health (Cresci & Bawden, 2015).

Additionally, gut microbiota reacts and adapts to dietary changes (Muegge et al., 2011) even rapidly within days. The introduction of an animal-based diet leads to changes in the beta diversity even one day after this diet reaches the distal gut and reverts to the original gut microbiota composition two days after the end of the diet (David et al., 2014).

ATB treatment disturbs gut microbiota in every life stage; however, especially devastating is ATB administration in infancy and early childhood, when gut microbiota is being shaped (Korpela et al., 2016). Most types of ATB are non-specific, and while the pathogen is removed, many harmless microbes in the gut are eliminated as well. In a study observing gut microbiota in healthy individuals over time, day-to-day variability was observed; however, most of the microbiota was stable without ATB administration. By ATB treatment, rapid changes, with loss of diversity and shift in microbial population were observed. After ATB administration, the microbiota shifted back to a normal state; however, it remained altered compared to the initial state (Dethlefsen & Relman, 2011).

Significant changes in the microbial community, imbalance and reduction of bacterial diversity characterise the term dysbiosis. The recovery can be fast, or slow and even incomplete. Vangay et al. (2015) divided the causes of dysbiosis into several groups: loss of keystone taxa which maintain homeostasis, or overall loss of diversity, which pathogens can take advantage of and colonise. The incomplete recovery can then affect the functional capacity, resulting in a persistent functional and metabolic shift that elevates the disease risk (Vangay et al., 2015). Microbiota dysbiosis, especially in the early stages of life, enhances predispositions towards allergies (Bisgaard et al., 2011), such as atopic disease (Abrahamsson et al., 2012) or towards obesity (Korpela et al., 2016) and autism (Kang et al., 2019). The impact of dysbiosis on various cancers is under discussion since it remains unclear whether altered microbiota is an inducer or consequent effect that contributes to carcinogenesis (Chen et al., 2017).

2.3 Immune responses in the gut

The effect of gut microbiota on the IS is outstanding. It influences the maturation and development of the IS, modulation of immune response and contributes to oral tolerance (Butel et al., 2018). Importantly gut microbiota protects against pathogens by a process called colonisation resistance. For example, exogenous species are unlikely to colonise the gut since they have to compete with established microbiota for nutrients or face active antagonism, which means that gut microbiota produces anti-bacterial peptides and bacteriocins to exclude colonisation of new species (Sorbara & Pamer, 2019). An important component of colonisation resistance is the cross-talk between gut microbiota and the IS. Certain bacteria can enhance the epithelial barrier functions (Ewaschuk et al., 2008) or even activate the innate

immunity in the presence of pathogens; for example, commensal bacteria can translocate and induce expression of IL-1β in the presence of *Clostridium difficile* (Hasegawa et al., 2012).

More than 10^{14} microbes are separated in the lumen of the gut from the rest of the body (Qin et al., 2010). The constantly changing gut microbiota must be under continual supervision of IS to prevent pathogenic infections and bacterial invasions into sterile body tissues. There is a continuously ongoing physiological inflammation in the gut in order to maintain homeostasis. Various mechanisms contribute to the preservation of physical, chemical and biological barriers. Mucus secretion, antimicrobial peptides and secretory IgA are major pathways that continuously protect us against infection (D. Zheng et al., 2020).

The gut lumen is separated from the rest of the body by one layer of intestinal epithelial cells. This layer is a physical barrier and an important mediator of the interplay between IS and gut microbiota. It contains cells that contribute to defence mechanisms. Goblet cells produce mucus and therefore sustain viscous barrier; they sample antigen (ag) as well by goblet cell-associated ag passages (Kulkarni et al., 2020). Both, Paneth cells, localised in the small intestine and deep crypt secretory cells in the colon, produce large amounts of antimicrobial peptides, such as α-defensins. Microfold cells uptake ag and transfer it into lamina propria to dendritic cells (DC), which accumulate directly under the intestinal epithelial layer in the Peyer's patches (PP). DC can also directly sample the ag through trans-epithelial luminal sampling (Brown et al., 2013).

PP are the main component of gut-associated lymphoid tissues and consist of lymphoid follicles without encapsulation and always contain germinal centres. They are essential for the constant tuning of the IS. Mesenteric lymph nodes (MLN) that collect lymph from the small and large intestine are typical secondary lymphoid organs. Intestinal epithelium structure and physiology differ in the small and large intestine, in accordance with different functions of each department, such as digestion and absorption in the small intestine and water resorption and stool formation in the colon (**Fig. 2**) (Brown et al., 2013).

Pattern recognition receptors (PRR), such as toll-like receptors and NOD-like receptors, are the primary sensors for pathogens. They recognise pathogen-associated molecular patterns, and in case of danger, signalling via these receptors activate inflammatory pathways.

PRR are expressed by various cells, such as DCs, macrophages (Mϕ), innate lymphoid cells (ILC), or even by intestinal epithelial cells (D. Zheng et al., 2020).

Cytokines produced by ILC tune the immune response. ILC type 3 are the most numerous cell population in the gut; therefore, they importantly contribute to the superiority of IL-17 immune response in this department, which sustains the barrier functions. Many regulatory T cells (Treg) maintain tolerance against commensal bacteria and various food ag (Allaire et al., 2018; Burgueño & Abreu, 2020; D. Zheng et al., 2020).

Secretory IgA produced by plasma cells in the lamina propria is transported via a poly-Ig receptor on epithelial cells through transcytosis. Secretory IgA neutralises microbes and toxins in the lumen. Additionally, IgG and IgM are also present in the gut lumen. IgM is transferred by the same receptor, while IgG is transported by the neonatal Fc receptor (Y. Li et al., 2020).

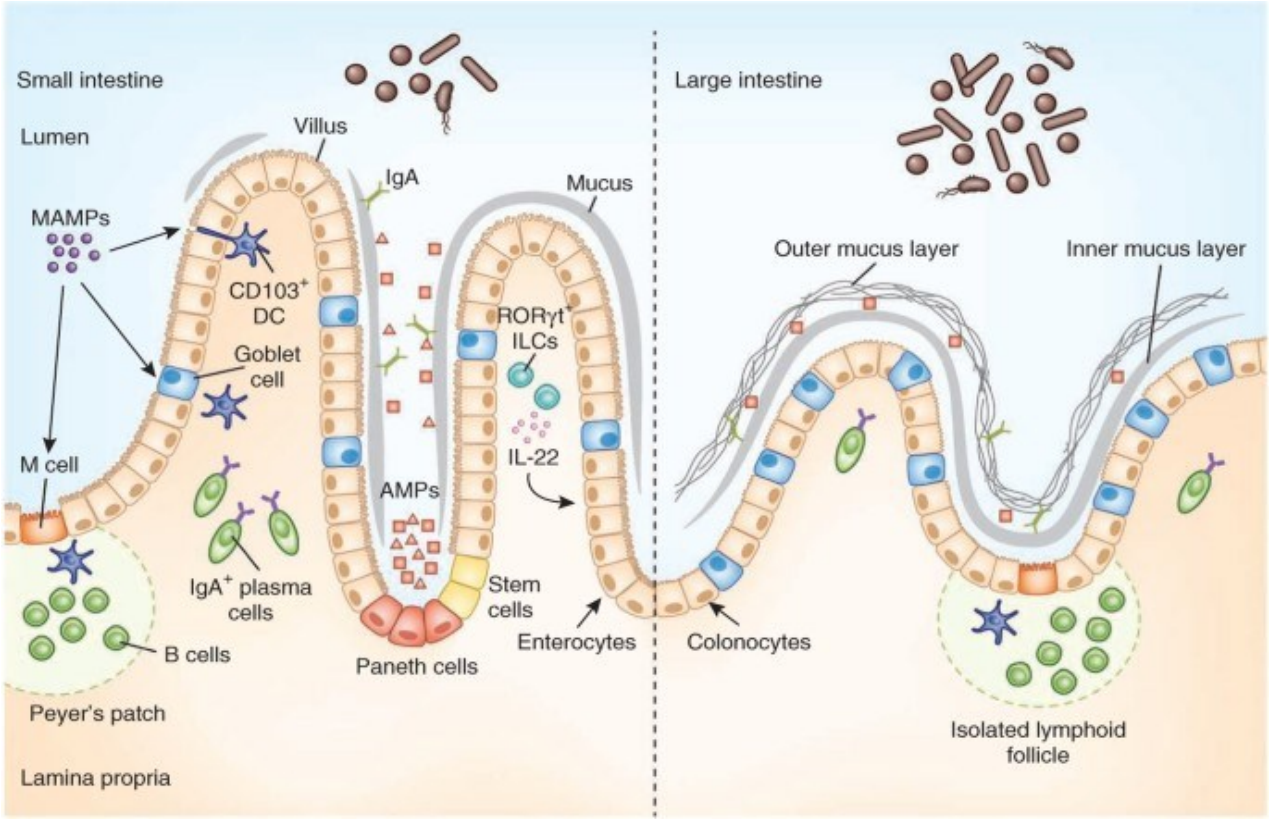

Figure 2 Structure of the gut: Different structure of small and large intestine reflects divergent functions of each compartment. The intestine consist of one epithelial layer; above it, in the lumen, is mucus that contains secretory IgA and antimicrobial peptides. In the small intestine ocurrs absorption per enterocytes; therefore, mucus layer is discontinuous. Through these ruptures is performed continuous ag sampling per Microfold cells, Goblet cells and DC. The large intestine has a thick mucus layer to strictly separate microbiota from the rest of the body. Picture from Brown et al., 2013. AMP = antimicrobial peptides, DC = dendritic cell, IgA = immunoglobulin A, IL = interleukin, ILCs = innate lymphoid cells M cell = Microfold cell, MAMPs = microbe-associated molecular pattern, RORγt = retinoic-acid-receptor-related orphan receptor gamma

2.4 Anti-tumour immune response

Immune responses to tumours can be divided into three states, elimination, equilibrium and escape. All together is this concept called cancer immunoediting, and each phase has typical properties. In the step of elimination are immune cells more effective. When anti-inflammatory and suppressor properties are balanced, the equilibrium phase is reached. Over time, mutations accumulate, and through the selection of clones arise once, that can overcome the IS and enable the tumour to escape immune control (**Fig. 3**) (Dunn et al., 2004).

Each cancer type is unique and different mechanisms or immune cells infiltration are associated with successful immune response. This section describes general mechanisms of the anti-tumour immune response. The main principle is a proper activation of innate immunity that later activates adaptive immunity, especially T helper (Th) 1 cells and cluster of differentiation (CD) 8^+ cytotoxic T lymphocytes (CTL) type 1. DC play an important role in triggering the immune response since they are capable of cross-presentation, which is needed for CTL activation. They also produce interleukin (IL)-12, which contribute together with interferon-gamma (IFN-γ) produced by activated natural killer (NK) cells, to Th1 development (Haniffa et al., 2012; Jorgovanovic et al., 2020).

Besides NK cells, Th1 and CTL also produce IFN-γ, a key molecule for enhancement of ag presentation, switch to IgG subclasses, Th1 differentiation and Mϕ activation. CTL are capable of direct killing through a perforin/granzyme pathway once they recognise tumour ag on major histocompatibility complex (MHC) I. One of the tumour defence mechanisms is the downregulation of those molecules. On that react NK cells that do not receive any or lowered inhibitory signals through MHC I and therefore activation pathways prevail and lead to cytotoxic killing. In addition, Ab binding to its Fc receptor induces Ab dependent cell-mediated cytotoxicity (Pahl et al., 2018). As a result, immune cells inhibit tumour growth and destroy tumour cells.

Mϕ are traditionally divided into pro-inflammatory type 1 Mϕ (M1) and anti-inflammatory type 2 Mϕ (M2). However, they should be instead described as a continuum of phenotypes, where M1 and M2 are extreme examples. Mϕ leaning towards M1 have enhanced expression of MHC II and costimulatory molecules, tumour necrosis factor-alpha (TNF-α), inducible NO synthase and other pro-inflammatory molecules. While M2 express anti-

inflammatory IL-10, transforming growth factor-beta (TGF-β), arginase, programmed death-ligand 1 (PD-L1), vascular growth factor or epithelial growth factor. To protumourigenic conditions contribute mainly also Tregs and myeloid-derived suppressor cells (MDSC) (DeNardo & Ruffell, 2019).

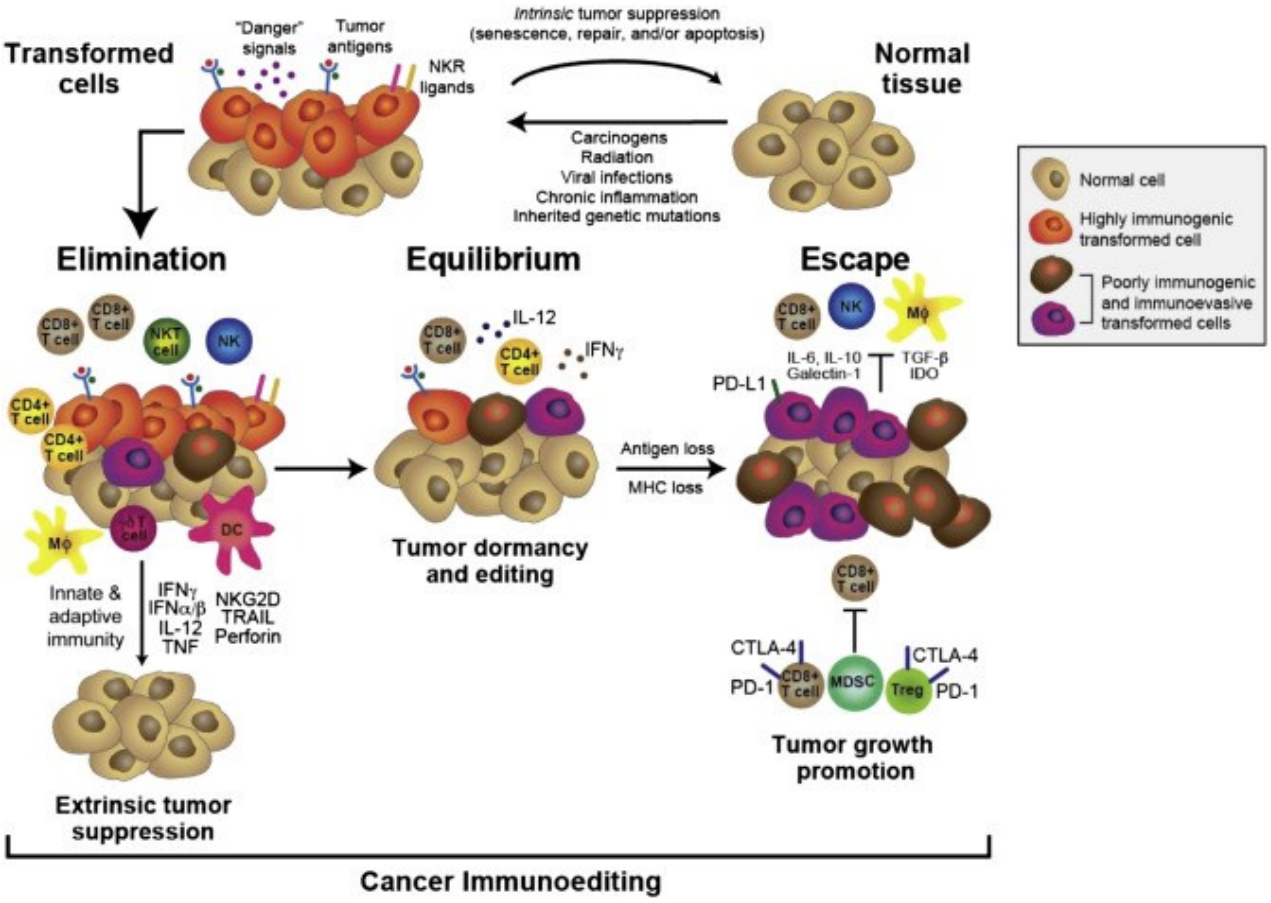

Figure 3 Carcinogenesis and cancer immunoediting: At the top of the figure, various carcinogenesis inducers are described, such as the presence of carcinogens or radiation, effects of viral infection, chronic inflammation and inherited genetic mutations. These factors cause the transformation of normal tissue. On these transformed cells react IS. Firstly, in the elimination phase, is IS more successful. Pro-inflammatory immune response through Th1, CTL, NK cells, NKT cells, M1 and DC is accompanied by secretion of pro-inflammatory molecules, such as IFN-γ, IL-12 and TNF-α. At this stage, can be tumour suppressed, or an equilibrium phase can be reached. In the equilibrium phase, neither IS, nor tumour has superiority. Over time tumour cells undergo mutations, and clones that can escape the immune system dominate and thereby, tumour escape begins. At this stage, tumour cells use some of their escape mechanisms, such as loss of MHC or ag presentation, induction of PD-L1 or expression of TFG-β. Many immune cells are exhausted and express their inhibitory molecules, such as CTLA-4 or PD-1 on T cells in this phase. In addition, more immunosuppressive cells, such as Treg, M2, MDSC accumulate in the tumour environment. And all this together leads to the tumour escape. Picture from Schreiber et al., 2011. CTLA-4 = cytotoxic T lymphocyte-antigen 4, DC = dendritic cell, IDO = indolamine 2,3-dioxygenase, IFN = interferon, IL = interleukin, Mϕ = macrophage, MDSC = myeloid-derived suppressor cells, NKG2D = natural killer group 2D, NKR = nature killer receptor, NKT = nature killer T, PD-1 = programmed cell death protein 1, PD-L1 = programmed death-ligand 1, TGF-β = transforming growth factor beta, TNF = tumour necrosis factor, TRAIL = TNF-related apoptosis inducing ligand, Treg = regulatory T cell

2.5 Immune checkpoint inhibitors (ICI)

Numerous checkpoint pathways regulate immune cells activation and functions to maintain homeostasis, self-tolerance and to prevent autoimmunity. Moreover, they regulate the length and magnitude of the immune response to prevent tissue damages. This exploits tumour cells as one of the very successful escape mechanisms. Tumour cells can effectively diminish anti-tumour immune response via recruitment of immunosuppressive cells and induction of expression of various inhibitory molecules such as PD-L1, programmed death-ligand 2 (PD-L2), cytotoxic T lymphocyte antigen-4 (CTLA-4), CD47 or TGF-β (Seidel et al., 2018; H. Wang et al., 2017; Zhang & Zheng, 2020).

Programmed cell death protein 1 (PD-1) and CTLA-4 generally protect us against prolonged immune response accompanied by pathological damages. Moreover, they contribute to central and peripheral tolerance, thus preventing autoimmune diseases.
In context of cancer, long fight and constant high ag load lead to upregulation of these molecules as a marker of exhaustion. Signalling through these receptors induces loss of proliferation, effector functions or even deletion, thereby it weakens the anti-tumour immune response. Treatment that consists of mAb blocking, such as anti-programmed cell death protein 1 (αPD-1) or anti-cytotoxic T lymphocyte antigen-4 (αCTLA-4), prevents inhibitory interaction and improves anti-tumour immune responses (**Fig. 4**) (Kumagai et al., 2020).

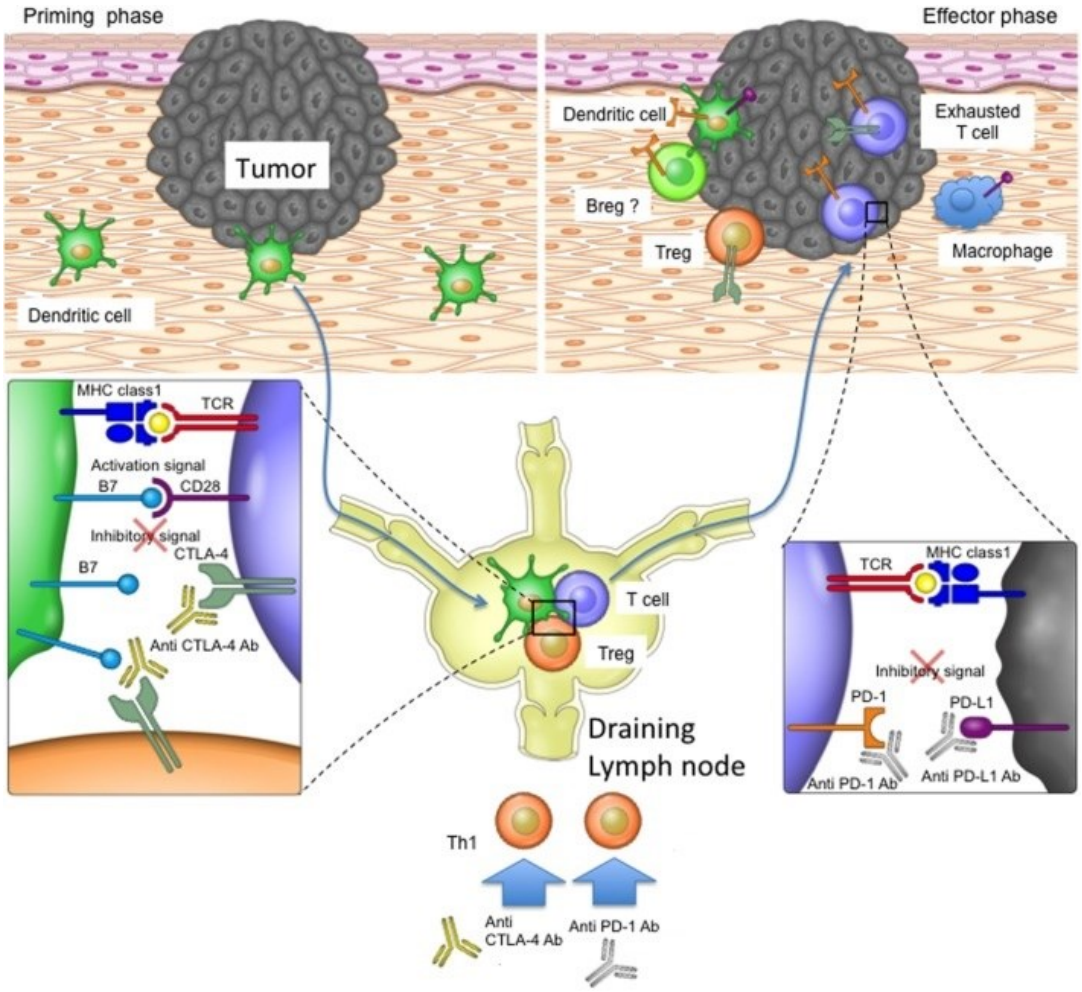

Figure 4 Role of αPD-1 mAb and αCTLA-4 mAb in the priming and effector phase of anti-tumour T cell mediated immune response. DC primed by tumour ag migrate to LN, where they present displayed ag on MHC. For T cell activation is MHC-T cell receptor interaction and CD28 with CD80/86 costimulation required. CTLA-4 upregulation on exhausted T cells or the presence of Tregs compete with CD28 for CD80/86 interaction. CTLA-4 has a much higher affinity to CD80/86. Once αCTLA-4 mAb is used, T cell activation is restored. These cells then migrate to the tumour site to kill cancer cells. Tumours and other cells express PD-L1 and PD-L2 that, in interaction with PD-1, impairs T cells functions. PD-1, PD-L1 or PD-L2 blockade restores anti-tumour properties of T cells. Picture from Seidel et al., 2018. Breg = regulatory B cells, CTLA-4 = cytotoxic T lymphocyte-antigen 4, LN = lymph nodes, MHC = major histocompatibility complex, PD-1 = programmed cell death protein 1, PD-L1 = programmed death ligand 1, TCR = T cell receptor, Th = T helper, Treg = regulatory T cells

2.5.1 CTLA-4

T cell receptor (TCR) and MHC interaction are required for proper T cell activation, but also many costimulatory pathways and cytokine environment are necessary. It seems that costimulation via CD28 and CD80/86 is the most important one. CTLA-4 is expressed on exhausted T cells, might be on tumour cells and is constitutively present in Tregs, where contributes to stopping potentially autoreactive T cells at the initial state. CTLA-4 is

a homolog of CD28 molecule that binds CD80/86 with much higher affinity, thereby preventing costimulation. Another suppressor mechanism of CTLA-4 interaction is the removal of CD80/86 from the surface of antigen presenting cells (APC) in a process called trans-endocytosis. It disables further interactions with CD28. This inhibitory effect occurs at the initial stages of the immune response, mainly in lymph nodes (Rotte, 2019; Seidel et al., 2018)

The αCTLA-4 mAb drug is registered to treat metastatic melanoma (MM) and surgically resectable "high-risk" melanoma. In addition, many clinical trials and studies are in progress in other cancer types, such as hepatocellular carcinoma (Duffy et al., 2017), advanced breast cancer (Vonderheide et al., 2010) or non-small cell lung carcinoma (NSCL) (Lynch et al., 2012).

2.5.2 PD-1

PD-1 molecule is an essential regulator of the immune response. It is expressed not only on T cells but also on B cells, myeloid DC, monocytes, Mϕ, NK cells and natural killer T (NKT) cells. Ligands for PD-1, PD-L1 and PD-L2, are mainly on APC; however, various cancer cells can also express them. Additionally, these ligands were also on T and B cells detected (Seidel et al., 2018). PD-1 expression is upregulated in the IFN-γ environment (Garcia-Diaz et al., 2017). While PD-1 is expressed on many other immune cells, the observed effect of αPD-1 blockade may also be T cell independent (Seidel et al., 2018). For example, the mouse model shows that PD-1 expression on NK cells is associated with suppressive functions (Niu et al., 2020). In addition, αPD-1 mAb therapy also works in patients with downregulated MHC I, suggesting T cell independent mechanism of action (Quatrini et al., 2020).

PD-1 signalling is mainly studied in T cells; however, the mechanism and overall effect remain the same in other immune cells. Signalling through PD-1 leads to phosphorylation of intracellular immunoreceptor tyrosine-based switch motif and immunoreceptor tyrosine-based inhibition motif. This is required for Src homology region 2 domain-containing phosphatase-2 (SHP-2) recruitment. Interaction of PD-1 with SHP-2 is essential for the downstream signalling (**Fig. 5**). As a result, T cells decrease cytokine production, especially IL-2, TNF-α and IFN-γ. Moreover, it impairs the effector properties and cytotoxic functions in $CD8^+$ T lymphocytes (Quatrini et al., 2020; Seidel et al., 2018).

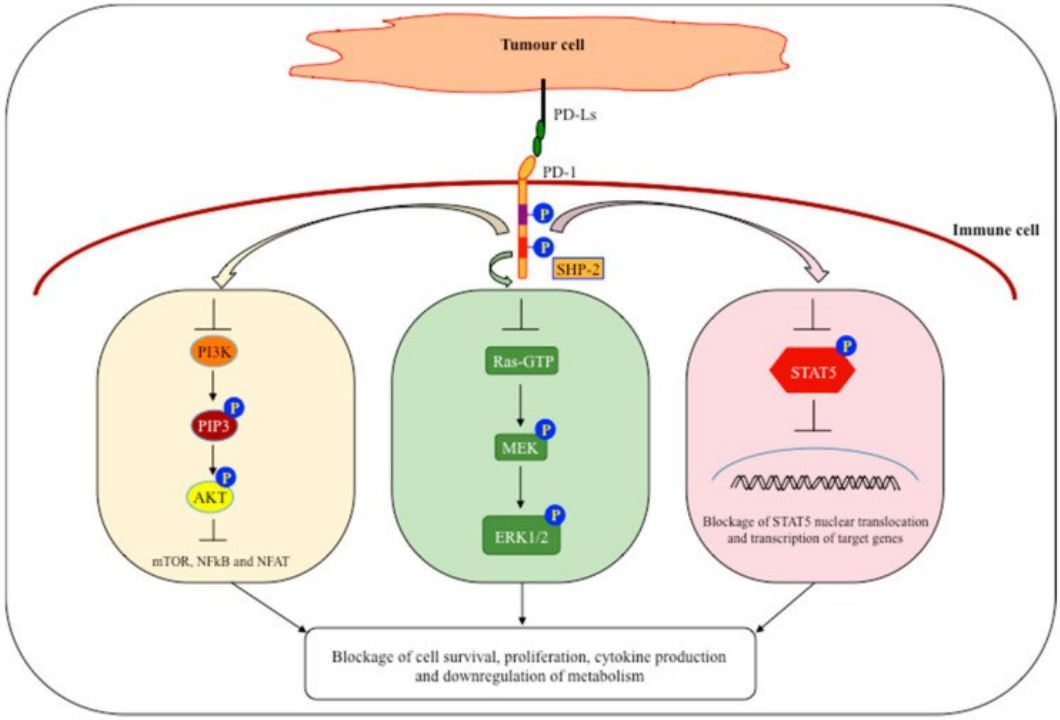

Figure 5 PD-1 signalling leads to phosphorylation of ITIM and ITSM motives in the intracellular PD1 domain. This recruits SHP-2 and blocks various pathways. It results in a negative effect on the innate and adaptive anti-tumour immune response. Picture from Quatrini et al., 2020. AKT = protein kinase B, GTP = guanosine triphosphate, ERK = mitogen-activated protein kinase, MEK = mitogen-activated protein kinase kinase, mTOR = mammalian target of rapamycin, NF-κB = nuclear factor kappa-light-chain-enhancer of activated B cells, NFAT = nuclear factor of activated T cells, P = phosphate, PD-1 = programmed cell death protein 1, PD-L = programmed death-ligand 1, PI3K = phosphoinositide 3-kinase, PIP3 = phosphatidylinositol 3,4,5-triphosphate, Ras = rat sarcoma, SHP-2 = Src homology region 2 domain-containing phosphatase-2, STAT = signal transducer and activator of transcription

The αPD-1 treatment is currently approved in metastatic melanoma, non-small-cell lung cancer (NSCLC), renal cell carcinoma (RCC), hepatocellular carcinoma and colorectal cancer (CRC) with mismatch repair aberration or gastric cancer (Rotte, 2019).

ICI therapy is enormous advancement in cancer therapy. For example, administration of αPD-1 to melanoma patients significantly prolongs progression-free survival and overall survival of the patients (Robert et al., 2015). Moreover, the ICI has fewer adverse effects than platinum-based chemotherapy (Reck et al., 2016); however, limitations persist, and the patients still face many side effects. For example, in αPD-1 treatment of NSCLC, common adverse effects are fatigue (19%) and pruritus (11%), in some cases hypothyroidism (7%), pneumonitis (4%) and diarrhoea (8%) (Garon et al., 2015). Therefore, the need for improved therapy, better patient stratification, more precise biomarkers recognition and possible modulation options is crucial. One possibility to improve ICI therapy is microbiota modulation.

2.6 Effect of microbiota on carcinogenesis

Carcinogenesis is a multiple-step process, and microbiota may contribute to its onset by the presence of oncogenic microbiota. Under specific genetic or environmental conditions, even a symbiont can promote carcinogenesis (termed pathobiont) (Mazmanian et al., 2008). For the cancer development or microbial tumorigenesis contribution, not only the presence of microorganisms is required, but also the whole interplay of microbial interactions and their metabolites is crucial (Goedert et al., 2015; Yachida et al., 2019). In some cases, there is a link to one specific microorganism (Guo et al., 2020); however, in others, is the carcinogenesis caused by generally altered and distracted microbiota (Goedert et al., 2015; Klimesova et al., 2013). Additionally, dynamic microbial shifts at different cancer stages occur (Yachida et al., 2019). On the other hand, microbiota may play a protective role in carcinogenesis. For example, bacteria that enhance intestinal barrier functions (C.-S. Alvarez et al., 2016), reduce inflammation (Ashraf et al., 2014) and cell proliferation (J. Zhang et al., 2015) or inhibit the activities of oncogenic microbiota (Bhatia et al., 1989) are considered to be protective against the development of CRC.

The most well-known and studied microorganism associated with carcinogenesis is *Helicobacter pylori*, which causes persistent inflammation in the stomach, leading to gastritis. *H. pylori* is the driving force of carcinogenesis, and in combination with other factors, can result in gastric cancer (Plottel & Blaser, 2011). If *H. pylori* is eradicated, the risk of gastric cancer is decreased (Guo et al., 2020). On the other hand, the presence of *H. pylori* lowers the risk of oesophageal adenocarcinoma (Z. Wang et al., 2018). This example underlines the complexity and heterogeneity of microbial effects on carcinogenesis.

2.6.1 Gut microbiota and CRC

Earlier, CRC was considered to be exclusively a genetic disorder, where the accumulation of mutations over time was a key trigger of carcinogenesis (Fearon & Vogelstein, 1990). However, deepening the knowledge about CRC revealed the effect of gut microbiota on carcinogenesis by different mechanisms, including induction of genetic instability. Significant contributions of gut microbiota to CRC tumourigenesis are dysbiosis and associated inflammation, barrier failure (García-Castillo et al., 2016) or bacterial toxins and metabolites (Schwabe & Jobin, 2013).

2.6.1.1 Dysbiosis, inflammation and barrier failure

Perturbation of gut microbiota homeostasis, gut barrier defects, and subsequent pro-inflammatory immune responses or inappropriate IS reaction are associated with microbiota driven carcinogenesis (**Fig. 6**). Moreover, these regulatory mechanisms are tightly linked together, and usually, disturbance in one mechanism disrupts the whole balance (Schwabe & Jobin, 2013).

Inflammation is a typical demonstration of immune response to pathogens or injuries that is traditionally divided into acute and chronic. Once the cause of inflammation persists or failure in termination of immune response occurs, the inflammation is prolonged to months or years and therefore shifted to chronic. Chronic inflammation causes damage to the gut barrier, allows even more host-microbiota interactions, and elevates immune responses (Schwabe & Jobin, 2013). This state is typically accompanied by cell mutations, prolonged cell survival and cell proliferation. Altogether, it creates appropriate conditions for cancer development (García-Castillo et al., 2016).

Cell mutations can also be caused by IS. Reactive oxygen species (ROS) and reactive nitrogen species (RNS) are produced mainly by phagocytes. ROS and RNS can interact and subsequently damage the DNA, thereby are a source of mutations that play an important role in tumourigenesis (Gorska-Ponikowska et al., 2020; Xie et al., 2018). Prolonged cell survival and proliferation are orchestrated by cytokine production, such as TNF-α, IL-1β and IL-6. These cytokines activate prosurvival and proliferatory pathways, including nuclear factor kappa-light-chain-enhancer of activated B cells, mitogen-activated protein kinase pathway and phosphatidylinositol 3-kinase/protein kinase B pathway, in the cells (Brás et al., 2020; Eyre et al., 2019; Jana et al., 2017; Zegeye et al., 2018).

One such example of how microbiota perturbation may lead to carcinogenesis are IBD; their development is tightly linked to gut microbiota alterations (dysbiosis) and subsequent inflammation (Gevers et al., 2014); additionally, chronic inflammation causes pro-neoplastic effects and therefore significantly increases the risk of CRC development in IBD patients (Rutter et al., 2004). Similarly, is associated celiac disease with dysbiosis (Caminero et al., 2016) and consequent enhanced risk of cancer (Han et al., 2015).

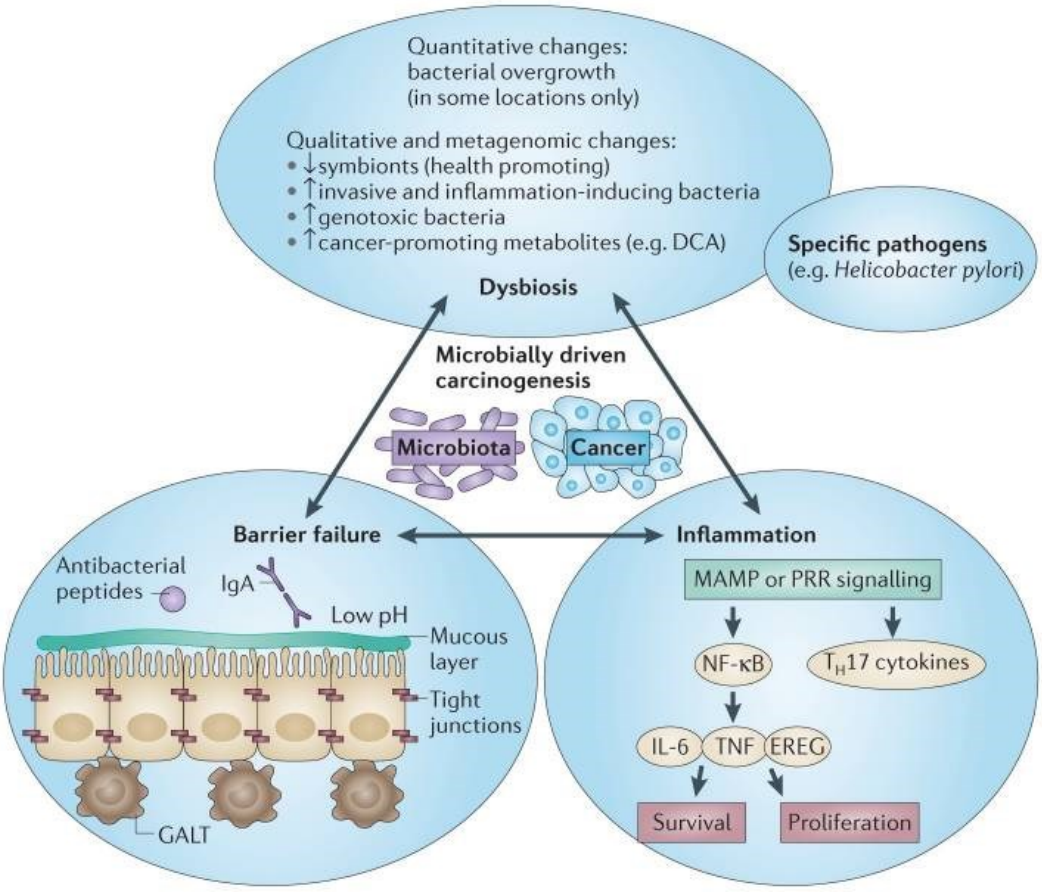

Figure 6 Microbially driven carcinogenesis: Dysbiosis occurs after perturbation, which induces a decrease of health-promoting symbiotic bacteria. This allows colonisation or overgrowth of invasive and inflammation-inducing bacteria, genotoxic bacteria or bacteria that produce cancer-promoting metabolites. In some cases, the abundance of only one specific pathogen, such as *H. pylori*, induces dysbiosis. **Barrier failures**, such as a defect in tight junctions or mucus secretion, disturb strictly controlled lumen and host milieu borders. These conditions activate IS via PRR and induce **inflammation**, which results in the survival and proliferation of epithelial cells. Picture from Schwabe & Jobin 2013. DCA = deoxycholic acid, EREG = epiregulin, GALT = gut associated lymphoid tissue, IgA = immunoglobulin A, IL = interleukin, MAMP = microbe-associated molecular pattern, NF-κB = nuclear factor kappa-light-chain-enhancer of activated B cells, Th = T helper, TNF = tumour necrosis factor, PRR = pattern recognition receptor

2.6.1.2 Specific microbiota and CRC

Similar to *H. pylori* and gastric cancer, the development of CRC is also related to specific bacteria species that in various mechanisms disrupt gut microbiota homeostasis and therefore contribute to carcinogenesis (**Table 1**).

Table 1 Examples and mechanisms of certain microorganisms contributing to carcinogenesis

Microorganism	Toxin	Mechanism
Bacteroides fragilis (enterotoxigenic)	*Bacteroides fragilis* toxin	Structure and function alteration in the epithelial barrier, ↑ permeability, ↑ cell proliferation, DNA damage, ↑ inflammation (Boleij et al., 2015)
Campylobacter jejuni	Cytolethal distending toxin	DNA brakes (Z. He et al., 2019)
E2 group *E. coli*	Colibactin, cytotoxic necrotising factors	Colibactin translocates into the nucleus and causes ds DNA brakes, ↑ inflammation (Morgan et al., 2019)
Fusobacterium nucleatum	FadA	FadA adhesin binds to E-cadherin and activates Wnt/β catenin signalling, ↑ expression of oncogenes – c-Myc, cyclin D1, ↑cell proliferation, ↑ inflammation, microsatellite instability, barrier dysfunctions (Raskov et al., 2017; Rubinstein et al., 2019)

CRC patients have consistent similarities in microorganism composition compared to healthy controls, described as CRC microbiome signature. The complex cooperation of microorganisms is expected to play a role in the carcinogenesis of CRC. "Bacterial driver-passenger model" explains the shifts in microbiota composition. Above, in table 1, are examples of driver microorganisms that disrupt barrier functions, enhance inflammation and cell proliferation, which is required to induce dysbiosis leading to carcinogenesis. The "driver bacteria" actively contribute to carcinogenesis. Over time, under these conditions, commensal bacteria are replaced by "passenger bacteria" that first do not play any active role; however, they can later actively contribute to tumour progression (Garza et al., 2020; Raskov et al., 2017).

2.6.2 Effects of gut microbiota on non-intestinal tissues malignancies

Many studies revealed a link between non-intestinal tissues such as the breast (Urbaniak et al., 2016), pancreas (Pushalkar et al., 2018) or respiratory tract (Kovaleva et al., 2019) and local specific microbiota that associate with local-tissue malignancies. However, it seems there exists a link between gut microbiota and non-intestinal tissues malignancies as well. In the case of breast cancer, specific changes in gut microbiota have been observed. For example, breast cancer patients have alterations in gut microbiota associated with estrogen metabolism and lowered bacterial diversity compared to healthy controls (Goedert et al., 2015). In another study, breast cancer patients have lower lysine decarboxylase (LDC) DNA and protein expression in the faeces. LDC is expressed in human cells but also in many gut bacteria. Through lysine decarboxylation performed by LDC, is cadaverine produced (Kovács et al., 2019). Differently, in other studies with different cancers (CRC and lung cancer), high cadaverine levels were associated with cancer patients (R. Liu et al., 2017; Yang et al., 2019). This shows how intricately, however, importantly bacterial metabolites can contribute to carcinogenesis.

Gut microbiota composition influences the microbiota composition in pancreatic tumours and shapes anti-tumour immune response. Pancreatic adenocarcinoma patients were divided into long term survivors (LTS) and short term survivors (STS). STS had lower alpha bacterial diversity and high levels of *Clostridia* and *Bacteroidea* in the tumour. In LTS, high alpha diversity correlated with enhanced frequencies of $CD8^+$ T lymphocytes and elevated levels of Granzyme B^+ cells. Approximately 25% similarity between the gut microbiome and tumour microbiome composition in cancer patients was observed. Therefore, mice pre-treated with ATB received FMT from LTS, STS or healthy controls and the tumours were inoculated. Mice from STS had the largest tumours compared to LTS and healthy control mice groups. Slowed tumour growth was associated with enhanced levels of $CD8^+IFN\text{-}\gamma^+$ T cells in the tumour tissue, whereas STS had higher frequencies of Treg and MDSC. Interestingly, in mice, after FMT were human bacteria and mice gut bacteria detected in the tumour, which suggests the bacterial migration from the gut to the tumour tissue. In mice's tumours without FMT were no bacteria detectable (Riquelme et al., 2019).

2.7 Gut microbiota and anti-tumour immune response

One of the pivotal studies to observe gut microbiota effects on anti-tumour immune response was done on mice pre-treated with ATB mix (vancomycin + imipenem + neomycin). Mice pre-treated with ATB had increased tumours sizes. In addition, gene expression analysis showed down-regulation of genes related to inflammation, phagocytosis, ag presentation and adaptive immune responses in the ATB pre-treated group (Iida et al., 2013).

The next study, which tried to elucidate whether gut microbiota can impact anti-tumour immune response, was performed using two genetically similar C57BL/6 mice strains from two different mouse facilities, Jack Laboratory (JAX) and Taconic Farms (TAC). The reason for that was different gut microbiota in mice from each facility (Ivanov et al., 2008). Firstly, tumour growth of JAX mice was slowed down, which was associated with enhanced intratumoural $CD8^+$ T cells infiltration and tumour-specific T cell responses compared to TAC mice. Then, the cohousing of JAX and TAC mice weakened TAC tumour growth, proposing that TAC mice could be simpler colonised by JAX mice commensal microbiota that facilitate anti-tumour immune response. Moreover, prophylactic oral gavage of JAX microbiota into TAC mice caused reduced tumour growth and enhanced infiltration of tumour-specific $CD8^+$ T cells. Reversed transfer of TAC microbiota into JAX mice did not have any effect; therefore, the dominant anti-tumour effect of JAX mice was described. This data shows a direct link between gut microbiota composition and anti-tumour immune response. The detailed analysis revealed that abundance of *Bifidobacterium* correlated with enhanced induction of tumour-specific T cells in the periphery and increased accumulation of ag specific $CD8^+$ T cells within the tumour. Live *Bifidobacteria* and $CD8^+$ T cells are needed for this indirect effect of the gut microbe to elevated anti-tumour immune response.

Further inspection revealed that JAX mice and JAX-fed TAC mice had increased frequency of MHC II^{high} DC and upregulated transcription of genes associated with anti-tumour immune responses, including genes important for $CD8^+$ T cells activation and costimulation, suggesting that DC trigger the immune response. Additionally, elevated tumour ag specific $CD8^+$ T cells in the tumour draining lymph node were observed and IFN-γ production was elevated in the tumour draining lymph node and spleen (Sivan et al., 2015).

That is in accordance with previous *in vitro* observation, where DC co-cultivated with *Bifidobacterium* expressed higher levels of IFN-γ and favoured Th1 $CD4^+$ T cells development (Dong et al., 2010). Sivan et al. (2015) study show critical interaction of *Bifidobacterium* and DC to trigger the anti-tumour immune response.

The gut microbiome modulates the anti-tumour immune response in liver cancer via bile acid regulated NKT cells. Many G+ bacteria contribute to bile acid metabolism. Depletion of these bacteria by ATB in drinking water enhance numbers of hepatic specific activated NKT cells within the mice liver tumour and results in enhanced anti-tumour immune response (Ma et al., 2018).

One more mechanism of how gut microbiota can influence remote anti-tumour immunity is molecular mimicry between specific gut microbiota and tumour neoantigens. Microbe-associated molecular patterns can trigger immune cells, and subsequent similarity to tumour neoantigens initiate a successful anti-tumour immune response (Vétizou et al., 2015). For example, Balachandran et al. (2017) showed that some tumour neoantigen specific T cells were cross-reactive to non-cancer microbial ag in LTS pancreatic cancer patients. In addition, Sivan et al. (2015) revealed a positive correlation of *Bifidobacterium* to ag specific T cell response within the tumour.

2.8 Effect of gut microbiota on αPD-1, αPD-L1 and αCTLA-4 ICI therapy

ICI therapy is beneficial for a subset of patients; approximately only one in four to one in five patients with NSCLC, melanoma or RCC respond to αPD-1 mAb therapy (Topalian et al., 2012). One variable factor is gut microbiota composition, which affects the anti-tumour immune response (Matson et al., 2018; Sivan et al., 2015). Once the synergy of ICI and microbiota is established, the final anti-tumour immunity is robust (Mager et al., 2020).

The first study that observed gut microbiota effect on ICI treatment of cancer was performed on JAX and TAC mice strains, which were previously shown to have different microbiota composition and therefore divergent Th17 cells differentiation in the lamina propria. The absence of Th17 promoting bacteria in JAX mice resulted in increased amounts of Treg (Ivanov et al., 2008). Treatment with αPD-L1 was sufficient only in JAX mice. FMT

from JAX mice broke the resistance of TAC mice. FMT with concomitant administration of αPD-L1 resulted in even smaller tumours and a more enhanced anti-tumour immune response (Sivan et al., 2015). The ATB administration is a commonly used method to induce changes in the gut microbiota; therefore, it is frequently used for studying the effect of microbiota on ICI. Mice with administrated αPD-1 mAb have significantly smaller tumours and prolonged survival compared to αPD-1/ATB (ampicillin + colistin + streptomycin) treated mice (Routy et al., 2018). Xu et al. (2020) used the same ATB mixture and came to the same conclusion. On the other hand, mice treated with ATB (metronidazole + neomycin + vancomycin) and antifungal amphotericin B have enhanced expression of PD-1 in tumour infiltrating $CD3^+$ T cells and therefore is the αPD-1 treatment in these mice more efficient. Additionally, αPD-1 treatment alone did not protect mice from tumour growth, and tumour size was similar to controls (Pushalkar et al., 2018). Xu et al. (2020) did not observe any difference in PD-1 expression among ATB treated/non-treated mice; however, they used another ATB mixture. The positive effect of ATB treatment on ICI is rather an exception (Pushalkar et al., 2018), many other studies associated ATB administration in mice (Vétizou et al., 2015) and humans (Huang et al., 2019; Routy et al., 2018) with enhanced tumour growth and poor prognosis since ATB administration causes gut microbiota perturbations, which disrupt homeostasis and microbiota diversity.

Less diverse microbiota and enrichment in Bacteroidales, *Escherichia coli,* and *Anaerotruncus colihominis* have been associated with poor prognosis. Especially abundance of Bacteroidales results in elevated frequencies of Treg and MDSC in the systemic circulation with reduced cytokine response. In contrast, responders (R) have higher bacterial alpha diversity in the DNA samples from the stool (Gopalakrishnan et al., 2018; Jin et al., 2019). MM patients with a high abundance of Clostridiales, *Ruminococcaceae* and *Faecalibacterium* in the gut have elevated $CD4^+$ and $CD8^+$ effector T cells in the systemic circulation with preserved cytokine response to αPD-1 ICI therapy (Gopalakrishnan et al., 2018). Controversially, *Ruminococcae* were associated with non-responders (NR) in the study on NSCLC (Jin et al., 2019). Additionally, patients with enriched *Faecalibacterium* in the gut have higher amounts of immune cells with markers of ag processing and presentation (Gopalakrishnan et al., 2018). Supporting this observation, patients with *Faecalibacterium* driven clusters have higher inducible costimulator (ICOS) and CD25 expression on $CD4^+$ T cells during αCTLA-4 treatment (Chaput et al., 2017). Enhanced ICOS expression is believed to be associated with αCTLA-4 treatment efficacy (Fu et al., 2011). *Akkermansia*

muciniphila and *Enterococcus hirae* are associated with favourable clinical outcomes in NSCLC and RCC patients that benefited from αPD-1 inhibition. IFN-γ secretion from peripheral blood memory Th1, CTL type 1 against *A. muciniphila* and CTL type 1 against *E. hirae* were observed. Additionally, the administration of *A. muciniphila* to mice previously treated by ATB mixture reinstated the αPD-1 mAb effect (Routy et al., 2018). *Akkermansia* species enhance IL-2 and IFN-γ expression in the tumours (Xu et al., 2020). The abundance of *Bifidobacterium longum*, *Collinsella aerofaciens* and *Enterococcus faecium* in the gut of MM patients are also associated with responsiveness to ICI. Additionally, in a total of 4 patients, all R, was detected *A. muciniphila* (Matson et al., 2018), which was previously described for its beneficial potential in αPD-1 treatment in Routy et al. (2018) study. The low number of positive patients disables to make any conclusions; however, it supports Routy et al. (2018) observation. Vétizou et al. (2015) suggest that αCTLA-4 mAb treatment may specifically change the gut microbiota composition of MM patients. This refutes Chaput et al. (2017), who did not observe any gut microbiota changes during αCTLA-4 mAb therapy of MM patients. These controversies suggest that the beneficial or deleterious effect of microbiota may not be a function of a single bacterium but interactions of several microbes with the host.

Many studies show the association of specific gut microbiota with responsiveness or unresponsiveness to ICI; however, the immune mechanisms are often missing. Nevertheless, it was shown that R, with higher microbiota diversity, have overall greater frequencies of unique memory $CD8^+$ T lymphocytes and NK cells (Jin et al., 2019). Concomitant administration of αPD-1 mAb and ATB enhances expression of CXCR3 and LFA-1 and activation of intratumoural $CD3^+$ cells (Pushalkar et al., 2018). Oral feeding of germ-free (GF) mice with *B. fragilis* and consequent tumour inoculation and αCTLA-4 mAb therapy promotes maturation of intratumoural DC and induces Th1 immune response in tumour draining lymph nodes (Vétizou et al., 2015). In summary, specific microbiota concomitantly with ICI leads to pro-inflammatory immune response, resulting in a better anti-tumour immune response.

Routy et al. (2018) and Gopalakrishnan et al. (2018) studied the effect of microbiota on ICI therapy not only in mice but they also transferred human faecal samples into GF mice to study the mechanisms of how certain human gut microbial consortia influence responsiveness to ICI. Mice colonised from R with subsequent tumour inoculation and αPD-

L1 treatment have a higher abundance of $CD8^+$ T cells and innate effector cells ($CD45^+CD11b^+Ly6G^+$) and lower frequencies of suppressive myeloid cells ($CD11b^+CD11c^+$) in the tumour. Elevated amounts of $CD45^+$ cells and $CD8^+$ T cells were observed in the gut (Gopalakrishnan et al., 2018). In addition, more $CXCR3^+CD4^+$ T lymphocytes infiltrate the tumour in the mice colonised by FMT from R (Routy et al., 2018). In contrast, tumours of mice colonised from NR have enhanced levels of Th17 cells and elevated levels of $CD4^+$IL- 17^+ T cells and Tregs in the spleen (Gopalakrishnan et al., 2018). Thus, microbiota from ICI R contributes to proper activation and ag presentation by DC and promotes tumour infiltration of T cells, especially Th1 cells and CTL. On the other hand, microbiota from individuals unresponsive to ICI supports the accumulation of suppressive myeloid cells and Treg in the tumour microenvironment. Unfortunately, the data describing immune responses outside the tumour microenvironment during these manipulations and the link between mucosal and systemic immune responses are scarce.

One well-described mechanism of how gut microbiota influences systemic immunity in the case of ICI treatment of tumours is the effect of *Bifidobacterium pseudolongum*. Monocolonisation of GF mice by *B. pseudolongum* before MC-38 tumour inoculation with subsequent αCTLA-4 mAb treatment provides the most robust anti-tumour immune response, mediated by Th1 cells. No effect on anti-tumour immune response and tumour growth reduction without αCTLA-4 was observed because the administration of αCTLA-4 disrupts the epithelial barrier and allows *B. pseudolongum* metabolites to promote systemic effect. Without αCTLA-4 therapy, *B. pseudolongum* is capable of inducing Th1, T-box expressed in T cells $(T\text{-bet})^+CD8^+$ T cells and IFN-γ^+ T cells within the GALT. The mediator of anti-tumour immune response is inosine, which is in elevated levels produced not only by *B. pseudolongum*, but also by *A. muciniphila*. Inosine binds to the adenosine 2A receptor and induces Th1 development. *In vitro* study revealed that inosine in the presence of IFN-γ has anti-tumour effects, while without IFN-γ has immunosuppressive properties (Mager et al., 2020). Additionaly, Xu et al. (2020) showed considerable changes in metabolic pathways, especially in glycerophospholipid metabolism among R and NR. These metabolic changes may affect the expression of IFN-γ and IL-2 in the tumour microenvironment, which may be the reason for a different response to αPD-1 among R and NR. Moreover, a cohort study of melanoma patients revealed the association of short-chain fatty acids in the stool and plasma with the efficacy of αPD-1 ICI therapy (Nomura et al., 2020). However, short-chain fatty acids restrain the αCTLA-4 therapy. Especially enhanced levels of butyrate in the patient´s

blood associate with elevated levels of Treg, decreased amounts of IL-2 and memory and $ICOS^+$ $CD4^+$ T cells (Coutzac et al., 2020).

The properties of each single bacteria and the complex microbial interactions are needed for the anti-tumour immune response. Tanoue et al. (2019) showed that the whole bacterial consortium and αPD-1 are necessary for the most effective anti-tumour immune response. They selected 11 bacterial strains capable of inducing enhancement of IFN-γ^+ $CD8^+$ T cells. Four non-Bacteroidales species possess better induction capacity; however, without the support of seven Bacteroidales strains, there was not established a full induction of anti-tumour immune response. These selected 11 bacterial strains preferentially localise the colon, and their systemic effect is not caused by bacterial dissemination or systemic circulation of gut-specific IFN-γ^+ $CD8^+$ T cells. Instead, it seems that their metabolites trigger the anti-tumour immune responses. GF mice colonised by these 11 bacterial strains with consequently inoculated MC-38 tumours were treated with αPD-1 mAb. Anti-tumour immune response was enhanced in comparison to GF mice colonised only with 10 bacterial strains, inoculated MC- 38 tumours and treated with αPD-1 (Tanoue et al., 2019). Since these 11 bacterial strains, if combined with ICI, induce an effective anti-tumour immune response, the collaboration of Bristol-Meyers Squibb and Vedanta was announced to start a clinical trial **(**NCT04208958). This study shows how important are the microbial interactions and how the disappearance of even one microbe may affect the whole outcome.

2.8.1 FMT and αPD-1 responsiveness in clinical trials

FMT showed promising results in the pre-clinical models. According to this success, a phase I clinical trial (NCT03353402) to prove safety, feasibility and impact on re-induction of αPD-1 therapy in MM patients was performed. FMT donors were two patients, who after αPD-1 mAb therapy, showed complete recovery at least for one year. Among nine recipients, previously unresponsive for αPD-1 mAb therapy, one achieved complete response and two partial responses. All nine recipients showed a progression-free survival milestone of 6 months. Recipients with complete and partial responses were from one healthy donor, who showed higher alpha diversity than the second one. Moreover, these recipients had enhanced genes expression related to APC activity, innate immunity, and IL-12 cytokine expression. All nine recipients showed post-treatment up-regulation of genes associated with ag presentation via MHC I in APC and IL-1 signalling. Overall the FMT was safe and feasible, accompanied by intra-tumoural immune activity in some patients (Baruch et al., 2021).

Results of one more phase I clinical trial (NCT03341143) on FMT effects on αPD-1 mAb resistant melanoma patients was published this year. Treatment provided clinical benefit in 6 out of 15 recipients and was accompanied by increased abundance of beneficial bacteria species, increased $CD8^+$ T cells activation, and improved cytolytic functions. It seems that FMT, together with αPD1 therapy, reduced myeloid-derived immunosuppression and induced the activation of cytotoxic $CD8^+$ T lymphocytes. Additionally, single-cell RNA analysis revealed a high Treg frequency in NR to FMT combined with αPD-1 therapy (Davar et al., 2021).

FMT shows high clinical potential for various cancers. However, gut microbiota interactions are too complex, and a deeper understanding for even more beneficial outcomes and proper selection of donors and recipients is needed. Indeed, even stricter safety controls need to be done in each donor to avoid unintentional harmful effects or even death. As it happened during FMT in *Clostridioides difficile* infected patient when drug-resistant *E. coli* bacteremia was transferred and resulted in the death of one recipient (DeFilipp et al., 2019).

2.9 Effect of gut microbiota on other cancer treatment options

2.9.1 Immunotherapeutic drugs

Gut microbiota affects other cancer immunotherapeutic drugs. Namely, CpG-oligodeoxynucleotides (ODN) that mimic bacterial unmethylated CpG motif, and therefore, serve as a ligand for TLR9 (Yu et al., 2020). CpG ODN combined with inhibitory anti-IL-10 receptor (αIL-10R) mAb causes hemorrhagic necrosis of tumours. The reason for that is a TNF-α production by tumour-associated myeloid cells that induce $CD8^+$ T cells response required for tumour eradication. Mice pre-treated with ATB mixture (vancomycin + imipenem + neomycin) and consequently administrated CpG ODN and αIL-10R have disrupted anti-tumour immune response in comparison to controls. ATB treatment reduces *TNF-α* expression and frequencies of TNF-α producing leukocytes in the tumour microenvironment. Furthermore, reduced *CD86* and *IL-12B* expression in the tumour-associated DC was observed, and an overall decrease in pro-inflammatory gene expression, such as *Il1a*, *Il1b*, *Il12b,* was detected. Iida et al. (2013) propose that bacterial products can activate, directly or indirectly, tumour-associated innate myeloid cells and boost them for

TLR9, CpG ODN dependent anti-tumour response. Another mechanism of gut microbiota-driven effects on immunotherapeutic drugs is the migration of *Bifidobacterium spp.* from the gastrointestinal tract to the tumour tissue, where contributes to enhanced effects of CD47 blockade through the production of secondary metabolites that increase cross-presentation and stimulate the STING pathway in DC, which leads to the robust adaptive immune response (Shi et al., 2020)

Another immunotherapeutic approach to treat cancer is lymphodepletion with total body irradiation (TBI), enhancing the efficiency of adoptively transferred tumour-specific $CD8^+$ T cells (Goff et al., 2016). TBI disturbs gut microbiota homeostasis and enables translocation of specific bacteria, such as *Enterobacter cloacae, E. coli*, *Lactobacillus spp.* and *Bifidobacterium spp.* to MLN. This activates innate immunity, and a higher abundance of activated $CD11c^+CD86^{high}$ DC and elevated serum levels of IL-1β, IL-6, TNF-α and IL-12 were detected. Moreover, high LPS levels were measured in the serum of these mice. ATB treatment with ciprofloxacin abolished pro-inflammatory immune response and promoted tumour growth (Paulos et al., 2007).

2.9.2 Chemotherapeutic drugs

The next question to elucidate was whether gut microbiota could influence cancer treatment that is not associated with immunotherapy. The effects of oxaliplatin, a chemotherapeutic drug causing DNA adducts, diminished in ATB pre-treated mice and GF mice. One mechanism of action of oxaliplatin is ROS production, mainly derived from tumour-associated inflammatory cells. In ATB treated group, lowered levels of ROS were detected (Iida et al., 2013).

Cyclophosphamide (CTX) is alkylating anticancer drug that cross-links DNA in the G1 phase of quickly proliferating cells, such as tumour cells and therefore causes programmed cell death. CTX therapy effect was reduced in GF mice compared to specific-pathogen-free mice. CTX treatment in mice causes discontinuities in the gut epithelial barrier and an increase in intestinal permeability. This leads to the translocation of commensal bacteria to MLN and spleen. The most prominent translocating bacteria are G+ microbes, such as *Lactobacillus johnsonii*, *Lactobacillus murinus* and *E. hirae*. These bacteria stimulate polarisation to Th1 and Th17 lymphocytes in these secondary lymphoid organs.

Administration of broad-spectrum ATB (ampicillin + colistin + streptomycin) to tumour bearing mice on CTX treatment abrogated IL-17 and IFN-γ expression in TCR-stimulated splenocytes and accelerate tumour growth. Colistin ATB (against G- bacteria) administration alone to CTX treated and control group decreased the tumour growth in CTX treated mice. On the other hand, vancomycin administration compromised the anti-tumour effects of CTX. It prevented the accumulation of Th17 lymphocytes in the spleen and reduced infiltrating of $CD3^+$ T cells and Th1 cells into the tumour microenvironment. Moreover, monocolonisation of segmented filamentous bacteria (SFB) that promote Th17 differentiation (Wu et al., 2010) to tumour-bearing GF mice did not show any effect on anti-tumour immune response combined with CTX compared to mice without CTX treatment (Viaud et al., 2013).

Translocation of *E. hirae* from the small intestine to MLN was observed in CTX treated patients as well. These patients had increased $CD8^+$ T cells and decreased Treg infiltration to the tumours. In addition, the abundance of *Barnesiella intestinihominis* in the colon enhanced levels of IFN-γ-producing gamma-delta T cells in the tumours. These both bacteria launched necessary effector and memory cancer-specific $CD4^+$ and $CD8^+$ T cells immune response. Interestingly, the NOD2 receptor limits anti-tumour stimulation of these bacteria and is proposed to be the gatekeeper to restrict certain microbiota immunogenicity (Daillère et al., 2016).

Recolonisation of *Parabacteroides distasonis* into ATB-pretreated mice reduces the anti-tumour effect of doxorubicin (Viaud et al., 2013). In addition, *P. distasonis* was previously shown to possess anti-inflammatory properties *in vivo* model of acute and chronic dextran sulphate induced colitis (Kverka et al., 2011).

3 Hypothesis and aims

The gut microbiota affects the anti-tumour immune response and influences the effectiveness of ICI. However, the observations differ among researcher groups mirroring the variability of gut microbiota composition among breeding facilities and complexity of microbe-microbe and host-microbe interactions. Additionally, many mechanisms of action are to be elucidated since the effect of microbiota on ICI has only recently been studied.

We hypothesized that mice bred in the breeding facility at the Institute of Microbiology of the CAS v.v.i. have different microbiota composition. Therefore, we can uncover a new mechanism of gut microbiota-mediated anti-tumour immune response to ameliorate the current knowledge about the effect of gut microbiota on the treatment of distant tumours.

Aims of the thesis:

- Establishment of a suitable mice model and methodology for studying the immune response within the tumour microenvironment and for studying the αPD-1 efficiency
- To study the effect of αPD-1 treatment on mice with modulated microbiota
- Study of immune mechanisms associated with reduced tumour growth

4 Material and methods

4.1 Material

4.1.1 Reagents and chemicals

Table 2: Reagents and chemicals

Name	Manufacturer
Ammonium chloride	Merck KGaA, Darmstadt, Germany #A9434
Anaerogen - anaerobic gas generator	Hardy Diagnostics, Santa Maria, CA, USA #AG025A
Brefeldin A solution (1000x)	Biolegend, San Diego, CA, USA # 420601
BSA (Bovine serum albumin)	Merck KGaA, #A7030
Citric acid	Penta, Prague, Czech Republic #18800-31000
Collagenase IV	Merck KGaA, # C-5138
Colistin	Merck KGaA, #C4461
Dextrin from maise starch	Merck KGaA, #31410
DMEM (Dulbecco's Modified Eagle Medium)	Merck KGaA, # D0697
DMSO[1]	Merck KGaA #20-139
DNase I	Merck KGaA, #11284932001
EDTA[2]	Merck KGaA, #E6758
FBS (Fetal bovine serum)	Thermo Fisher Scientific, Waltham, MA, USA, #10270106
HEPES[3]	Merck KGaA, #H4034
Hydrogen peroxide	Lach-Ner, Neratovice, Czech Republic #10064-A30-M1000-1
L-Glutamine	Merck KGaA, # G6392
Metronidazole	B. Braun, Melsungen AG, Germany, #D5353-5224
Monensin Solution (1000X)	Biolegend, #420601
Non-essential amino acids	Merck KGaA, # M7145

[1] Dimethyl sulfoxid
[2] Ethylenediamine tetraacetic acid
[3] 4-(2-hydroxyethyl)-1-piperazineethanesulfonic acid

PBS (phosphate-buffered saline)	Merck KGaA, #P5493
Penicillin-Streptomycin	Merck KGaA, # P4333
Potassium bicarbonate	Merck KGaA, #237205
RPMI-1640 (Roswell Park Memorial Institute Medium)	Merck KGaA, # R0883
Saline 0.9% w/v NaCl	Ardeapharma, a.s., Ševětín, Czech Republic
Sodium bicarbonate	Merck KGaA, #S5761
Sodium citrate dihydrate	Penta, #11470-30500
Sodium L-ascorbate	Merck KGaA, #A7631
Sodium pyruvate	Merck KGaA, #P4562
Streptomycin	Merck KGaA, #S6501
TMB[4]	Merck KGaA, #CL07
Trehalose dihydrate	Merck KGaA, # 90210
Trypan blue	Merck KGaA, #302643
Trypsin-EDTA[5]	Biowest, Nuaillé, France # P5957
Tween 20	Merck KGaA, # P1379
UltraPure™ DNase/RNase-Free Distilled Water	Thermo Fisher Scientific, # 10977015
Vancomycin	Mylan, Canonsburg, PA, USA #0166265 (SÚKL code)

4.1.2 Solutions and buffers

Table 3: Solutions and buffers

Name	Components
Citrate solution	Demineralised water containing 2% w/v citric acid and 2.94% w/v sodium citrate dihydrate, pH = 4.2
Complete RPMI-1640 medium	RPMI-1640 containig 10% v/v FBS, 1% v/v Penicilin-streptomycin, 2mM L-Glutamine
Complete RPMI-1640 medium without ATB	RPMI-1640 containig 10% v/v FBS, 2mM L- Glutamine
eBioscience™ FOXP3/Transcription Factor Staining Buffer Set	Thermo Fisher Scientific, #00-5523-00

[4] 3,3′,5,5′-Tetramethylbenzidine
[5] Ethylenediamine tetraacetic acid

eBioscience™ IC Fixation Buffer	Thermo Fisher Scientific, #00-8222-49
eBioscience™ Permeablisation Buffer 10X	Thermo Fisher Scientific, #00-8333-56
ELISA buffer	PBS containing 1% w/v BSA
FACS buffer	PBS containing 0.1% v/v Brefeldin A and 0.1% v/v Monensin
Magnetic separation recommended medium	PBS containing 2% v/v FBS, 1mM EDTA
MC-38 medium	DMEM containing 10% v/v FBS, 0.1 mM non-essential amino acids, 1 mM sodium pyruvate, 2 mM L-glutamine, 10 mM HEPES, 1% w/v Penicillin-streptomycin solution, 0.15% w/v sodium bicarbonate
Permeabilisation buffer	Distilled water containing 10% v/v eBioscience™ Permeablisation Buffer 10X
Red blood cell lysis buffer	Distilled water containing 150 mM ammonium chloride, 10 mM potassium bicarbonate and 0.1 mM EDTA
Tumour tissue dissociation solution	RPMI-1640 containing 0.003% w/v DNase I, 0.125% w/v collagenase IV, 1% v/v FBS
Trypsin – EDTA solution	PBS containing 0.01% v/v EDTA and 0.25% v/v trypsin
Wash buffer	PBS containing 0.05% v/v Tween 20

4.1.3 Kits and other reagents

Table 4: Kits and other reagents

Name	Manufacturer
EasySep™ Mouse CD45 Positive Selection Kit	STEMCELL Technologies, Vancouver, Canada #18945
iQ™ SYBR® Green Supermix	Bio-Rad, Hercules, CA, USA #1708880
Tumour dissociation kit mouse	Miltenyi Biotec, Bergisch Gladbach, Germany, #130-096-730
UltraComp eBeads™ Plus Compensation Beads	Thermo Fisher Scientific, # 01-3333-42
ZymoBIOMICS™ DNA Miniprep Kit	Zymo Research, Irvine, CA, USA # D4300

4.1.4 Antibodies

Table 5: Antibodies

Functional antibodies	Dilution	Clone	Manufacturer	Cat. number	RRID
CD16/32	1:200	93	Thermo Fisher Scientific	14-0161-86	AB_467135
InVivoMab anti-mouse PD-1 (CD279)	1:4.925	29F.1A12	BioXcell, Lebanon, PA, USA	BE0273	AB_2687796
Ultra-LEAF™ purified anti-mouse CD3	1:200	145-2C11	Biolegend	100359	AB_2616673
Ultra-LEAF™ Purified anti-mouse CD28	1:125	37.51	Biolegend	102116	AB_11147170
Analytical antibodies					
CD3 – FITC	1:100	145-2C11	BioLegend	100306	AB_312671
CD4 – BV 605	1:100	GK1.5	Biolegend	100451	AB_2564591
CD8 – BV 650	1:100	53-6.7	Biolegend	100741	AB_11124344
CD11c – BV 711	1:100	N418	Biolegend	117349	AB_2563905
CD25 – APC	1:100	PC61.5	Thermo Fisher Scientific	17-0251-82	AB_469366
CD38 - FITC	1:100	90	Biolegend	102705	AB_312926
CD45 – Alexa Fluor 700	1:100	30-F11	Biolegend	103128	AB_493715
CD45R/B220 – BV510	1:100	RA3-6B2	Biolegend	103247	AB_2561394
CD49b – eFluor450	1:50	DX5	Thermo Fisher Scientific	48-5971-82	AB_10671541
CD80 – PerCP-Cy5.5	1:100	16-10A1	Biolegend	104722	AB_2291392
F4/80 - PE	1:100	BM8	Thermo Fisher Scientific	17-4801-82	AB_2784648
Fixable Viability Dye - eFluor™ 780	1:200 1:100 (tumour)	-	Thermo Fisher Scientific	65-0865-14	-
FOXP3 - PE	1:100	FJK-16s	Thermo Fisher Scientific	12-5773-82	AB_465936
IFN-γ - PE	1:100	XMG1.2	Thermo Fisher Scientific	12-7311-81	AB_466192
IL-17 - APC	1:100	17B7	Thermo Fisher Scientific	17-7177-81	AB_763580
PD-1 – PE-Cy7	1:100	RMP1-30	Biolegend	109109	AB_572016

RORγt – BV 421	1:100	Q31-378	BD Biosciences, Franklin Lakes, NJ, USA	562894	AB_2687545
T-bet – PerCP-Cy5.5	1:50	4B10	Thermo Fisher Scientific	45-5825-80	AB_953658
TNF-α – PE-Cy7	1:100	TN3-19.12	Thermo Fisher Scientific	25-7423-82	AB_494228

4.1.5 Plastics

Table 6: Plastics

Name	Manufacturer
Cell culture flask 75 cm^2	Thermo Fisher Scientific, #156499
Centrifuge tubes 50 ml	JET Biofil, Guangzhou, China, #CFT011500
Corning® Cell strainer 70 µm	Merck KGaA, #CLS431751-50EA
Corning® 96 Well Clear Polystyrene Microplate	Merck KGaA,# CLS3788-100EA
GentleMACS™ C tubes	Miltenyi Biotec, #130-093-237
Faeces collection container	Dispolab, Troubsko, Czechia, #1085
MACS® Smartstrainer 30 µm	Miltenyi Biotec, #130-098-458
Microtubes loose 1.2 ml	Alpha Laboratories, Eastleigh, UK #QS845
Milex-GP syringe filter 0.22 µm	Merck KGaA, #SLGP033RS
Nunc MaxiSorp™ flat-bottom	Thermo Fisher Scientific, #44-2404-21
Tissue culture test plates 96 wells	TPP, Trasadingen, Switzerland #92097

4.1.6 Technical devices and instruments

Table 7: Technical devices and instruments

Name	Manufacturer
Cell culture incubator – MCO-15AC	Sanyo, Osaka, Japan
CFX96 Touch Real-Time PCR detection system	Bio-Rad
EasyPlate™ EasySep™ Magnet	STEMCELL™ #18102
FastPrep®-24 homogenizer	MP Biomedicals, Santa Ana, CA, USA #116004500
GentleMACS™ Dissociator	Miltenyi Biotec, #130-093-235
Hettich Universal 32R centrifuge	DJB Labcare, Buckinghampshire, UK

LSR II Flow cytometer with High-throughput sampler	Beckton Dickinson, Franklin Lakes, NJ, USA
Microcentrifuge Minispin™	Eppendorf, Hamburg, Germany
Microscope Zeiss TELAVAL 2	Zeiss, Oberkochen, Germany
Multi Bio 3D programmable mini-shaker	Biosan, Riga, Latvia
Multiskan Ascent Plate Reader 96/384	Labsystems Diagnostics Oy, Vantaa, Finland
NanoDrop 2000™ spectrophotometer	Thermo Scientific
Nuve NB 5 unstirred water bath	Henderson Biomedical, London, UK
Tecan Columbus Pro microplate washer	Gemini, Apeldoorn, Netherlands #04969

4.1.7 Softwares

Table 8: Softwares

Name	Manufacturer
Ascent (version 2.4.1)	Thermo Scientific
Bio-rad CFX manager (version 3.0)	Bio-Rad
BD FACS DIVA (version 6.0)	Beckton Dickinson
FlowJo (version 7.2.5/9.9.4)	Tree Star Inc., Ashland, OR, USA
GraphPad Prism (version 8.0.2)	GraphPad Software, Inc., La Jolla, CA, USA

4.2 Methods

4.2.1 Culture of MC-38 cells

For all experiments, the MC-38 murine colon adenocarcinoma cell line (CVCL_B288; Kerafast, Boston, MA, USA, #ENH204-FP) was used. This tumour cell line was obtained as a kind gift from the Laboratory of Tumour Immunology at the Institute of Microbiology of the CAS v.v.i.

4.2.1.1 Cell thawing

The frozen aliquots (0.5×10^6 cells in 1 ml) were stored at -150 °C freezer. On the day of thawing (Day 0), the MC-38 cultivation medium (**Table 3**) was prepared. Then it was preheated and saturated with CO_2 in the cell culture incubator (37 °C, 5% CO_2) for 15 min. Afterwards, were the cells thawed and transferred into the sterile 50 ml tube already containing 9 ml of MC-38 cultivation medium. The solution was well mixed and centrifuged for 5 min at 200 × g, 20 °C. The supernatant was discarded, and the cell pellet was resuspended in 2 ml of MC-38 cultivation medium, then 8 ml of MC-38 cultivation medium were added, and the solution was mixed well. To entirely eliminate the DMSO cryoprotectant, the suspension was again centrifuged for 5 min at 200 × g, 20 °C. Afterwards, the supernatant was discarded, and the cell pellet was resuspended in 2 ml of MC-38 cultivation medium, then 8 ml of MC-38 cultivation medium were added, and the solution was mixed well. The suspension was transferred into two cell culture flasks (75 cm^2), 5 ml each time. Then 10 ml of MC-38 cultivation medium was added and mixed in each cell culture flask. The lower amount of medium allows cells to better adhere to plastic. The cell culture flasks were put into the cell culture incubator (37 °C, 5% CO_2) overnight. The next day (Day 1), the cell adhesion, shape and possible contamination were checked under the microscope. Then, all the medium was removed, and fresh 25 ml of medium was added.

4.2.1.2 Cell passaging

In order to get fully recovered cells after freezing and to obtain a sufficient amount of cells for inoculation into mice, the cells were passaged. Usually, on day 4, when the bottom of the cell cultivation flask was fully covered by cells.

Trypsin-EDTA solution (**Table 3**) and saline (0.9% w/v NaCl) were warmed in a 37°C water bath for 15 min. MC-38 cultivation medium was warmed and saturated with CO_2

for 15 min in the cell culture incubator (37 °C, 5% CO_2). The cell culture flasks were checked under the microscope, and the MC-38 cultivation medium was removed. The cells were washed by saline to eliminate all FBS that contains protease inhibitor, which may inhibit trypsin activity. Then, the saline was removed, 5 ml of trypsin-EDTA was added, and the flask was gently shaken manually. The solution was cultured for 3 min in the cell culture incubator (37 °C, 5% CO_2). Subsequently, in order to stop trypsinisation, 10 ml of MC-38 culture medium were added and mixed well. The solution was transferred into a 50 ml tube and centrifuged for 5 min at 270 × g, 28 °C. The supernatant was discarded, the cell pellet was resuspended, and the MC-38 cultivation medium was added up to 20 ml. Into new cell culture flask (75 cm^2) was 10 ml of cell suspension transferred and 15 ml of new MC-38 cultivation medium added. The culture flasks were then added back to the cell culture incubator (37 °C, 5% CO_2).

4.2.1.3 Cell harvesting

On the day of MC-38 cells inoculation into mice, usually at day 6 of here described procedure, were the cells treated the same as described in 4.2.1.2 cell passaging, to the step with adding 10 ml of MC-38 cultivation medium. Then, the solution was mixed well and transferred into a 50 ml tube via a 70 µm cell strainer to get a single-cell suspension. After 5 min centrifugation at 270 × g, 28 °C, the supernatant was discarded, and the cell pellet was resuspended in 10 ml of saline. The solution was strained again through a 70 µm strainer and centrifuged for 5 min at 270 × g, 28 °C. Again, the supernatant was discarded, and 5 ml of saline was added. The cell concentration was counted in the Bürker counting chamber using trypan blue to distinguish death cells. Subsequently, the cell suspension was diluted to the desired concentration and immediately inoculated into the right flank of mice (4.2.2.1).

4.2.2 Mice

For all experiments, eight to ten-week-old wild-type C57BL/6 male and female mice were used, which were obtained and housed at the breeding facility at the Institute of Microbiology of the CAS v.v.i. Except for the colonisation experiment, where were used GF mice from the Laboratory of Gnotobiology in Nový Hrádek at the Institute of Microbiology of the CAS v.v.i . Prior and during the experiments, mice were fed *ad libitum*. Mice had free access to clean tap water except for ATB-treated mice.

The experiment was terminated either by the death of all mice or between days 18 to 21 post tumour inoculation by cervical dislocation. The experiments were carried out in accordance with the recommendations of the ethics standards defined by the European Union legislation on the use of experimental animals (2010/63/EU) and the Czech animal welfare act. Furthermore, all mice were used according to the procedures approved by the Institute of Microbiology Animal Care and Use Committee.

4.2.2.1 Tumour induction and treatment

Before the experiment started, the mice were shaved around the right flank, divided into groups and marked. On day 0, 0.5×10^6 MC-38 cells in 100 µl of saline were subcutaneously inoculated. Except for the first experiment, which determined the convenient amount of MC-38 tumour cells inoculated per mouse. In that experiment were 0.1×10^6, 0.25×10^6, 0.5×10^6 or 1×10^6 MC-38 cells in 100 µl of saline subcutaneously inoculated. The tumour growth was measured every 2-3 days by calliper, and mice were weighed the same day until the experiment termination. A modified ellipsoid formula (length × width × width)/2 was used to calculate tumour volume.

The mice were treated intraperitoneally on days 7, 10 and 13 with 200 µg of InVivoMab anti-mouse PD-1 in 100 µl of PBS. Control mice received only 100 µl of sterile PBS. For the experiment that determined the effective dosage of InVivoMab anti-mouse PD-1 were also administrated 12.5 µg, 50 µg of αPD-1 in 100 µl of sterile PBS.

4.2.2.2 Microbiota manipulation by ATB

One group of mice was treated with ATB from day -18 till the experiment termination to establish disruption of gut microbiota. Before the beginning of the experiment, the stool was collected from αPD-1 and αPD-1 + ATB groups into sterile pre-weighed 2 ml microcentrifuge tubes, then weighed again to determine stool weight and subsequently stored at – 80 °C. ATB + αPD-1 group was treated with ATB mix dissolved in autoclaved drinking water: colistin (7.5 mg/l), streptomycin (5 g/l) and vancomycin (250 mg/l). Every 2-3 days, received mice 300 µl of metronidazole (5 mg/ml) per gavage with steel bulb-tipped gavage needle. The tumour induction and αPD-1 were performed as described above in 4.2.2.1 tumour induction and treatment. On day18, stool from αPD-1 and αPD-1 + ATB groups was collected; mice were sacrificed by cervical dislocation. MLN, PP and tumours were collected for immediate processing (see sections below). Additionally, gut microbiota content was collected for subsequent GF mice colonisation.[6]

4.2.2.3 Collection, storage and administration of gut microbiota

The collection fluid was prepared under sterile conditions. Faeces collection container was filled with 0.5% w/v Sodium L-ascorbate, 6% w/v trehalose dehydrate and 19% w/v dextrin from maise starch in saline. The solution was filtered through a 0.22 µm Milex-GP syringe filter, and 1 ml was distributed to sterile 2 ml microcentrifuge tubes. Subsequently, anaerobic conditions were maintained by an anaerobic gas generator, and the solution was incubated for 48 hrs. Then the lids were closed, and 2 ml microcentrifuge tubes were stored at 5 °C.

On the day of experiment termination, ileal and colon + caecum content was collected separately to 2 ml microcentrifuge tubes with the prepared solution. The solution and gut content were mixed well by pipette and frozen at -80 °C. For mice colonisation, the frozen samples were thawed in the water bath at 37 °C for 10 min, the samples from ileum from one group separately and colon + caecum of one group were pooled together, and mice were colonised as described below in 4.2.2.4 GF mice colonisation.

4.2.2.4 GF mice colonisation

GF mice were divided into two groups, R were mice, which were colonised with the gut microbiota from αPD-1 + ATB group from the previous ATB experiment. NR were colonised with the gut microbiota from the αPD-1 group. Mice were colonised per os with 200 µl of ileal content and per rectum with 100 µl of content from colon + cecum via steel bulb-tipped gavage needle. After the transfer, mice were given autoclaved water and a sterile diet and were kept in individually ventilated cages for 16 days before MC-38 tumour inoculation. On day 0, 0.5×10^6 MC-38 tumour cells were inoculated subcutaneously, and mice were treated on day 7, 10 and 13 with 200 µg αPD-1 in 100 µl PBS intraperitoneally. The mice were weighed, and tumour growth was measured (length and width) by calliper every 2-3 days until day 19 when was stool from both groups collected and mice were sacrificed by cervical dislocation. MLN, PP, spleen and tumours were collected for immediate processing (see sections below). Additionally, gut microbiota content from ileum, colon and caecum were collected for subsequent GF mice colonisation and sequencing. [6]

[6] On the day of experiment termination were approximately 7 people working together. I planned the work, prepared protocols, solutions, materials etc.. On day of experiment termination, I coordinated the work and participated in the tumour processing, magnetic separation and all flow cytometry stainings. Additionally, I have participated in all the steps that are needed for the tissue processing, countings and cell cultivation/stimulation described in this master thesis, however in other experiments. The previous and subsequent parts of the experiment and data analysis were done on my own.

4.2.3 Cell suspension preparation

4.2.3.1 MLN and spleen

Spleen and MLN were collected and then mashed separately under sterile conditions. The cell suspension was then filtered through a 70 µl strainer into a 50 ml centrifugation tube. MLN were centrifuged for 5 min at 300 × g, 4 °C, the supernatant was discarded, and the pellet was resuspended in 0.5 ml of saline. Spleen suspension was centrifuged, the supernatant was discarded, and the cells were treated with 5 ml of Red blood cell lysis buffer lysing buffer (**Table 3**) for 5 min to get rid of red blood cells. Then, was diluted Red blood cell lysis buffer in saline to a total amount of 20 ml, and the tubes were centrifuged. The supernatant was discarded, and the cell pellet was diluted in 5 ml of complete RPMI-1640 medium without ATB. Cells were then counted in the Bürker chamber and diluted to 0.2×10^6 concentration. The cell suspension was used for intracellular flow cytometry staining into the nucleus, anti-CD3/anti-CD28 stimulation for 12 hrs + 4 hrs with brefeldin + monensin for intracellular flow cytometry staining for cytokines and for anti-CD3/anti-CD28 stimulation for 48 hrs with subsequent Enzyme-linked Immunosorbent Assay (ELISA).

4.2.3.2 Tumour

Tumours were weighed and put into gentleMACS™ C tubes containing 1.5 ml of tumour tissue dissociation solution (**Table 3**). At the beginning of this project was also the tumour dissociation kit from Miltenyi Biotec (**Table 4**) used to compare effectivity. First, the tumour tissue was cut into small pieces with surgical scissors. Subsequently, was gentleMACS™ Dissociator used twice at standard programme m-imp_tumour_02. The tubes were incubated at 37 °C under continuous rotation at 4 rpm for 40 min. Afterwards, gentleMACS™ Dissociator at standard programme m-imp_tumour_03 was used twice. Then the dissociated tissue solution was diluted with saline and transferred into a 50 ml tube through a 70 µm strainer. After centrifugation for 5 min at 300 × g, 4 °C, was the supernatant carefully removed, and red blood cells were lysed by 5 ml of Red blood cell lysis buffer lysing buffer for 10 min. Then the Red blood cell lysis buffer was diluted by saline to the total amount of 20 ml and centrifuged. Afterwards, was the supernatant discarded, the cell pellet was resuspended in the saline and saline was added in total to 5 ml. The cell solution was strained through MACS® Smartstrainer 30 µm, centrifuged again and diluted in 5 ml of complete RPMI-1640 medium with ATB for direct cell counting and dilution to 5×10^6

cells/ml or in 400 µl of recommended magnetic separation medium (**Table 3**) for CD45 positive magnetic separation.

4.2.3.3 CD45 positive magnetic separation

In order to get more immune cells from the tumour tissue, CD45 positive magnetic separation was performed with EasySep™ Mouse CD45 Positive Selection Kit. The procedure was done according to manufacturer protocol with slight changes. Firstly, single-cell tumour suspension from each sample was divided into two wells in round-bottom Corning® 96 Well Clear Polystyrene Microplate, in each well was 200 µl of suspension. Subsequently, a selection cocktail was prepared; for each well, 2 µl of component A and 2 µl of component B were mixed. Then, 4 µl of selection cocktail were added to each well, mixed and incubated for 5 min at room temperature (RT). Rapidspheres™ were vortexed for 30 secs, 2 µl were added to each sample and mixed well. After 3 min incubation at RT, was 50 µl of recommended magnetic separation medium added to each well and mixed gently 3 times. The plate without the lid was then placed on the EasyPlate™ EasySep™ Magnet and incubated for 5 min. The supernatant was carefully pipetted off and discarded. The plate was removed from the magnet, and 250 µl of recommended magnetic separation medium was added to each well, then was the plate put on the magnetic plate again and incubated for 5 min. The supernatant was discarded, and 250 µl of complete RPMI-1640 medium with ATB was added to each well, wells from one sample were pooled together, and the cells were counted and diluted to concentration 5×10^6 cells/ml. The cell suspension was used for intracellular flow cytometry staining into the nucleus, anti-CD3/anti-CD28 stimulation for 12 hrs + 4 hrs with brefeldin + monensin for intracellular flow cytometry staining for cytokines and for anti-CD3/anti-CD28 stimulation for 48 hrs with subsequent indirect ELISA.

4.2.4 Flow cytometry analysis of T cell subsets and mononuclear cells

Tumour, spleen and MLN cell suspensions were used for flow cytometry analysis of 2 panels. The 96-well plates were used and in each well was 2×10^5 spleen or MLN cells or 5×10^5 cells from the tumour. Firstly, the plates were centrifuged for 5 min, 300 × g at 4 °C and the supernatant was gently discarded by gentle tap of the plate on the paper towel. The samples, except native and other single stains, were stained with 10 µl of Fixable Viability Dye eFluor™ 780 in PBS (**Table 5**). To native and other single stains was added 10 µl of PBS. After 30 min incubation in the dark at 4 °C was added 150 µl of PBS, and the plates

were centrifuged. The supernatant was discarded, and the pellet was resuspended in 160 µl of PBS and centrifuged again. Next, were the cells fixed and permeabilised in 140 µl of eBioscience FOXP3/Transcription Factor Staining Buffer Set (**Table 3**) for 45 min in the dark at 4 °C. Then the plates were centrifuged for 5 min, 350 × g at 4 °C because higher speed is needed for fixed cells. Next, the plates were washed two times with 170 µl of permeabilisation buffer (**Table 3**). Then, were cells blocked with 20 µl of 10% normal mouse serum and Fc block (CD16/32) in permeabilisation buffer for 20 min in the dark at 4 °C to prevent non-specific binding of mAb. After incubation, 10 µl of properly vortexed UltraComp eBeads™ Plus Compensation Beads were added to wells prepared for single stains bead controls. Then, 10 µl of Ab (**Table 5**) in permeabilisation buffer were added and incubated for 20 min in the dark at 4 °C. Subsequently, plates were washed twice in permeabilisation buffer and finally resuspended in 100 µl of PBS. Samples were measured on Beckton Dickinson LSR II flow cytometer and captured by BD FACS DIVA. Data were analysed with the FlowJo software. Flow cytometry data analysis was performed according to native, single stains on cells and UltraComp eBeads™ Plus Compensation Beads and FMO controls. Gating strategies are in supplementary Figure 1 and 2 depicted.

4.2.5 Flow cytometry analysis of intracellular cytokines

For flow cytometry analysis of intracellular cytokines was the 96-well plate pre-treated with 50 µl of the Ultra-LEAF^{TM} purified anti-mouse CD3 mAb (5 µg/ml) diluted in saline. The liquid was then removed, and each well was washed two times with 200 µl of saline in the first washing and complete RPMI-1640 (tumour samples every time in medium with ATB and spleen + MLN in medium without ATB) in the second. Then, 2×10^5 MLN and spleen cell suspensions and 5×10^5 tumour cell suspension were transferred to wells, and consequently, 100 µl of Ultra-LEAF^{TM} purified anti-mouse CD28 mAb (4 µg/ml) diluted in RPMI-1640 was added. The plate was cultured for 12 hrs in the cell incubator (37 °C, 5% CO_2). After 12 hours was into each well 50 µl of 0.5% Brefeldin A + 0.5% Monensin diluted in RPMI-1640 medium, added. After 4 hours, the plate was centrifuged for 5 min 300 × g, 4 °C, 100 µl of solution was discarded, and the rest was transferred into a new 96-well plate. The plate was centrifuged, and 10 µl of Fixable Viability Dye eFluor™ 780 diluted in FACS buffer (**Table 3**) was added for 20 min, the plate was kept in the dark at 4 °C. Afterwards, was 160 µl of FACS buffer added, and the plate was centrifuged and washed again with 170 µl of FACS buffer. Then were the cells permeabilised in 140 µl of eBioscience™ IC Fixation

Buffer (**Table 3**) for 45 min at 4 °C in the dark. After that, was the plate centrifuged for 5 min 350 × g, 4 °C. Cells were washed two times in 170 µl of permeabilisation buffer (**Table 3**). After centrifugation, were cells blocked by 20 µl of 10% normal mouse serum and Fc block (CD16/32) in permeabilisation buffer for 20 min, in the dark at 4 °C. Afterwards, 10 µl of properly vortexed UltraComp eBeads™ Plus Compensation Beads were added to wells designed for beads control single stains, and 10 µl of Ab (**Table 5**) in permeabilisation buffer were added to samples. After 20 min incubation in the dark at 4 °C was 140 µl of permeabilisation buffer added, and the plate was centrifuged and washed with 170 µl of permeabilisation buffer. After centrifugation were cells resuspended in 100 µl of PBS and were measured on Beckton Dickinson LSR II flow cytometer and captured by BD FACS DIVA. Data were analysed with the FlowJo software. Flow cytometry data analysis was performed according to native, single stains on cells and UltraComp eBeads™ Plus Compensation Beads and FMO controls. Gating strategy is in supplementary figure 3 depicted.

4.2.6 Cell cultivation

Cell suspensions from spleen, MLN and tumour were cultured for 48 h on 96-well pre-treated with 50 µl of the Ultra-LEAF^{TM} purified anti-mouse CD3 mAb (5 µg/ml) diluted in a complete RPMI-1640 (tumour samples every time in medium with ATB and spleen + MLN in medium without ATB) and incubated for 2 h in the cell incubator (37 °C, 5% CO_2). The liquid was then removed, and each well was washed two times with 200 µl of saline in the first washing and complete RPMI-1640 without ATB in the second. Then, were transferred 2 × 10^5 MLN and spleen cell suspensions and 5 × 10^5 tumour cell suspension in doublets to wells and consequently 100 µl of Ultra-LEAF^{TM} purified anti-mouse CD28 mAb (4µg/ml) diluted in RPMI-1640 was added. Next, the plate was cultured for 48 hrs in the cell incubator (37 °C, 5% CO_2). Then was the plate centrifuged for 5 min at 300 × g, RT, and supernatant from doublets was collected into 1.2 ml loose microtubes and samples were frozen at -20 °C until analysis.

Three distal PP, one sample of three-millimetre punch biopsy of distal colon and ileum were washed in sterile saline, blotted dry, weighted and cultured for 48 hours in the 48-well plate in the complete RPMI-1640 medium with ATB. The supernatant was carefully collected into 1.2 ml loose microtubes, and samples were frozen at -20 °C until ELISA analysis.

4.2.7 ELISA

Supernatants from 48 h cell stimulation or 48 h tissue biopsies culture were used for ELISA analysis. The procedure was done with DuoSet® ELISA Development Systems (**Table 9**), and all the dilutions were performed according to the manufacturer recommendations. On day 1 were capture Ab thawed and diluted in PBS, then were capture Ab added to the the 96-well Nunc MaxiSorp™ flat-bottom plate and coated with capture Ab overnight. On day 2 was the plate washed by Tecan Columbus Pro microplate washer with wash buffer (**Table 3**). This washing was performed after each incubation step. Then was added ELISA buffer (**Table 3**) to each well to prevent non-specific binding. After 1 h incubation were samples and control standards added in doublets into the plate. Subsequently, was the plate incubated for 1.5 h. Then was added biotinylated detection Ab diluted in ELISA buffer to each well. After 1.5 h incubation, was added streptavidin conjugated to horseradish peroxidase diluted in ELISA buffer. After 20 min incubation in the dark was added substrate (TMB + citrate (**Table 3**) + H_2O_2) to start the enzymatic reaction. The plate was incubated for 20 min and then was the enzymatic reaction stopped by 2M H_2SO_4, and the optic density was measured by spectrophotometer at wavelength 450 nm and 650 nm. The plate was analysed with Ascent software. The concentration of cytokine was quantified with the use of standard diluted series. Quantified cytokines are described in **Table 9**.

Table 9: Analysed cytokines

colon	
IL-33	Bio-Techne, Minneapolis, USA, #DY3626
TNF-α	Bio-Techne, #DY410
S100A8	Bio-Techne, #DY3059
MLN	
IFN-γ	Bio-Techne, #DY485
IL-2	Bio-Techne, #DY402
TNF-α	Bio-Techne, #DY410
PP	
IL-1β	Bio-Techne, #DY401
IL-6	Bio-Techne, #DY406
IL-33	Bio-Techne, #DY3626
S100A8	Bio-Techne, #DY3059
TNF-α	Bio-Techne, #DY410
spleen	
IL-17	Bio-Techne, #DY421

4.2.8 Microbiome analysis

From collected stool was bacterial DNA isolated with ZymoBIOMICS™ DNA Miniprep Kit according to manufacturer protocol. Firstly, were stool samples transferred to ZR BashingBead™ Lysis tubes and 750 µl ZymoBIOMICS™ Lysis solution was added, the tube content was homogenised three times at 6.5 m/s for 1 min in FastPrep®-24 homogenizer. Then were the tubes centrifuged in the microcentrifuge at 10 000 × g for 1 min. Into new tube with Zymo-Spin™ III-F filter was supernatant transferred and centrifuged at 8 000 × g for 1 min. Then, 1200 µl of ZymoBIOMICS™ DNA Binding Buffer was added to the filtrate and mixed well. To new collection, the tube was 800 µl of filtrate added through the Zymo-Spin™ IICR column and centrifuged at 10 000 × g for 1 min. The supernatant was discarded, and this step was repeated with the remaining solution. Next, the column was transferred into a new collection tube, and 400 µl of ZymoBIOMICS™ DNA wash buffer 1 was added, and the tube was centrifuged. The supernatant was discarded, and 700 µl of ZymoBIOMICS™ DNA wash buffer 2 was added to the column, and the tube was centrifuged. In the next step, was 200 µl of ZymoBIOMICS™ DNA wash buffer 2 added and centrifuged. The column was then transferred into a sterile 1.5 ml microcentrifuge, and 50 µl of ZymoBIOMICS™ DNase/RNase free water was added directly to the column matrix, incubated for 1 min and centrifuged to elute the DNA. The new Zymo-Spin™ III-HRC filter was placed into a new collection tube, and 600 µl of ZymoBIOMICS™ HRC Prep solution was added and centrifuged. The eluted DNA was transferred into a prepared Zymo-Spin™ III-HRC filter placed in a new sterile 1.5 ml microcentrifuge tube, and centrifuged at 16 000 × g for 3 min.

The amount and quality of harvested DNA was measured by Thermo Scientific™ NanoDrop 2000. Then the abundance of total bacteria, lactobacilli and SFB was measured by quantitative reverse transcription polymerase chain reaction (RT-qPCR) using specific 16S ribosomal RNA (rRNA) gene primers (**Table 10**). The amplification was performed in a 25 µl reaction (**Table 11**). The samples and standards were in doublets, and each pair of primers had its negative control. Diluted PCR products served as standards to validate the absolute copy number of each sample in 10-fold dilution series. The cycling parameters were as follows: 4 min at 94 °C, 35 cycles of 10 s at 94 °C, 25 s at 60 °C for SFB primers, 58 °C for *Lactobacilli* primers or 57 °C for universal bacterial primers, and 35 secs at 72 °C, and a final extension for 7 min at 72 °C. The CFX96 Touch Real-Time PCR detection system was used for qPCR and the data were analysed in the Bio-rad CFX manager.

Table 10: Primers

Name	Sequence (5´- 3´)	Target	Reference
Uni926F Uni1062R	AAACTCAAAKGAATTGACGG CTCACRRCACGAGCTGAC	Universal bacterial 16S rRNA	Bacchetti De Gregoris et al., 2011
Lacto157F Lacto379R	TGGAAACAGRTGCTAATACCG GTCCATTGTGGAAGATTCCC	Lactobacilli 16S rRNA	(Byun et al., 2004)
SFB225F SFB558R	AGGAGGAGTCTGCGGCACATTAGC CGCATCCTTTACGCCCAGTTATTC	SFB 16S rRNA	(Suzuki et al., 2004)

Table 11: RT-qPCR reaction

Name	Volume
iQ™ SYBR® Green Supermix, Biorad	12.5 µl
Forward primer	1 µl (10 µM)
Reverse primer	1 µl (10 µM)
DNA template	4 µl (5 ng/µl)
UltraPure™ DNase/RNase-Free Distilled Water	6.5 µl

4.2.9 Statistical analysis

Shapiro-Wilk test was performed to investigate the normal distribution. Paired two-tailed student´s t-test was used to determine the difference in the experiment with different tumour dissociation buffers and magnetic separation. The unpaired Student´s t-test was used to compare two experimental groups and one-way analysis of variance (ANOVA) with Tukey´s multiple comparison test to compare more groups. Two-way ANOVA with Bonferroni post hoc test was used for the analysis of the tumour growth. The Kaplan-Meier survival curve was analysed by long-rank (Mantel-Cox) test and the log-rank test for trend. All data are expressed as the mean ± standard deviation, except for the tumour growth timeline graph, where is SD omitted for clarity. Data were considered statistically significant when $p \leq 0.05$; for the statistical analysis was used GraphPad Prism software.

5 Results

5.1 Establishment of a mice model and convenient methodology for studying the effect of αPD-1 mAb on the anti-tumour immune response

In order to study the effect of gut microbiota on the αPD-1 ICI therapy, a suitable mice model and methods had to be established. This includes the amount of inoculated tumour cells, αPD-1 dosage, the length of the experiment and subsequent methods of tumour processing.

5.1.1 Amount of inoculated MC-38 tumour cells

In the first experiment, 0.1×10^6, 0.25×10^6, 0.5×10^6 or 1×10^6 MC-38 cells in 100 µl of saline were inoculated s.c. to C57BL/6 mice to determine the number of tumour cells, which induce visible tumours on day 7, when αPD-1 treatment starts. On day 7 were the tumours detected in the groups with 0.5×10^6 and 1×10^6 inoculated MC-38 tumour cells (**Fig. 7A**). Additionally, both groups have similar tumour growth (**Fig. 7B**) and survival rate (**Fig. 7C**). Since similar results of 0.5×10^6 and 1×10^6 MC-38 tumour xenografts were observed and there was no excessive tumour growth associated with rapid death, we decided to inoculate the lower amounts of tumour cells to additionally give space for a more robust adaptive immune response and also with respect to the model organism and material saving.

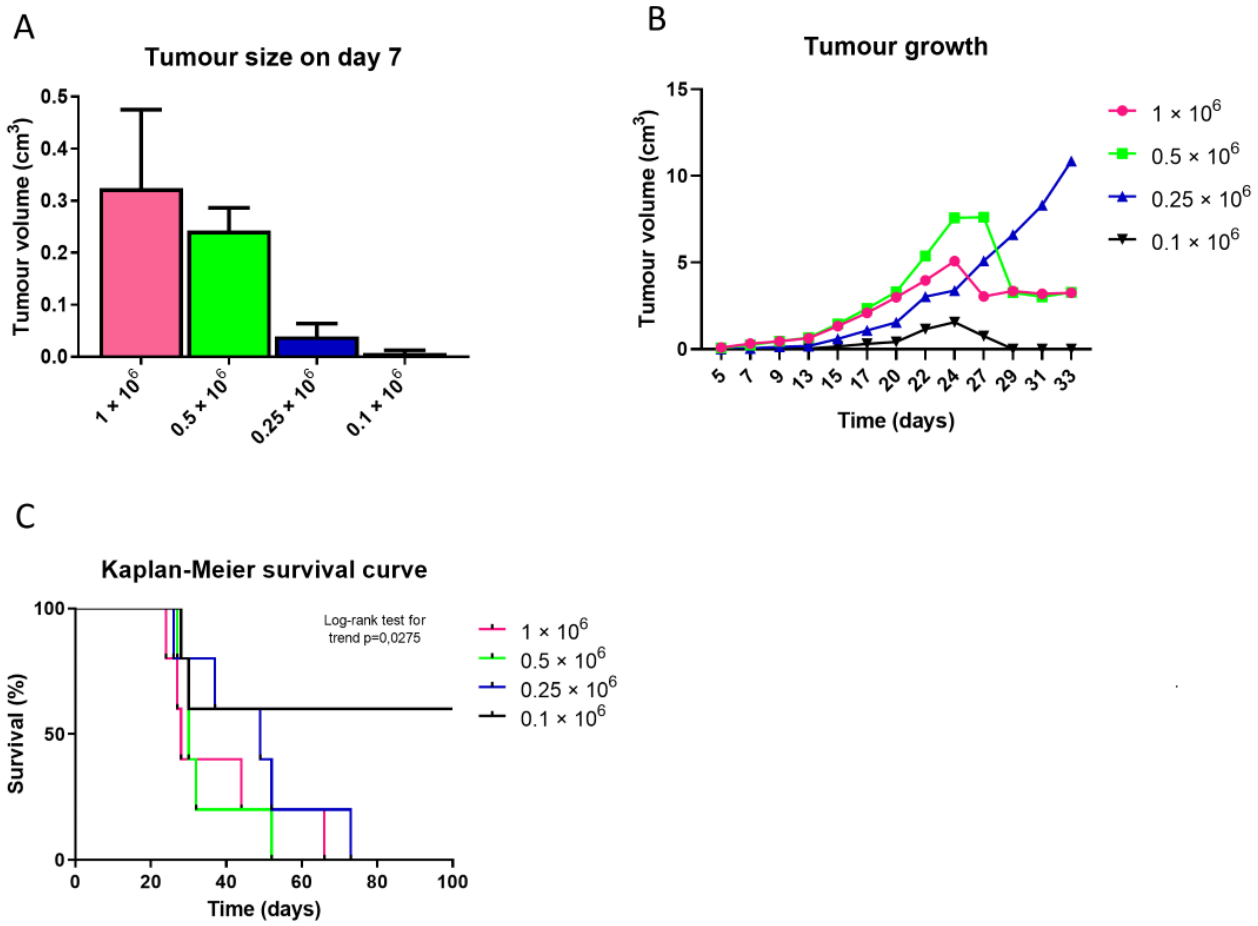

Figure 7 Determining the optimal amount of inoculated MC-38 tumour cells. C57BL/6 mice (n=5 per group) were inoculated subcutaneously with 1×10^6, 0.5×10^6, 0.25×10^6 or 0.1×10^6 MC-38 cells in 100 µl of saline into the right flank. Tumours size was measured by calliper from day 7 (**A**) and was continuously monitored every 2-3 days (**B**). The survival (**C**) was observed as well. Tumour growth was analysed by two-way ANOVA with Bonferroni post hoc test; the Kaplan-Meier survival curve was analysed by long-rank (Mantel-Cox) test and long-rank test for trend. Experiment was done only once. Data are shown as mean ± SD. The SD is omitted for clarity in the graph of tumour growth. αPD-1 = anti-programmed cell death protein 1

5.1.2 Three doses of 200 µg of αPD-1 are needed to slow the tumour growth but do not affect survival

In the next step, the effective dose of αPD-1 was determined. For αPD-1 treatment of tumour xenografts in mice is commonly used 200 µg of αPD-1 per dose (Juneja et al., 2017). We wonder if we could lower the administered amount, and therefore while testing 200 µg of αPD-1, we added also lowered amounts of 50 µg and 12.5 µg of αPD-1 in 100 µl of PBS to treat MC-38 tumour xenografts. The administration of 200 µg of αPD-1 mAb on day 7, 10 and 13, slows the tumour growth (**Fig. 8A**). However, a visible acceleration after day 21 was detected (data not shown). Therefore, it was decided to terminate the following experiments on day 21 in order to observe immune changes related to αPD-1 administration. Interestingly, the overall survival was not affected by αPD-1 treatment with this dosing schedule (**Fig. 8B**), leaving space for improvement by microbiota manipulation.

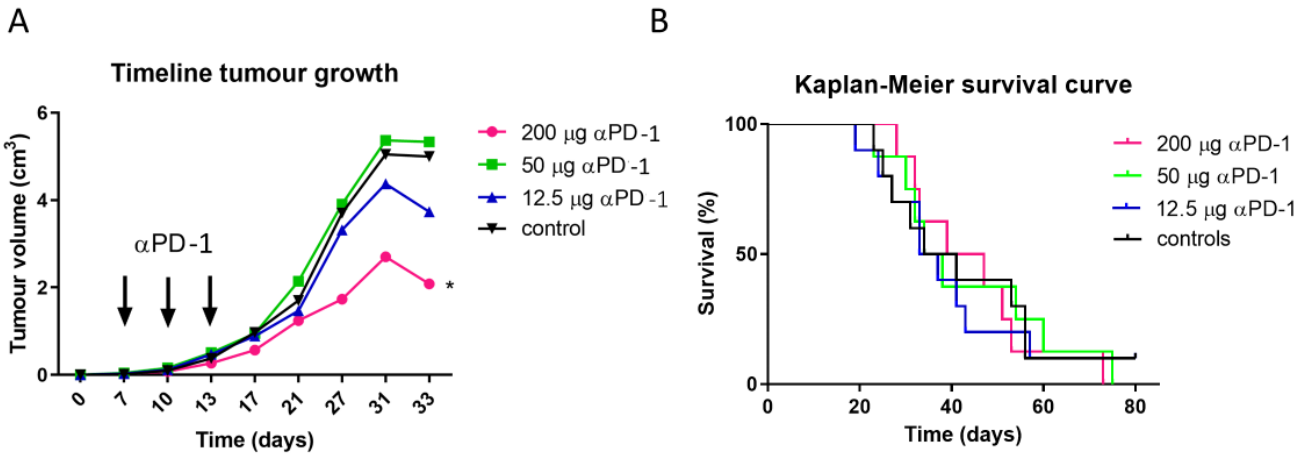

Figure 8 Determination of effective αPD-1 doses. C57BL/6 mice (n=8-10 per group) were inoculated subcutaneously with 0.5 × 10^6 MC-38 cells in 100 µl of saline and were treated with 200 µg, 50 µg and 12.5 µg of αPD-1 in 100 µl of PBS. The Control group received only 100 µl of PBS. The tumour growth (**A**) and survival (**B**) were monitored. Experiment was done only once. Tumour growth was analysed by two-way ANOVA with Bonferroni post hoc test; the Kaplan-Meier survival curve was analysed by long-rank (Mantel-Cox) test and long-rank test for trend. The SD is omitted for clarity in the graph of tumour growth. * $p < 0.05$. αPD-1 = anti-programmed cell death protein 1

5.1.3 Collagenase IV and DNase I for tumour tissue dissociation combined with positive CD45 magnetic separation as convenient methods to study MC-38 tumour infiltrating immune cells

To evaluate the tumour infiltrating immune cells, suitable methods for isolation of these cells had to be established. Firstly, two different buffers for tumour tissue dissociation were compared, the commercial one, tumour dissociation kit from Biotec and the classic combination for tissue dissociation, collagenase IV and DNase I. In the case of MC-38 tumours, the combination of collagenase IV and DNase I was more efficient. As a result, more $CD45^+$ cells with similar viability were isolated from the same tumour of one mice and the same amount of cells (**Fig. 9A**); however, the frequency of $CD45^+$ cells among live cells remained the same (**Fig. 9B**).

The tissue dissociation method alone was not sufficient to study the small fractions of immune cells. Therefore, the positive CD45 magnetic separation was tested. Importantly, more immune cells were obtained when CD45 magnetic separation was performed **(Fig. 9C**), and population frequencies differed (**Fig. 9D**). Especially, the amounts of certain immune cells, such as $CD8^+$ T lymphocytes producing IFN-γ, was increased (**Fig. 9E**). That enabled the precise analysis of small population subsets. Furthermore, besides the higher yield of immune cells, magnetic separation facilitates and ameliorates the data analysis since the positive populations are easier to separate (**Fig. 9F**).

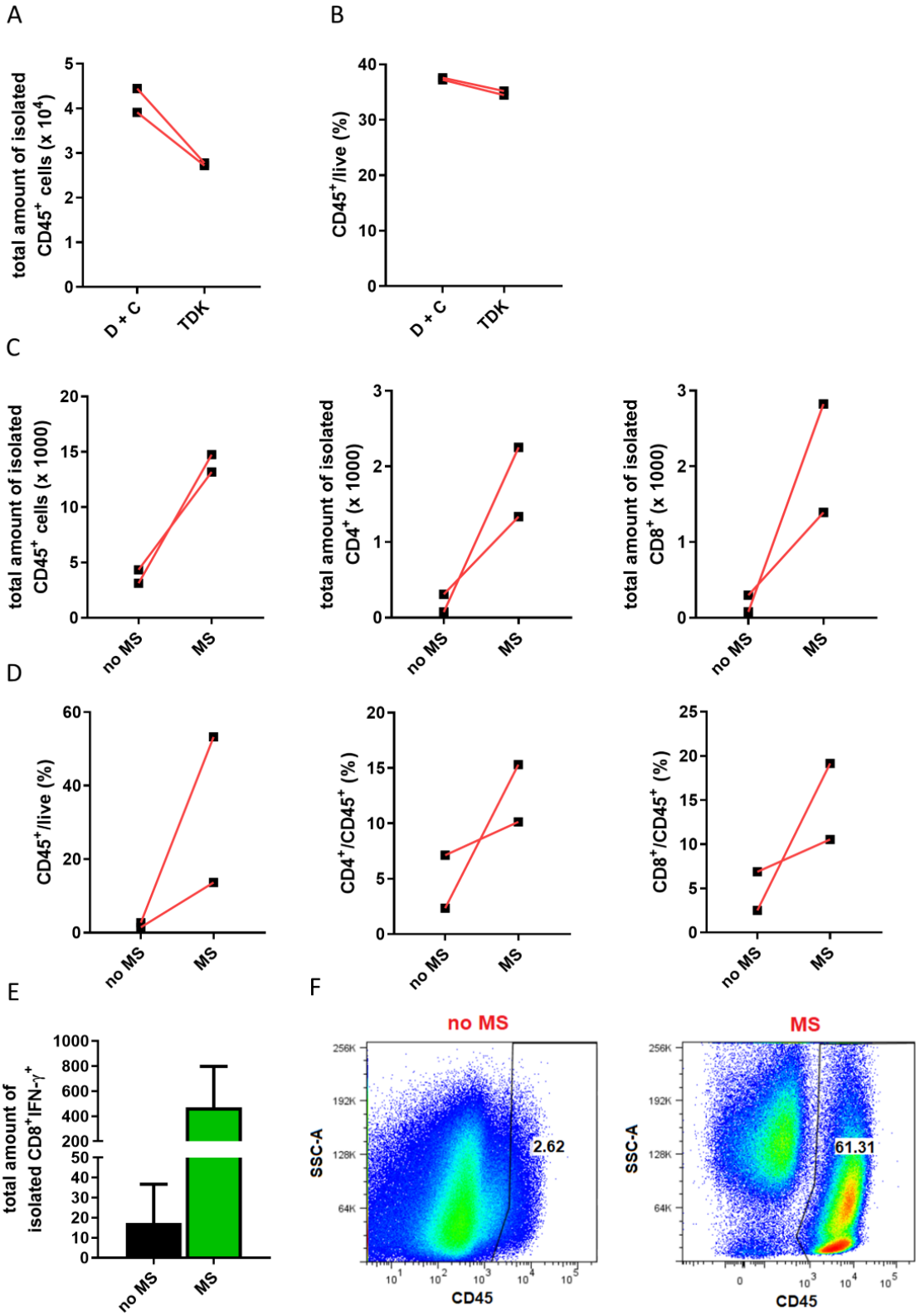

Figure 9 Establishment of methods for the analysis of tumour infiltrating immune cells. The MC-38 tumours (n= 2) were processed in two different ways, with a tumour dissociation kit (TDK) from Biotec or with collagenase IV + DNase I (C + D) buffer. The yield of $CD45^+$ immune cells (**A**) and their frequency among live (**B**) in both buffers were observed. The MC-38 tumours (n=2) were processed and either separated by CD45 positive magnetic separation (MS) or not (no MS). The yield (**C, E**) and frequency (**D**) of tumour infiltrating immune cells was measured. Additionally, the magnetic separation ameliorate date analysis from the flow cytometry (**F**). Experiment with DNase I and collagenase IV was done once, the experiments with magnetic separation twice; therefore, data presented are from one representative experiment out of 2. The difference between groups was analysed by paired two-tailed student´s t-test. Data are shown as mean ± SD.
CD = cluster of differentiation, IFN-γ = interferon gamma

5.1.4 Treatment by αPD-1 slows the MC-38 tumour growth; however, the immune mechanism remains unclear

The last set-up experiment aimed to test and ameliorate previously established methods, and experimental design, before more extensive experiments with microbiota manipulation would be performed. Mice were divided into two groups, αPD-1 treated and untreated. After 21 days, the immune response in the tumour was evaluated by flow cytometry. The treated mice had smaller tumour volumes after day 13; however, the tumour growth accelerated after day 19 (**Fig. 10A**). Therefore, to better see the effect of αPD-1 treatment, the following experiments were terminated on day 19. Decreased tumour weight in αPD-1 treated mice confirmed the tumour measurements (**Fig. 10B**). Overall infiltration of $CD45^+$ cells, $CD4^+$, and $CD8^+$ T cells into the tumour did not differ among groups. Therefore, the distinction of tumour growth is expected to be at the subpopulation levels of these cells. Additionally, slightly more Treg ($CD25^+$ Forkhead Box P3 $(FOXP3)^+CD4^+$) were observed in the tumours of the αPD-1 treated group (**Fig. 10C**).

The flow cytometry analysis did not reveal any possible explanations or mechanisms responsible for a more effective anti-tumour immune response in αPD-1 treated mice. Therefore, the Ab repertoire for flow cytometry was extended and divided into two panels in future experiments to study the immune cells in detail.

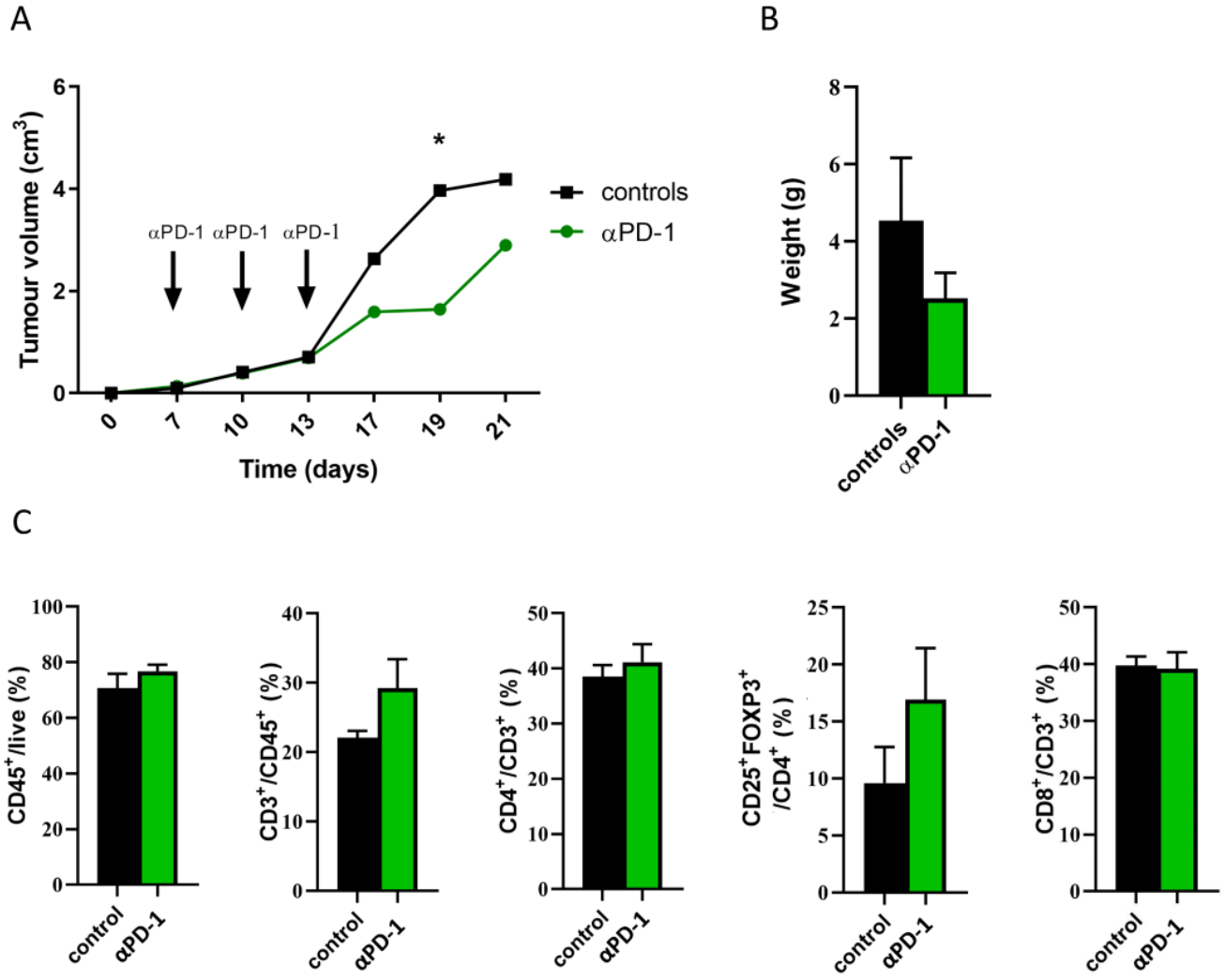

Figure 10 The effects of αPD-1 treatment on MC-38 tumour growth and immune response. Tumours of αPD-1 treated and untreated mice (n=7 per group) were processed and analysed by flow cytometry. The tumour growth was measured during the experiment (**A**), and tumours were weighted after experiment termination (**B**). The frequencies of tumour infiltrating immune cells were analysed by flow cytometry (**C**). The Experiment was performed once. The tumour growth was analysed by two-way ANOVA with Bonferroni post hoc test, the tumour weight and frequencies of immune cells by unpaired two-tailed student´s t-test. Data are shown as mean ± SD. The SD is omitted for clarity in the graph of tumour growth. * $p < 0.05$, αPD-1 = anti-programmed cell death protein 1, CD = cluster of differentiation, FOXP3 = Forkhead Box P3

5.2 Mice pre-treated with ATB and concomitantly administrated αPD-1 have reduced tumour growth

In the set-up experiments, we observed a reduction in the tumour growth after αPD-1 administration. Therefore, we wondered whether microbiota dysbiosis affects the αPD-1 therapy and what are the mechanisms responsible for it. The experiment was performed as depicted in **figure 11A**. The mice treated with ATB in addition to αPD-1 had smaller tumours than either these treated only with αPD-1 or controls. The αPD-1 mAb treatment alone did not affect the tumour growth in this experiment (**Fig. 11B**). Moreover, the tumour weight was even higher than in the controls. Interestingly, the αPD-1 + ATB group had considerably reduced tumour weight (**Fig. 11C**). The ATB treatment or decrease of specific bacteria that stimulate the IS caused a reduction in the weight of PP (**Fig. 11D**). The RT-qPCR analysis revealed that ATB treatment did not affect the total amount of bacteria in the gut and the amounts of SFB were slightly reduced in ATB treated mice, lactobacilli remained unchanged (**Fig. 11E**). To get more accurate results of bacterial changes after ATB treatment, the DNA isolated from the stool has been sequenced on the MiSeq platform at the CEITEC Genomics Core Facility (Brno, Czech Republic) recently, and the data is being processed.

The addition of ATB increased the production of various pro-inflammatory molecules in the PP (**Fig. 12A**). This was reflected in the MLN by a significant increase of activated ($CD80^+$) DC and ILC type 1 compared to controls and αPD-1 only treated groups (**Fig. 12B**). The activation of the adaptive IS was observed as well. Increased levels of $CD8^+$ T lymphocytes, especially CTL type 1, were detected in the MLN of the αPD-1 + ATB group (**Fig. 12C**). Additionally, $CD8^+$ cells together, probably with ILC type 1 and Mϕ, produce increased amounts of TNF-α **(Fig. 12D**).

The pro-inflammatory activation of IS was not gut-restricted and positively influenced the anti-tumour immune response. Enhanced expression of IFN-γ was in the tumour microenvironment of αPD-1 + ATB group detected, namely in $CD3^-$ cells, $CD4^+$ and $CD8^+$ T lymphocytes (**Fig. 13A**). This pro-inflammatory environment supports the infiltration of $CD3^+$ T lymphocytes, primarily $CD8^+$ T lymphocytes and the formation of Th1 and CTL type 1. This increased IFN-γ production may be responsible for slightly increased Mϕ frequencies in αPD-1 + ATB-treated group (**Fig. 13B**).

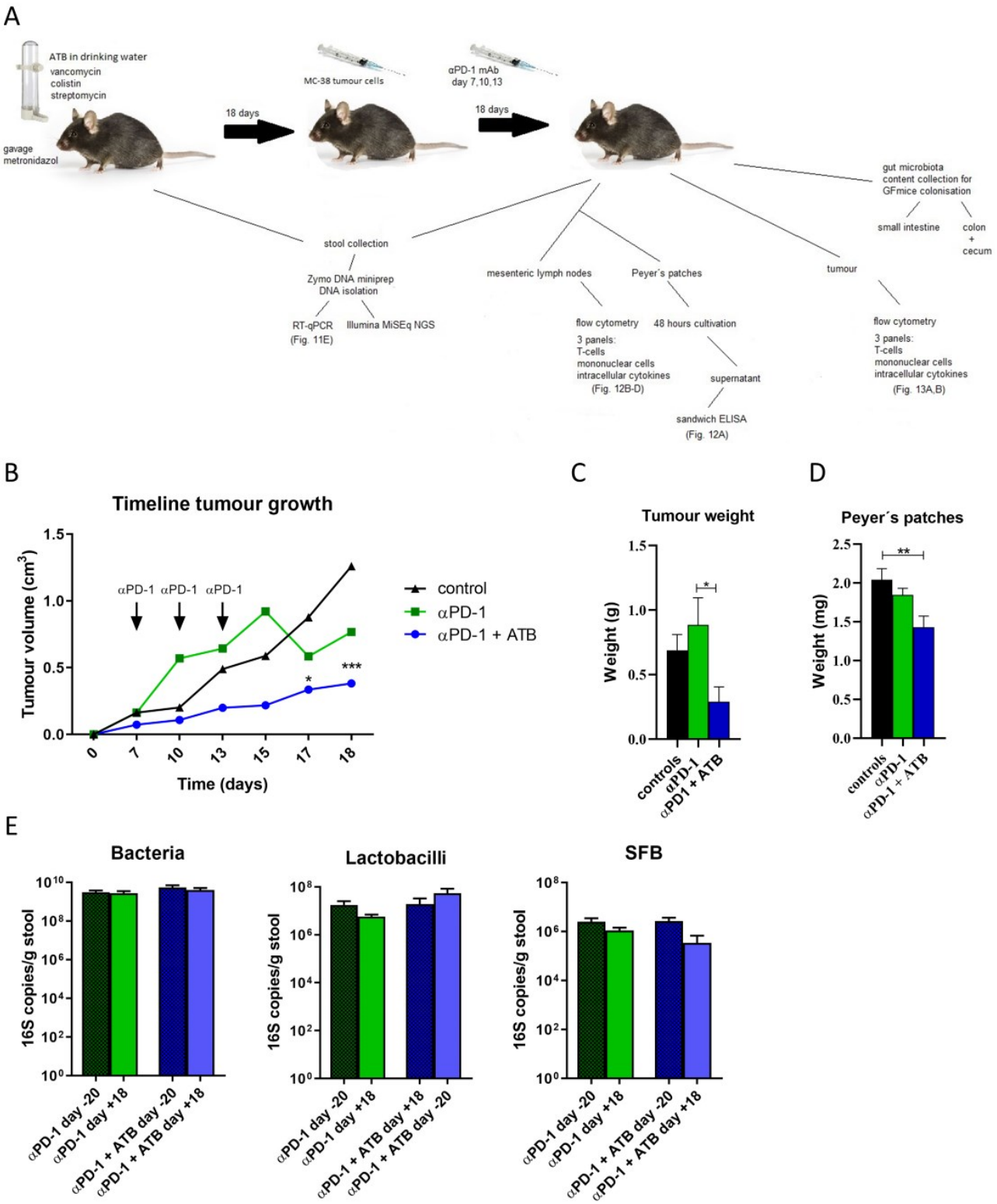

Figure 11 The effect of ATB on the αPD-1 treatment of MC-38 tumours. The experiment consisted of 3 groups, controls, αPD-1 or αPD-1 + ATB treated mice (n=7 per group) and was performed according to experimental layout (**A**). The tumour growth was measured during the experiment (**B**). Tumours (**C**) and PP (**D**) were weighted after experiment termination. The total amount of bacteria, Lactobacilii and SFB DNA was quantified by RT-qPCR (**E**). The experiment was performed once. The tumour growth and total amount of bacteria were analysed by two-way ANOVA with Bonferroni post hoc test, the tumour and PP weight was analysed by one-way ANOVA with Tukey´s post hoc test. Data are shown as mean ± SD. The SD is omitted for clarity in the graph of tumour growth. * $p < 0.05$, ** $p < 0.01$; *** $p < 0.001$, αPD-1 = anti-programmed cell death protein 1, ATB = antibiotics, ELISA = Enzyme-linked immunosorbent assay, GF = germ free, mAb = monoclonal antibody, RT-qPCR = quantitative reverse transcription polymerase chain reaction SFB = segmented filamentous bacteria

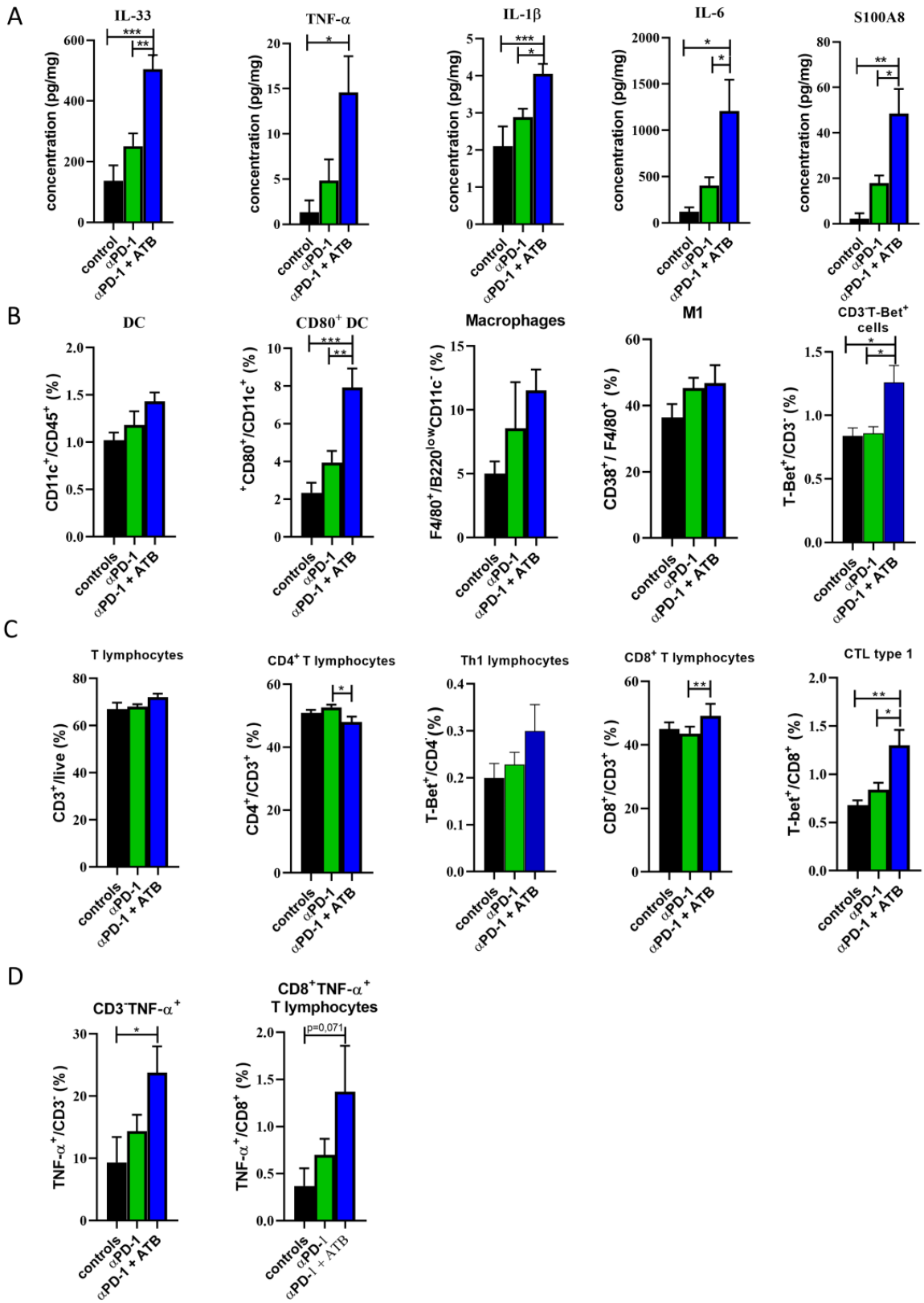

Figure 12 The immune response in the gut. The cytokine production after 48 hrs cultivation of PP was measured by ELISA (**A**). The innate (**B**) and adaptive (**C**) immune response in the MLN was measured by flow cytometry directly on the day of experiment termination. The cytokine expression was evaluated by flow cytometry after 12 hrs of anti-CD3/anti-CD28 + 4 hrs with brefeldin + monensin stimulation (**D**). Experiment was performed once. The frequencies of immune cells were analysed by one-way ANOVA with Tukey´s post hoc test. Data are shown as mean ± SD. * $p < 0.05$, **$p < 0.01$; *** $p < 0.001$, αPD-1 = anti-programmed cell death protein 1, ATB = antibiotics, CD = cluster of differentiation, CTL = cytotoxic T lymphocytes, DC = dendritic cells, IL = interleukin, M1 = type 1 macrophages, T-bet = T box expressed in T cells, Th = T helper, TNF-α = tumour necrosis factor-alpha

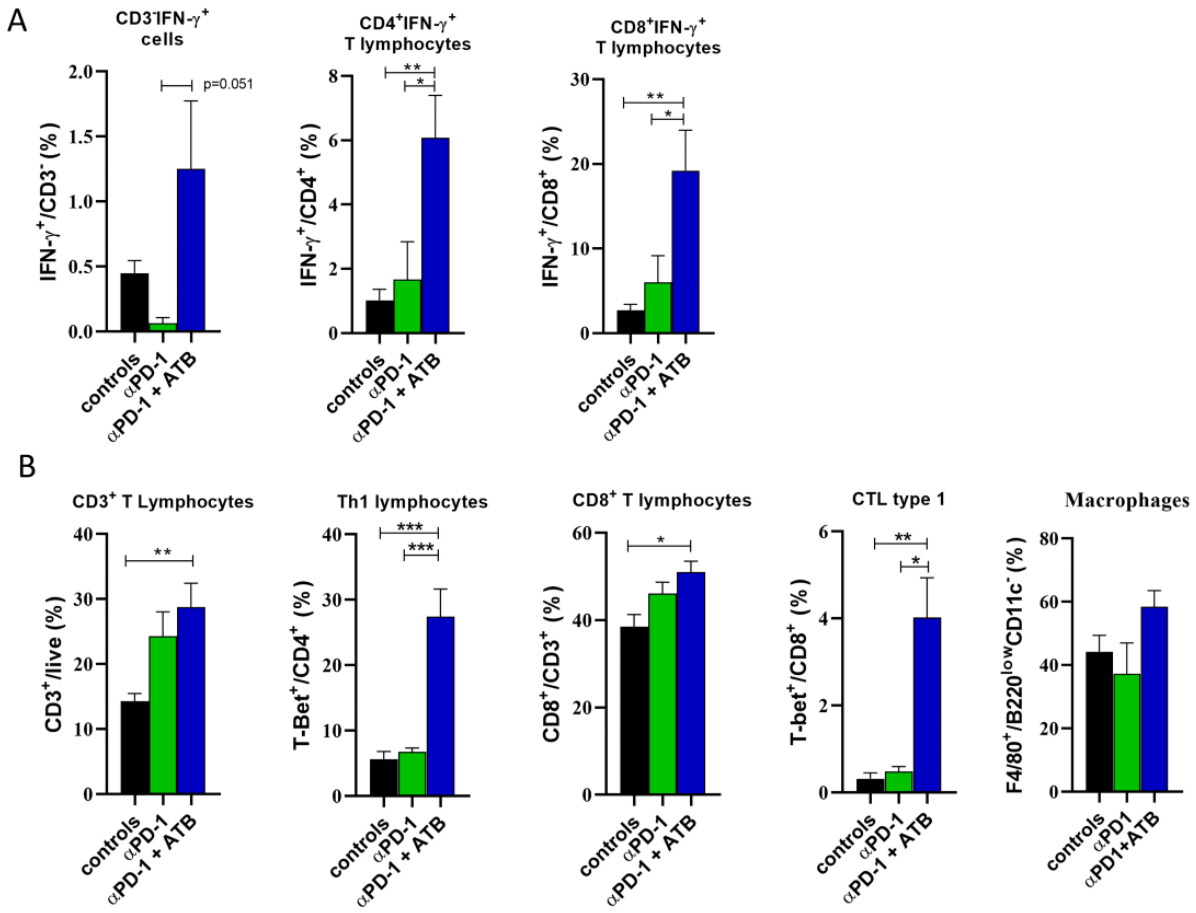

Figure 13 The immune response in the tumour. Flow cytometry analysis of 12 hrs anti-CD3/anti-CD28 + 4 hrs brefeldin + monensin stimulated cells from tumour microenvironment (**A**). The immune response in the tumour was analysed on the day of experiment termination (**B**). Experiment was performed once. The frequencies of immune cells were analysed by one-way ANOVA with Tukey´s post hoc test. Data are shown as mean ± SD. * $p < 0.05$, **$p < 0.01$; *** $p < 0.001$, αPD-1 = anti-programmed cell death protein 1, ATB = antibiotics, CD = cluster of differentiation, CTL = cytotoxic T lymphocytes, IFN-γ = interferon gamma, T-bet = T box expressed in T cells,Th = T helper

5.3 Gut microbiota transfer concomitantly with αPD-1 administration causes tumour growth reduction

In the previous experiment, we saw that the anti-tumour immune response was positively influenced in the αPD-1 + ATB treated group. We wondered whether this was the effect of shifted microbiota, ATB administration or both together. Therefore, the mice were colonised with the gut microbiota from the previous experiment. The mice part of the experiment was performed as described in the methods (4.2.2), and the overall experimental design is depicted in **figure 14A**. Mice were divided into two groups. Mice colonised by microbiota from αPD-1 + ATB treated group were marked as R. NR were colonised by microbiota from the αPD-1 treated group. R had smaller tumours during the measurements with the highest tumour size difference on the day of experiment termination compared to NR (**Fig 14B**). The tumour weight (**Fig. 14C**), although not significantly, was decreased in R (**Fig. 14D**). PP of R were heavier, suggesting enhanced stimulation of the mucosal IS (**Fig. 14E**). The R had a higher abundance of lactobacilli and SFB (**Fig. 14F**), which agrees with the previous data from sequencing of bacterial DNA from the stool of mice treated with the same ATB mix (Stehlikova et al., 2019). To get more detailed information about the gut microbiota composition, DNA from the stool of these mice has been sequenced on the MiSeq platform at the CEITEC Genomics Core Facility (Brno, Czech Republic) recently. Bioinformatics is processing these data.

Next, the immune response in the gut was analysed. No significant changes in the cytokine production in the PP were observed (**Fig. 15A**). The pro-inflammatory cytokines, TNF-α and IFN-γ, were elevated in the MLN of R (**Fig. 15B**). The frequencies of immune cells did not show any difference (data not shown) except for $CD3^-$ retinoic-acid-receptor-related orphan receptor gamma $(ROR\gamma t)^+$ cells and a slight increase of DC and activated DC in the R group (**Fig. 15C**). No difference in adaptive immune response was observed among the groups; however, the IL-2 was increased in the R group (**Fig. 15D**). Next, the colon's cytokine production was analysed to observe whether the shifted microbiota influences the immune reactions in the colon. There was no significant difference in this department (**Fig. 15E**).

To observe systemic immune response, spleen analysis was included in the experiment. It seems that the systemic immunity is shifted into type 17 immune response. Elevated levels of Th17 lymphocytes and $CD8^{+}PD\text{-}1^{+}$ T lymphocytes in the R group were detected (**Fig. 16A**). Cells stimulated with anti-CD3/anti-CD28 from the spleen of R mice were more prone to secrete IL-17 than these cells from NR (**Fig. 16B**). Interestingly decreased frequencies of activated DC were observed in the spleen of R (**Fig. 16C**). The type 17 immune response was reflected within the tumour as well by the production of IL-17 from $CD4^{+}$, $CD8^{+}$ and $CD3^{-}$. Additionally, R showed increased infiltration of $CD3^{+}$ T lymphocytes and slight enhancement of $CD4^{+}IFN\text{-}\gamma^{+}$ in the tumour microenvironment of R (**Fig. 16D**).

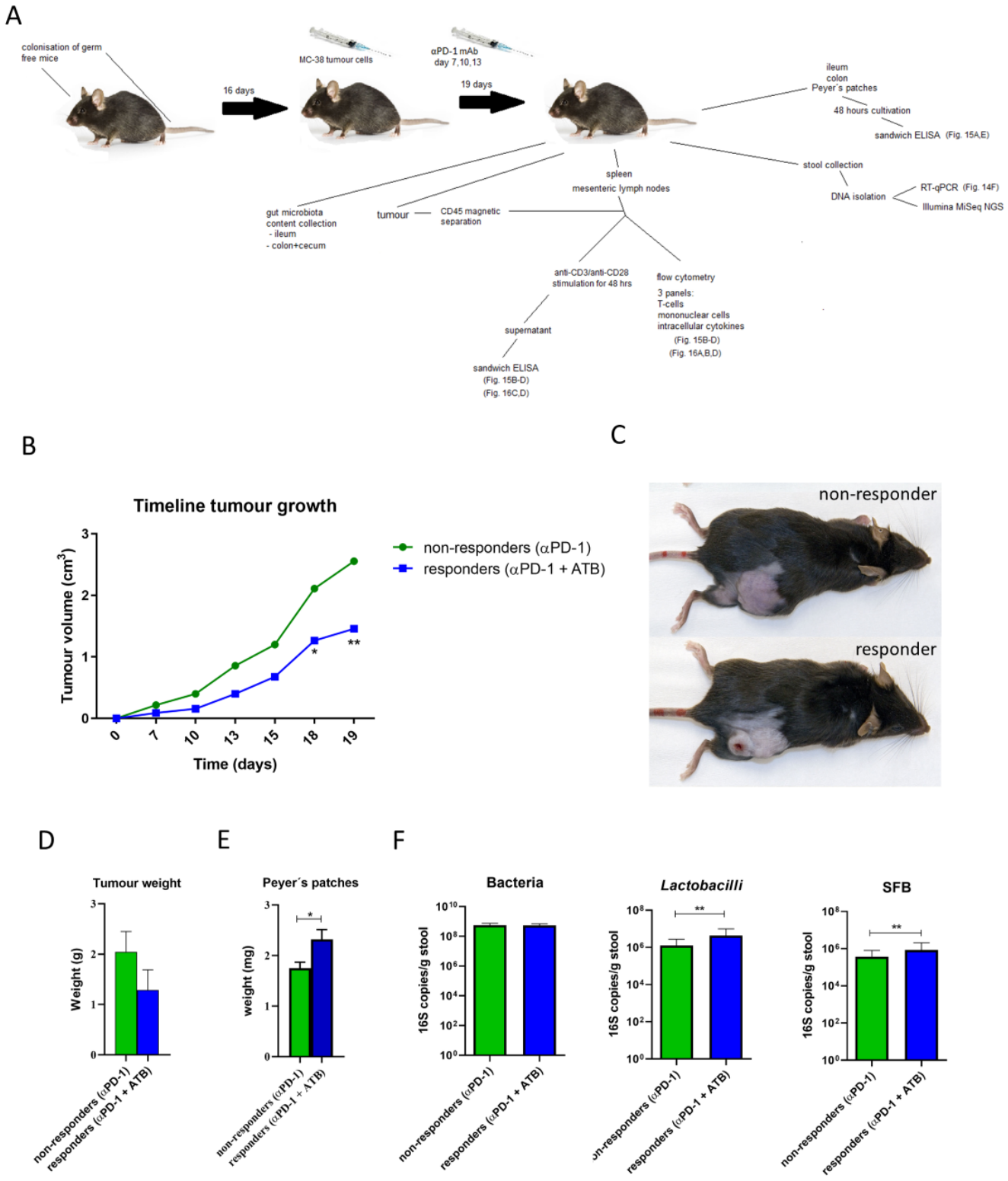

Figure 14 The effect of gut microbiota transplantation combined with αPD-1 treatment on the MC-38 tumours growth. The experiment consisted of 2 groups; GF mice were colonised by microbiota either from αPD-1 or αPD-1 + ATB group from the previous experiment (n=9 per group). The experiment was performed according to the experimental layout (**A**). The tumour growth was measured during the experiment every 2-3 days (**B**) and the tumours were photographed at the end of experiment (**C**). Tumours (**D**) and PP (**E**) were weighted after experiment termination. The total amounts of bacteria, Lactobacilli and SFB DNA, was quantified by RT-qPCR (**F**). The experiment was performed once. The tumour growth and total amount of bacteria were analysed by two-way ANOVA with Bonferroni post hoc test, the tumour and PP weight was analysed by unpaired two-tailed student´s t-test. Data are shown as mean ± SD. The SD is omitted for clarity in the graph of tumour growth. * $p < 0.05$, ** $p < 0.01$; αPD-1 = anti-programmed cell death protein 1, ATB = antibiotics, CD = cluster of differentiation, ELISA = enzyme-linked immunosorbent assay, mAb = monoclonal antibody, RT-qPCR = quantitative reverse transcription polymerase chain reaction SFB = segmented filamentous bacteria

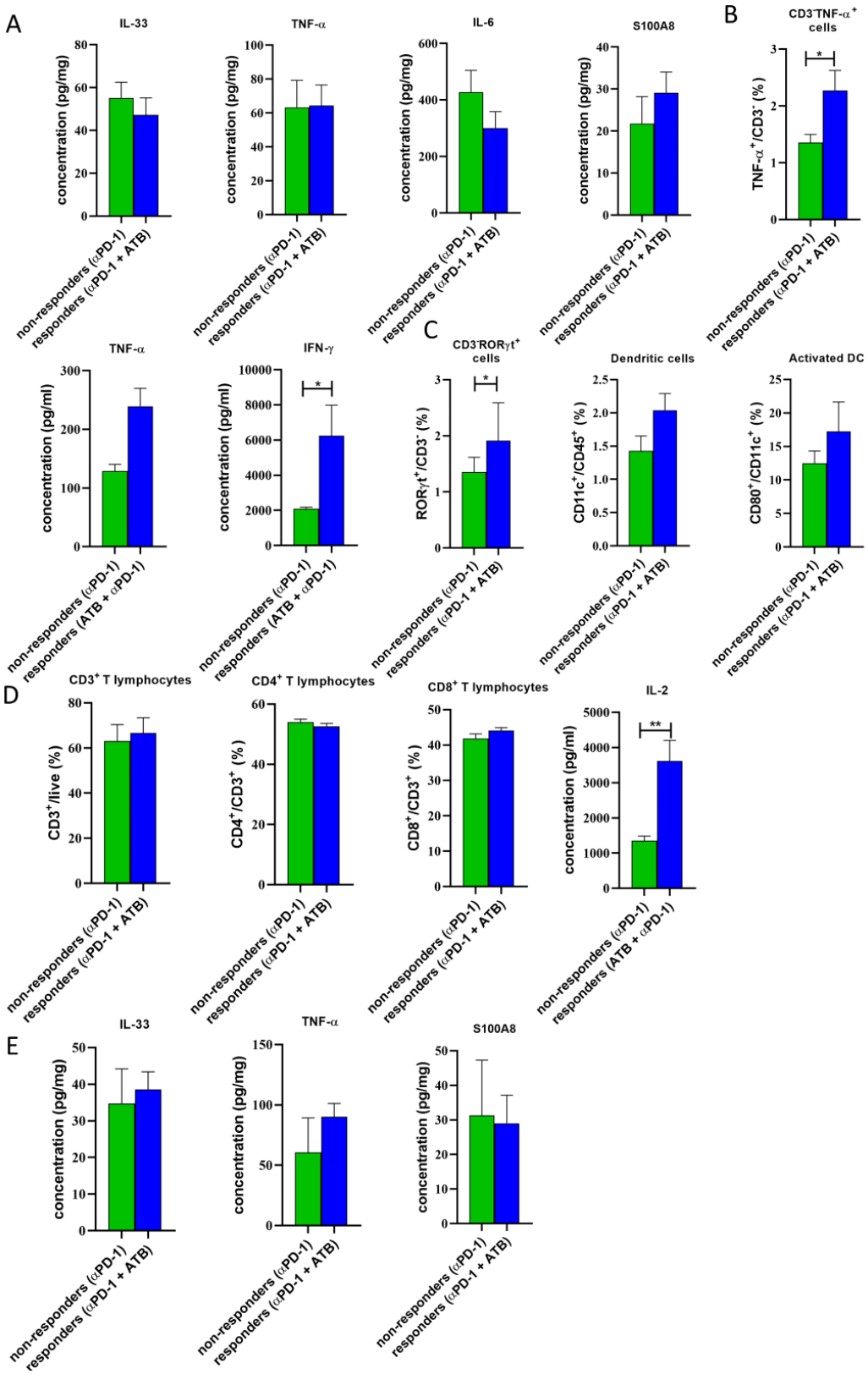

Figure 15 Immune response in the PP and MLN. The cytokine production after 48 hrs cultivation of PP was measured by ELISA (**A**). The immune response in the MLN was evaluated by ELISA, which was performed from the supernatant of MLN cell suspension after anti-CD3/anti-CD28 stimulation for 48 hrs. The flow cytometry was performed either on the day of experiment termination or after 12 hrs anti-CD3/anti-CD28 + 4 hrs brefeldin+ monensin stimulation (**B-D**). Next, the cytokine production was evaluated from the supernatant of colon biopsy after 48 hrs cultivation (**E**). The frequencies of immune cells were analysed by unpaired two-tailed student´s t-test. Data are shown as mean ± SD. * $p < 0.05$, ** $p < 0.01$, αPD-1 = anti-programmed cell death protein 1, ATB = antibiotics, CD = cluster of differentiation, DC = dendritic cells, IL = interleukin, IFN-γ = interferon gamma, Rorγt = retinoic-acid-receptor-related orphan receptor gamma TNF-α = tumour necrosis factor-alpha

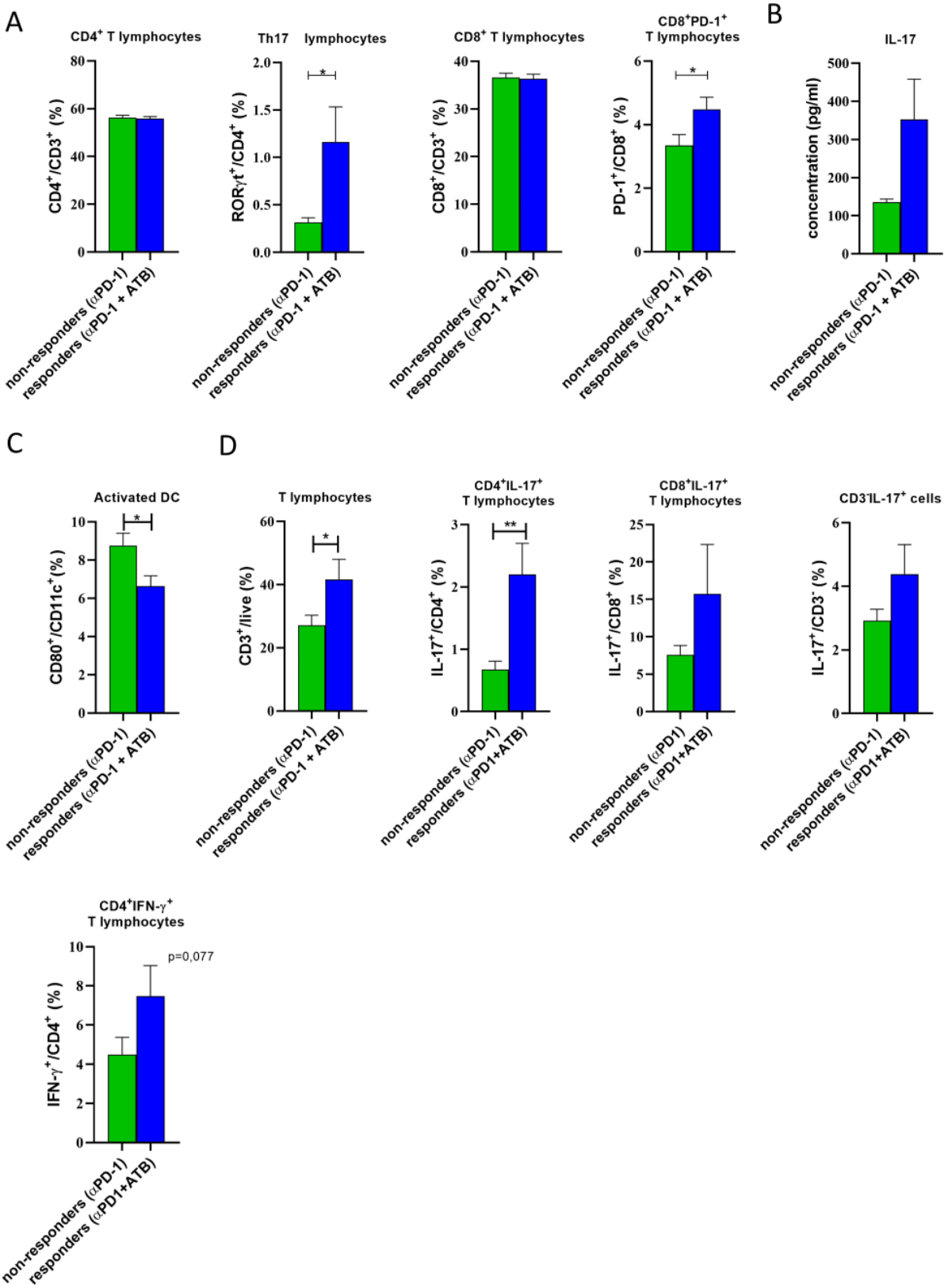

Figure 16 Immune response in the spleen and tumour. Flow cytometry analysis of adaptive immune response in the spleen (**A,C**). IL-17 detection from the supernatant of 48 hrs anti-CD3/anti-CD28 stimulated splenocytes by ELISA (**B**). Immune response in the tumour was evaluated either by flow cytometry analysis on the day of experiment termination or after 12 hrs of anti-CD3/anti-CD28 + 4 hrs brefeldin + monensin stimulation (**D**). The frequencies of immune cells were analysed by unpaired two-tailed student´s t-test. Data are shown as mean ± SD. * $p < 0.05$, ** $p < 0.01$, αPD-1 = anti-programmed cell death protein 1, ATB = antibiotics, CD = cluster of differentiation, DC = dendritic cells, IL = interleukin, IFN-γ = interferon gamma, PD-1 = programmed cell death protein 1, Th = T helper

6 Discussion

Gut microbiota significantly influences not only anti-tumour immune response (Iida et al., 2013; Sivan et al., 2015), but also fundamentally changes responsiveness to certain cancer therapies, such as chemotherapeutic (Daillère et al., 2016; Viaud et al., 2013) and immunotherapeutic drugs (Iida et al., 2013; Paulos et al., 2007). ICI are successfully used to treat various cancers; however, the responsiveness among patients with the same diagnosis differ (Gopalakrishnan et al., 2018; Routy et al., 2018). This master thesis shows a link between gut microbiota and αPD-1 mediated anti-tumour immune response, which is transferable through colonisation of GF mice by gut microbiota. Next, it describes key molecules and immune cells responsible for effective anti-tumour immune response. Moreover, it challenges the generally accepted view of negative impact of ATB on αPD-1 ICI treatment and proposes that this incongruence is due to the variability of colonizing microbes of each individual.

The influence of the gut microbiota may be mediated through a specific organism or the whole consortium (Mager et al., 2020; Tanoue et al., 2019). Since the microbial diversity is enormous and the importance of microbiota has been overlooked for a long time, many mechanisms underlying the responsiveness to ICI associated with gut microbiota composition need to be discovered. Therefore we started to study the effect of gut microbiota on ICI treatment in mice bred at the facility at the Institute of Microbiology of the CAS v.v.i. The breeding facility and its breeding conditions, such as diet, contribute significantly to microbiota composition (Sivan et al., 2015) and might explain different observations among research groups.

Firstly, the convenient mice model had to be established. The MC-38 tumour cell line was chosen for its high PD-L1 expression and high immunogenicity with elevated T cell infiltration into the tumour (Okada et al., 2020). In the first place, we had to choose the counting formula for tumour volumes to avoid easy data distortion. We ended up using the most suitable method, the modified ellipsoid formula (length × width × width)/2 (Tomayko & Reynolds, 1989), however always having in mind that the observations might be misleading because two widths are counted instead of one height, and the width is not always the same as the height. Additionally, the tumours may also differently grow on the other side towards the

peritoneum, and consequently this part may not be counted correctly. Therefore, the most reliable method is the tumour weighing at the end of the experiment.

We decided to inoculate 0.5×10^6 MC-38 tumour cells per mice since the tumours were measurable on day 7, when αPD-1 therapy starts, in contrast with 0.25×10^6 and 0.1×10^6. Importantly, the mice survival was not excessive, allowing easier observation of survival changes related to therapeutic interventions. Furthermore, the higher amount, 1×10^6 of inoculated MC-38 cells, did not differ from 0.5×10^6 administration and additionally, the lower amount of inoculated cells gives space for a more robust immune response (Juneja et al., 2017).

Since the amount of effective αPD-1 doses differ among the researcher groups (da Fonseca-Martins et al., 2019; Juneja et al., 2017), the efficiency of different amounts was tested. The administration of 200 μg of αPD-1 mAb on day 7, 10 and 13 was chosen, according to Juneja et al. (2017), since this schedule was tested on the 0.5×10^6 MC-38 tumours with 100% tumour clearance. While 200 μg of αPD-1 is commonly used amount, we also tested 50 μg and 12.5 μg of αPD-1 in order to titrate the responsiveness to ICI and to leave space for microbiota-driven improvement or impairment of the anti-tumour immune response. However, only 200 μg of αPD-1 resulted in reduced tumour growth. The survival rate was not affected; it is expected that repeated administration would be needed to affect the survival positively (Agrawal et al., 2016). Nevertheless, for our type of experiment was the reduction in tumour growth, reflecting improved anti-tumour immune response, more important. The survival rate could have been improved by modifying the therapeutic approach to keep newly recruited T cells protected (Agrawal et al., 2016).

Next, we compared collagenase IV + DNase I and tumour dissociation kit from Biotec for processing of the tumour tissues. Both methods are commonly used for MC-38 tumour tissue processing (Beyrend et al., 2019; Taylor et al., 2019). We did not see any difference in the viability of $CD45^+$ cells while using the collagenase IV + DNase I or tumour dissociation kit from Biotec. Nevertheless, collagenase IV + DNase I enabled us to obtain higher yields of immune cells than the tumour dissociation kit; therefore, we decided to use it in future experiments. The possible issue with all these methods using proteolytic enzymes may be the loss of extracellular markers during tumour processing, which may affect the flow cytometry results (Autengruber et al., 2012). However, neither method resulted in the major populations losses (data not shown), which agrees with Autengruber et al. (2012), who showed that

collagenase IV has only minor effects on the surface molecules when the cells are directly processed after enzymatic digestion.

Although MC-38 tumours are marked as “hot tumours” (Efremova et al., 2018), we were unable to harvest sufficient amounts of immune cells, and therefore we tested positive magnetic separation to increase the yields of immune cells (G. Wang et al., 2017). The amounts of immune cells were remarkably higher when magnetic separation of $CD45^+$ cells was performed. Moreover, magnetic separation removes many tumour cells and dead cells, and therefore the flow cytometry analysis is easier and more precise.

In the next experiment, the efficiency of 200 μg of αPD-1 was confirmed to slow the tumour growth. However, our dosing schedule seems to be limited in time as the tumour growth accelerated even in the αPD-1 treated mice approximately one week after the last dose. A slight elevation of $CD25^+FOXP3^+$ Treg was observed in the αPD-1 treated group. There is constant cancer immunoediting, and over time more immune cells are exhausted and express their inhibitory molecules on their surface, and more immunosuppressive cells are present in the tumours (Dunn et al., 2004). The αPD-1 treatment may have boosted the $PD\text{-}1^+CD25^+FOXP3^+$ Treg resulting in increased immunosuppression (Kamada et al., 2019). Therefore, we added PD-1 Ab to the flow cytometry panel to analyze this in the subsequent experiments. Additionally, to avoid the tumour escape, we decided to terminate the future experiments earlier, on day 19, to see the immune-related changes by αPD-1 administration.

For the gut microbiota manipulation already well-established ATB mixture was used to disrupt the gut microbiota homeostasis (Stehlikova et al., 2019; Zákostelská et al., 2016). Colistin (against G-), streptomycin (against G+ and G-) and vancomycin (against G+) were in the drinking water. Metronidazole (against anaerobes G+ and G-) was gavaged three times a week. The decrease of SFB in the ATB treated mice is consistent with the previous experiments performed in our laboratory (Stehlikova et al., 2019).

The observation that ATB administration concomitantly with αPD-1 treatment causes reduction in the tumour growth was quite surprising and rather unexpected. Since ATB administration causes dysbiosis and many previous studies linked ATB administration as a negative prognostic marker not only in mice experiments (Iida et al., 2013; Routy et al., 2018) but also in human patients (Routy et al., 2018; Xu et al., 2020). Notably, the mice microbiota composition differs among breeding facilities (Sivan et al., 2015), and the different ATB

mixtures have a diverse effect on gut microbiota (He et al., 2019), which may explain the different results among the scientific groups.

ATB treatment combined with αPD-1 resulted in the elevation of various pro-inflammatory molecules in the PP. These cytokines are products of cells of innate immunity and non-immune cells, which as a result, lead to the activation of adaptive immunity later. Increase in IL-33 may not be strictly associated with Th2 immune response, as this pleiotropic cytokine can also induce Th1 immune response (F. Alvarez et al., 2019). IL-33 is stored in the nucleus of epithelial barrier tissues and lymphoid organs (Pichery et al., 2012), once the cells die, IL-33 is released, and immune cells get activated (F. Alvarez et al., 2019). IL-33 increases the production of IL-1β, TNF-α and IL-6 in mouse Mϕ in response to LPS (Espinassous et al., 2009), which could have happened in this experiment. Another inducer of inflammation is a DAMP molecule S100A8, which is constitutively expressed by myeloid cells and can be induced in monocytes, endothelial and epithelial cells (Srikrishna, 2011). An increase of S100A8 in the PP contributes to the inflammation. S100A8 is actively or passively released in response to environmental stimuli or damage, and triggers inflammation, promotes phagocytes migration, binds to RAGE or TLR4 and induces expression of IL-1β and IL-6 (Simard et al., 2013). As a result of the inflammatory immune response, activated ($CD80^+$) DC accumulate in the MLN and activate $CD8^+$ T cells into ($CD8^+$T-Bet^+) CTL type 1 under the pro-inflammatory conditions, such as in the presence of TNF-α. However, the TNF-α production may not be independent, and probably other cytokines, such as IL-12 (Gao et al., 2019), contribute to the pro-inflammatory immune response in the gut.

Not microbial load, but a shift in microbiota leads to the pro-inflammatory effects. Eradication of some bacteria could give antibiotic-resistant bacteria chance to overgrow the sensitive ones, or elimination of certain immunosuppressive bacteria resulted in the enhanced pro-inflammatory immune responses (Neuman et al., 2018). This elevation could be a result of specific bacteria (Mager et al., 2020) or the whole bacterial network of relationships (Tanoue et al., 2019). These gut microbiota changes have distinct consequences on the tumour growth.

The link between the gut and distant tumours remains mostly poorly explained, although this is crucial information. The possible mechanisms of action are: the presence of certain bacteria that stimulate the IS against tumour neoantigens (Balachandran et al., 2017; Sivan et al., 2015; Vétizou et al., 2015), bacterial metabolites that directly or indirectly affect

the anti-tumour immune response (C. Ma et al., 2018; Mager et al., 2020) or bacterial translocation which induces inflammation and the immune cells are more prone to eradicate the tumours (Viaud et al., 2013) or even the bacteria themselves migrate to the tumour tissue (Riquelme et al., 2019). Another possibility is that the presence of certain bacteria stimulates the immune cells, which then migrate through the systemic circulation (McAleer et al., 2016). The elucidation of the mechanism is the next step of this research project.

Strong type 1 immunity with IFN-γ production is associated with reduced tumour growth in ATB + αPD-1 treated mice. Because IFN-γ affects the Mϕ (DeNardo & Ruffell, 2019), their levels within the tumour were also elevated, however not significantly. We tried to elucidate whether they were M1 type; however, only a tiny amount of tumour-infiltrating Mϕ expressed CD38, the marker for type 1 Mϕ (Jablonski et al., 2015). Induction of type 1 immune response within the tumour by gut microbiota modulation was previously shown when the administration of αCTLA-4 to mice colonised with *B. pseudolongum* elevated anti-tumour immunity through robust induction of type 1 immune response accompanied by the production of IFN-γ in T cells. The pro-inflammatory effects are gut-restricted without ICI (Mager et al., 2020). Colonization of the gut with simple consortium of 11 bacterial strains can induce IFN-γ production in the tumour that leads to remarkably enhanced anti-tumour immunity as well (Tanoue et al., 2019).

In our experiment, administration of αPD-1 alone did not decrease tumour growth; however, there was a slight elevation of various pro-inflammatory molecules and immune cells in this group. The remarkable anti-tumour effect is observed only in ATB + αPD-1 treated mice and since new colleague Anietie Udoumoh DVM., PhD. started to work on the same project and repeated the experiment two more times[7] also with ATB only treated group, he proved that αPD-1 + ATB treated mice show the most notable slowing of tumour growth, while tumours in αPD-1 treated mice have only modest reduction and ATB alone does not affect the anti-tumour immune response (Fig. S1). However, as he was the responsible person for that experiments and did all the work, these data are not presented in this master thesis.

[7] My experiment was the first big tumour experiment performed in our lab and therefore, the need for magnetic separation, change of the Ab for NK cell distinction by flow cytometry and addition of ATB only treated group was revealed in order to generate more reliable results. Since the mice part of this experiment takes around five weeks and the subsequent analysis even longer, I could perform this experiment only once. However, I suggested and tested all the improvements before the next experiments were performed by my colleague.

The question is, what may be the mechanism behind the interplay of altered microbiota and αPD-1. The αPD-1 blockade may have limited the protective functions of the intestinal epithelial cells, which express PD-L1 (Scandiuzzi et al., 2014). Additionally, αPD-1 protects the activated immune cells against PD-L1$^+$ immunosuppressive cells in various departments and against PD-L1$^+$ tumour cells, whose levels are even increased in the presence of IFN-γ (Juneja et al., 2017). This favours the pro-inflammatory immune response; however, the blockade alone is not as effective if compared with ATB administration/shifted microbiota. It can be expected that microbiota shift, maybe concomitantly with ATB effects, increases the activation of various immune cells, which in reaction elevate the expression of PD-1, and because αPD-1 mAb blocks these inhibitory molecules, the activities of PD-1$^+$ cells are not limited. The positive effect of ATB + αPD-1 combination on the anti-tumour immune response was shown previously by Pushalkar et al. (2018), administration of oral ATB (amphotericin + metronidazole + neomycin + vancomycin) caused elevation of PD-1 expression on CD3$^+$ T cells entering the tumour, and if ATB mix was combined with αPD-1, the anti-tumour immunity was effective. To evaluate the PD-1 expression in my experiment, I added the PD-1 Ab for flow cytometry to the panel. When the GF mice were colonised by gut microbiota from ATB + αPD-1, they had elevated levels of PD-1$^+$CD8$^+$ T cells in the spleen, which supports the idea, that gut microbiota composition affects the activation of immune cells or the expression of PD-1; therefore, αPD-1 mAb protects these activated cells.

Next, we hypothesised how and if ATB administration might contribute to the observed pro-inflammatory immune response. ATB might be a source of damages and apoptosis of intestinal cells in the gut, which might be accompanied by a release of DAMPs (Konstantinidis et al., 2020) or translocation of bacteria (Knoop et al., 2016; Paulos et al., 2007) and that may lead to the inflammation. Moreover, ATB can cause bacterial death in an inflammatory manner due to the release of PAMPs such as lipopolysaccharides or peptidoglycans (Wolf et al., 2017), which directly activate PRR and induce the whole cascade of pro-inflammatory cytokines. Additionally, the type of ATB affects the activation of the IS; for example, vancomycin-treated bacteria are more susceptible to killing by Mϕ if compared with other ATB (Wolf et al., 2011). To test the need of ATB administration for the full anti-tumour immune response, we colonised GF mice with the microbiota from αPD-1 + ATB and αPD-1 treated mice.

When microbiota from ATB-treated mice was transferred to GF mice, we observed mixed type 1 and 17 immunity, which is a different pattern of immune response compared to

ATB-treated mice, where we detected type 1 immune response. Therefore, ATB administration may affect the immune response as well. Nevertheless, both experiments resulted in a more effective anti-tumour immune response accompanied by reduced tumour growth. Several mechanisms can explain the difference between both experiments. Firstly, the IS of GF mice is altered due to the absence of microbes that contribute to the development and stimulation of the IS (Round & Mazmanian, 2009). Next, ATB administration may affect the immune response (Wolf et al., 2011) or gut microbiota transplantation to the GF mice, which possess a free niche, allows creating a new community with altered interactions (Lozupone et al., 2012). Alternatively, the absence of ATB pressure allows certain bacterial species to grow and dominate (Palleja et al., 2018).

The administration of vancomycin kept SFB suppressed (McAleer et al., 2016), but once the ATB pressure relented after the transfer into GF mice, the amounts of SFB have increased. This increased SFB could subsequently trigger type 17 immune response (Ivanov et al., 2009) not only in the intestine but also at the systemic level resulting in decreased tumour growth. SFB are known to stimulate the development of Th17 lymphocytes, which can subsequently migrate to the systemic circulation and therefore can be present in the spleen (Yang et al., 2014) or even tune the immune response in the lungs (McAleer et al., 2016). Therefore Th17 might have migrated to the tumours as well.

The *Lactobacillus* genus contains members of both resistant and susceptible to streptomycin or vancomycin (Klare et al., 2007), therefore similarly as in the case of SFB, when ATB pressure vanished, certain lactobacilli may have overgrown. Lactobacilli are generally known as beneficial and protective bacteria, which decrease inflammation predominantly through Treg formation (Jang et al., 2012); however, some strains can induce Th1 immune response accompanied by the production of TNF-α, IFN-γ, IL-12 and other pro-inflammatory cytokines in immune cells (Ding et al., 2017). This pro-inflammatory effect of lactobacilli may contribute to the mixed type 1 and 17 pro-inflammatory immune responses in the gut of R.

Unexpectedly there is no noticeable elevation of pro-inflammatory cytokines produced in PP after 48 hrs cultivation, although this should be the starting point of IS activation, and SFB attach to the ileal mucosa where they directly stimulate the IS. Additionally, SFB preferentially adhere to follicle associated epithelium of PP (Jepson et al., 1993; Lécuyer et

al., 2014). However, these bacteria can induce non-specific Th17 immune response in mice lacking organised gut lymphoid tissue suggesting the capacity of SFB to stimulate multiple intestinal inductive sites, such as isolated lymphoid follicles (Lécuyer et al., 2014).

A slight reduction of IL-33 in PP of R may contribute to an increase of amounts and unrestricted properties of SFB since IL-33 deficient mice have elevated levels of SFB (Malik et al., 2016). A decrease of IL-6 in PP of R is unexpected because IL-6 is crucial for induction of Th17 immune response and inhibition of Treg formation (Korn et al., 2008). Additionally, SFB promote the expression of serum amyloid A, which can induce the production of IL-6 (Ivanov et al., 2009; W. Li et al., 2017). Levels of S100A8 in the presence of SFB can increase due to enhanced ROS production caused by SFB attachment (Cheng et al., 2019).

Geem et al. (2014) have not observed Th17 enrichment in the MLN of SFB colonised mice, and therefore they suggest that Th17 differentiate in situ, which is in concordance with my observation where no increased levels of Th17 in the MLN were detected. Since the pro-inflammatory environment (IFN-γ and TNF-α) in the MLN is also linked to type 1 immune response, the involvement of other bacteria in the activation of the IS is expected. The increased levels of TNF-α in R are in agreement with the observation that the presence of TNF-α indirectly, however relevantly, contribute to IL-17 expression in $CD4^+$ T cells (Sugita et al., 2012; Y. Zheng et al., 2014), which can be lately seen within the spleen and tumour. Elevated levels of IFN-γ may contribute to the increased activation of DC in the MLN of R as it was shown that IFN-γ together with TLR stimulus enhances activation and functions of DC (Sheng et al., 2013). Despite the elevation of IFN- γ in R, there was no increase of Mϕ. $CD3^-$ $ROR\gamma t^+$ may support the pro-inflammatory immune response by the production of cytokines that were not detected, such as IL-22 (Zhang et al., 2020). Alternatively, they may present ag to T lymphocytes under microbiota-induced conditions in the presence of IFN-γ (Lehmann et al., 2020).

Accumulation of Th17 cells in the spleen supports SFB-driven changes in the immune response. The effect of SFB on PD-1 expression is not known so far. However, elevated amounts of $PD\text{-}1^+CD8^+$ T cells in the spleens of R may also be caused by other bacteria species (Pushalkar et al., 2018), or it is simply the outcome of increased activation of the IS. Activated DC are expected to migrate to the tissue and therefore are decreased in the spleen.

The connection between SFB and cancer is not much studied since the role of the Th17 immune response to anti-tumour immunity remains controversial. Th17 infiltration is associated with poor prognosis in gastric cancer (T. Liu et al., 2012) or CRC (Tosolini et al., 2011), where elevated levels of Th17 may be a reflection of barrier failure (Sano et al., 2015). However, they are a marker of a good prognosis in ovarian cancer (Bilska et al., 2020). It seems that the effect of Th17 cells on the immune response is unique to the type of malignancy or therapy approach. Th17 cells possess high plasticity and, under a particular condition, can be transformed to suppressor RORγt^{+}FOXP3^{+} but also to RORγt^{+} T-bet^{+} cells (Bailey et al., 2014).

This topic is even more interesting because the first genomic sequence from human-derived SFB has been presented recently (Jonsson et al., 2020), and more than 20 bacterial strains from the human gut, such as *Bifidobacterium adolescenti,* can induce Th17 immune response in colonised mice (Atarashi et al., 2015; Tan et al., 2016), therefore studying of mechanisms how bacteria-stimulated Th17 immune cells affect the anti-tumour immunity may be very beneficial.

It is expected that IFN-γ producing cells importantly contribute to the anti-tumour immune response. Elevated levels of IFN-γ can induce expression of CXCL9 and CXCL10 (Groom & Luster, 2011), which may result in higher infiltration of T lymphocytes. Concomitantly IL-17 can elevate the expression of CXCL2 or CXCL5, which potentiates neutrophil recruitment (Kuang et al., 2011; S. Xu & Cao, 2010). Additionally, IL-17 increases the killing capacity of tumour-infiltrating neutrophils through increased myeloperoxidase, ROS, TRAIL and IFN-γ (Chen et al., 2018). Among other mechanisms how IL-17 may contribute to the anti-tumour immune response is the promotion of cytotoxic activity, such as expression of perforin, granzymes and FasL in CD8+ T cells (Acharya et al., 2017).

The main limitation of these results is that the colonisation experiment was performed only once. Nevertheless, the experiment will be repeated in the future to confirm the observations.

7 Proposed models

According to observed results and literature review, proposed models of how gut-tumour axis together with αPD-1 therapy may contribute to anti-tumour immune response are depicted in Fig. 17 and Fig. 18. ATB experiment and following colonisation experiment showed distinctions in the immune responses, and therefore different microbiota composition or mechanism can be expected. For this reason, two models are described in this chapter.

ATB administration causes a shift in the microbiota composition, which may allow the overgrowth of certain ATB resistant species or ATB administration suppresses a protective microbe, which results in the secretion of alarmin, IL-33 and DAMP molecule S100A8, which activates the inflammation and production of pro-inflammatory cytokines, such as TNF-α, IL-1β and IL-6. In addition, monocytes, neutrophils and macrophages are expected to be recruited into the site of inflammation.

Already activated $CD80^+$ DC migrate from the inflammation site into MLN to activate T lymphocytes. Higher amounts of TNF-α trigger the pro-inflammatory immune response. Under specific pro-inflammatory conditions (not detected), supported by $CD3^-$T-Bet^+, is type 1 immune response developed. These CTL type 1 and Th1 immune cells then migrate through the body.

ATB-changed microbiota activates the IS and consequent αPD-1 administration boost and prolong immune response, which is evident in the tumour tissue, as enhanced and prolonged presence of T lymphocytes, especially Th1 cells and type 1 CTL. In addition, to effective anti-tumour immune response contribute IFN-γ secretion from $CD3^-$, Th1 lymphocytes and CTL type 1 cells. Furthermore, IFN-γ induces the pro-inflammatory properties of Mϕ.

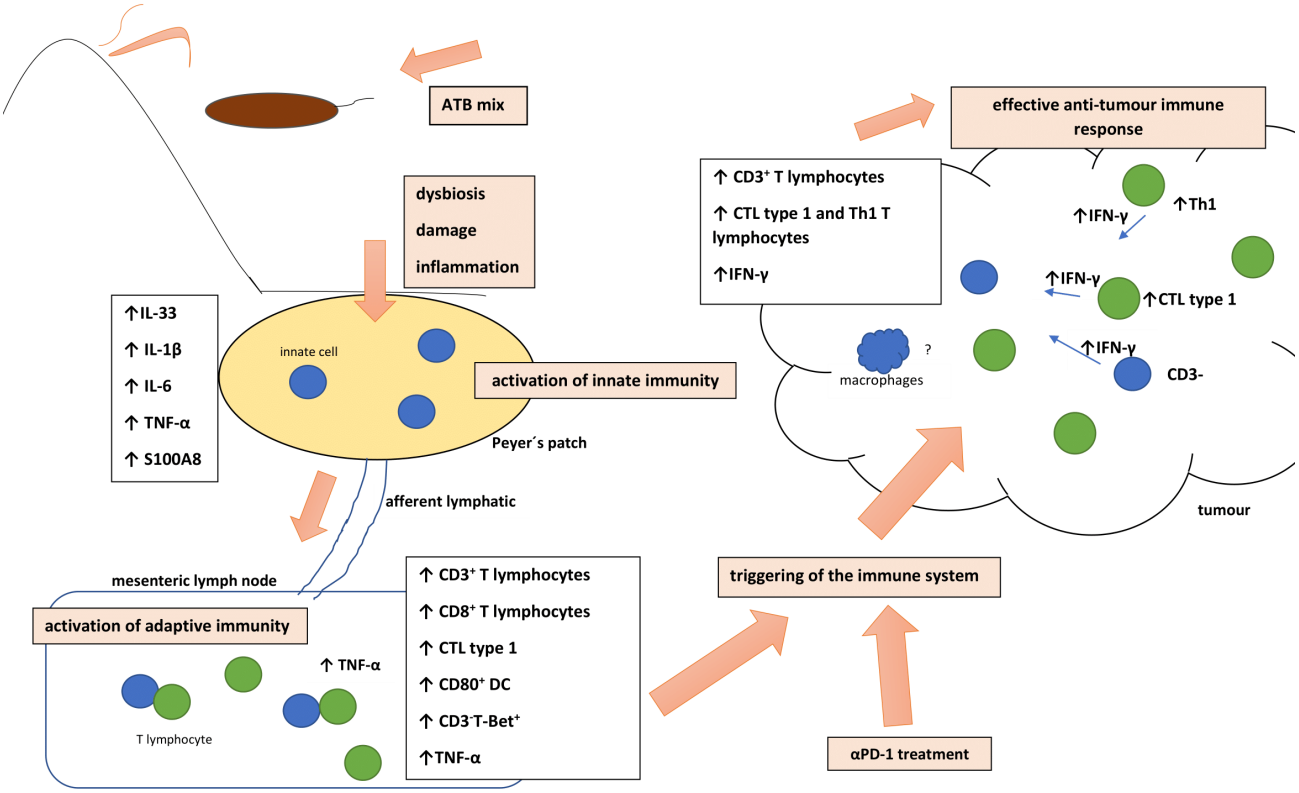

Figure 17 Proposed mechanism how gut microbiota driven changes in the immune reactions concomitantly with αPD-1 treatment lead to effective anti-tumour immune response in MC-38 tumour xenografts. αPD-1 = anti-programmed cell death protein 1, ATB = antibiotics, CD = cluster of differentiation, CTL = cytotoxic T lymphocytes, DC = dendritic cells, IFN-γ = interferon gamma, IL = interleukin, T-bet = T-box expressed in T cells, Th = T helperTNF-α = tumour necrosis factor-alpha,

In the subsequent experiment, mice colonised by ATB-changed microbiota and treated with αPD-1 showed distinction in the immune responses in the gut, spleen and tumour, which resulted in a more effective anti-tumour immune response. Different microbiota composition, such as increased amounts of lactobacilli and SFB (the rest is to be elucidated by 16S rRNA gene sequencing), activate the IS into the pro-inflammatory type, which is manifested by the production of pro-inflammatory cytokines (IFN-γ, TNF-α) in the MLN. $CD3^{-}ROR\gamma t^{+}$ support the pro-inflammatory immune response and also, in the presence of IFN-γ, may present the ag to T cells.

The pre-activated IS by microbial changes is even more triggered by αPD-1 administration. For example, in the spleen are elevated levels of activated ($PD\text{-}1^{+}$) $CD8^{+}$ T lymphocytes, which are protected by αPD-1 mAb and therefore are even more effective. Th17 lymphocytes primed in the gut migrate through the circulation and accumulate in the spleen and tumours. IFN-γ and IL-17 induce the expression of various chemokines, and therefore

more T lymphocytes accumulate in the tumour tissue. IL-17, in the unknown mechanism so far, considerably contributes to the anti-tumour immune response.

Altogether, pro-inflammatory immune response in the gut influences systemic immune response, which can be seen in the spleen. Importantly, the gut-tumour axis exists, and gut microbiota stimulate the effective anti-tumour immune response.

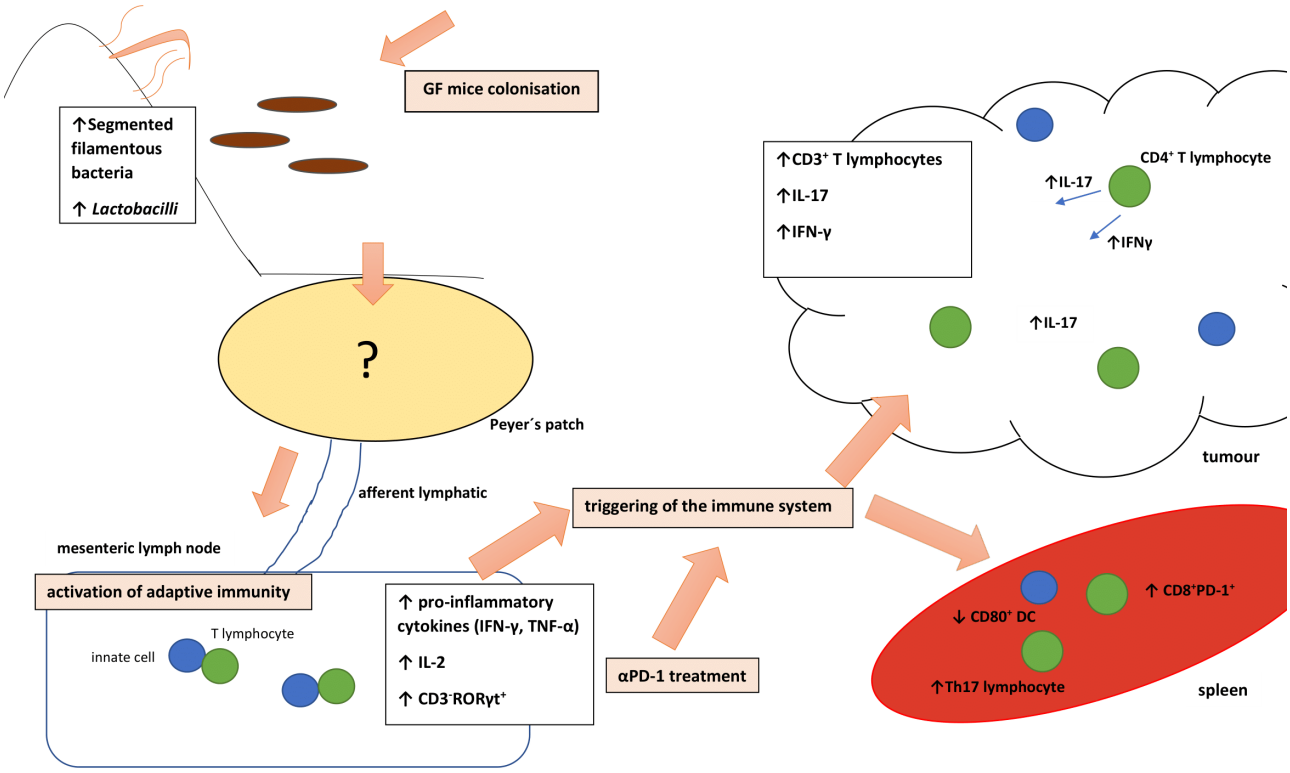

Figure 18 Proposed mechanism how gut microbiota combined with αPD-1 treatment may affect the anti-tumour immune response. αPD-1 = anti-programmed cell death protein 1, CD = cluster of differentiation, DC = dendritic cells, GF = germ free, IFN-γ = interferon gamma, PD-1 = programmed cell death protein 1, Rorγt = retinoic-acid-receptor-related orphan receptor gamma, TNF-α = tumour necrosis factor-alpha

8 Conclusion

The mice model for studying the effect of gut microbiota on the αPD-1 therapy of tumours was established, and therefore we were able to prove the existence of the gut microbiota – tumour axis. The results of this master thesis indicate the potential of the gut microbiota to influence the αPD-1 treatment or even the possibility to reach a more beneficial outcome if acting synergistically.

Moreover, this master thesis reveals the complexity of gut microbiota interactions since the ATB + αPD-1 experiment led to different effective anti-tumour mechanisms compared with the colonisation experiment. ATB combined with αPD-1 treatment results in enhanced T cell activation and overall production of pro-inflammatory cytokines within PP, MLN and incredibly in the tumours. This observation denies the generally accepted negative impact of ATB on anti-tumour therapies. Importantly the anti-tumour immune response could be transferred through colonisation of GF mice by ATB-changed gut microbiota if concomitantly αPD-1 mAb is administrated.

Additionally, this master thesis opens the question of the role of microbiota-induced Th17 lymphocytes in the anti-tumour immune response, which is poorly understood so far. We showed that SFB induces systemic immune response with increased expression of IL-17 and elevated amounts of Th17 cells. However, it is probable that to the activation of the IS in the gut contribute other bacterial species as well, which underlines the complexity of bacterial interactions in the gut.

9 References

*review article

Abrahamsson, T. R., Jakobsson, H. E., Andersson, A. F., Björkstén, B., Engstrand, L., & Jenmalm, M. C. (**2012**). **Low diversity of the gut microbiota in infants with atopic eczema**. *The Journal of Allergy and Clinical Immunology*, *129*(2), 434–440, 440.e1-2. https://doi.org/10.1016/j.jaci.2011.10.025

Acharya, D., Wang, P., Paul, A. M., Dai, J., Gate, D., Lowery, J. E., Stokic, D. S., Leis, A. A., Flavell, R. A., Town, T., Fikrig, E., & Bai, F. (**2017**). **Interleukin-17A promotes CD8+ T cell cytotoxicity to facilitate west Nile virus clearance**. *Journal of Virology*, *91*(1). https://doi.org/10.1128/JVI.01529-16

***Agrawal, S.**, Feng, Y., Roy, A., Kollia, G., & Lestini, B. (**2016**). **Nivolumab dose selection: Challenges, opportunities, and lessons learned for cancer immunotherapy.** *Journal for Immunotherapy of Cancer*, *4*. https://doi.org/10.1186/s40425-016-0177-2

***Allaire, J. M.**, Crowley, S. M., Law, H. T., Chang, S.-Y., Ko, H.-J., & Vallance, B. A. (**2018**). **The intestinal epithelium: Central coordinator of mucosal immunity**. *Trends in Immunology*, *39*(9), 677–696. https://doi.org/10.1016/j.it.2018.04.002

Alvarez, C.-S., Badia, J., Bosch, M., Giménez, R., & Baldomà, L. (**2016**). **Outer membrane vesicles and soluble factors released by probiotic Escherichia coli Nissle 1917 and commensal ECOR63 enhance barrier function by regulating expression of tight junction proteins in intestinal epithelial cells.** *Frontiers in Microbiology*, *7*. https://doi.org/10.3389/fmicb.2016.01981

***Alvarez, F.**, Fritz, J. H., & Piccirillo, C. A. (**2019**). **Pleiotropic effects of IL-33 on CD4+ T cell differentiation and effector functions**. *Frontiers in Immunology*, *10*. https://doi.org/10.3389/fimmu.2019.00522

Ashraf, R., Vasiljevic, T., Day, S. L., Smith, S. C., & Donkor, O. N. (**2014**). **Lactic acid bacteria and probiotic organisms induce different cytokine profile and regulatory T cells mechanisms.** *Journal of Functional Foods*, *6*, 395–409. https://doi.org/10.1016/j.jff.2013.11.006

Atarashi, K., Tanoue, T., Ando, M., Kamada, N., Nagano, Y., Narushima, S., Suda, W., Imaoka, A., Setoyama, H., Nagamori, T., Ishikawa, E., Shima, T., Hara, T., Kado, S., Jinnohara, T., Ohno, H., Kondo, T., Toyooka, K., Watanabe, E., Honda, K. **(2015**). **Th17 cell induction by adhesion of microbes to intestinal epithelial cells.** *Cell*, *163*(2), 367–380. https://doi.org/10.1016/j.cell.2015.08.058

Autengruber, A., Gereke, M., Hansen, G., Hennig, C., & Bruder, D. (**2012**). **Impact of enzymatic tissue disintegration on the level of surface molecule expression and immune cell function.** *European Journal of Microbiology & Immunology*, *2*(2), 112–120. https://doi.org/10.1556/EuJMI.2.2012.2.3

Bacchetti De Gregoris, T., Aldred, N., Clare, A. S., & Burgess, J. G. (**2011**). **Improvement of phylum- and class-specific primers for real-time PCR quantification of bacterial taxa.** *Journal of Microbiological Methods*, *86*(3), 351–356. https://doi.org/10.1016/j.mimet.2011.06.010

Bäckhed, F., Roswall, J., Peng, Y., Feng, Q., Jia, H., Kovatcheva-Datchary, P., Li, Y., Xia, Y., Xie, H., Zhong, H., Khan, M. T., Zhang, J., Li, J., Xiao, L., Al-Aama, J., Zhang, D., Lee, Y. S., Kotowska, D., Colding, C., Wang, J. (**2015**). **Dynamics and stabilization of the human gut microbiome during the first year of life.** *Cell Host & Microbe*, *17*(5), 690–703. https://doi.org/10.1016/j.chom.2015.04.004

Bailey, S. R., Nelson, M. H., Himes, R. A., Li, Z., Mehrotra, S., & Paulos, C. M. (**2014**). **Th17 Cells in Cancer: The Ultimate Identity Crisis.** *Frontiers in Immunology*, *5*. https://doi.org/10.3389/fimmu.2014.00276

Balachandran, V. P., Łuksza, M., Zhao, J. N., Makarov, V., Moral, J. A., Remark, R., Herbst, B., Askan, G., Bhanot, U., Senbabaoglu, Y., Wells, D. K., Cary, C. I. O., Grbovic-Huezo, O., Attiyeh, M., Medina, B., Zhang,

J., Loo, J., Saglimbeni, J., Abu-Akeel, M., Leach, S. D. (**2017**). **Identification of unique neoantigen qualities in long term pancreatic cancer survivors.** *Nature*, *551*(7681), 512–516. https://doi.org/10.1038/nature24462

Baruch, E. N., Youngster, I., Ben-Betzalel, G., Ortenberg, R., Lahat, A., Katz, L., Adler, K., Dick-Necula, D., Raskin, S., Bloch, N., Rotin, D., Anafi, L., Avivi, C., Melnichenko, J., Steinberg-Silman, Y., Mamtani, R., Harati, H., Asher, N., Shapira-Frommer, R., Boursi, B. (**2021**). **Fecal microbiota transplant promotes response in immunotherapy-refractory melanoma patients.** *Science*, *371*(6529), 602–609. https://doi.org/10.1126/science.abb5920

Beyrend, G., van der Gracht, E., Yilmaz, A., van Duikeren, S., Camps, M., Höllt, T., Vilanova, A., van Unen, V., Koning, F., de Miranda, N. F. C. C., Arens, R., & Ossendorp, F. (**2019**). **PD-L1 blockade engages tumor-infiltrating lymphocytes to co-express targetable activating and inhibitory receptors**. *Journal for Immunotherapy of Cancer*, *7*. https://doi.org/10.1186/s40425-019-0700-3

Bhatia, S. J., Kochar, N., Abraham, P., Nair, N. G., & Mehta, A. P. (**1989**). **Lactobacillus acidophilus inhibits growth of Campylobacter pylori in vitro.** *Journal of Clinical Microbiology*, *27*(10), 2328–2330.

Bilska, M., Pawłowska, A., Zakrzewska, E., Chudzik, A., Suszczyk, D., Gogacz, M., & Wertel, I. (**2020**). **Th17 cells and IL-17 as novel immune targets in ovarian cancer therapy.** *Journal of Oncology*, *2020*, 8797683. https://doi.org/10.1155/2020/8797683

Bisgaard, H., Li, N., Bonnelykke, K., Chawes, B. L. K., Skov, T., Paludan-Müller, G., Stokholm, J., Smith, B., & Krogfelt, K. A. (**2011**). **Reduced diversity of the intestinal microbiota during infancy is associated with increased risk of allergic disease at school age.** *The Journal of Allergy and Clinical Immunology*, *128*(3), 646-652.e1-5. https://doi.org/10.1016/j.jaci.2011.04.060

Boleij, A., Hechenbleikner, E. M., Goodwin, A. C., Badani, R., Stein, E. M., Lazarev, M. G., Ellis, B., Carroll, K. C., Albesiano, E., Wick, E. C., Platz, E. A., Pardoll, D. M., & Sears, C. L. (**2015**). T**he Bacteroides fragilis toxin gene is prevalent in the colon mucosa of colorectal cancer patients.** *Clinical Infectious Diseases: An Official Publication of the Infectious Diseases Society of America*, *60*(2), 208–215. https://doi.org/10.1093/cid/ciu787

Brás, J. P., Bravo, J., Freitas, J., Barbosa, M. A., Santos, S. G., Summavielle, T., & Almeida, M. I. (**2020**). **TNF-alpha-induced microglia activation requires miR-342: Impact on NF-kB signaling and neurotoxicity.** *Cell Death & Disease*, *11*(6), 415. https://doi.org/10.1038/s41419-020-2626-6

***Brown, E. M.**, Sadarangani, M., & Finlay, B. B. (**2013**). **The role of the immune system in governing host-microbe interactions in the intestine.** *Nature Immunology*, *14*(7), 660–667. https://doi.org/10.1038/ni.2611

***Burgueño, J. F., & Abreu, M. T**. (**2020**). **Epithelial Toll-like receptors and their role in gut homeostasis and disease.** *Nature Reviews Gastroenterology & Hepatology*, *17*(5), 263–278. https://doi.org/10.1038/s41575-019-0261-4

Burisch, J., Pedersen, N., Cukovic-Cavka, S., Turk, N., Kaimakliotis, I., Duricova, D., Bortlik, M., Shonová, O., Vind, I., Avnstrøm, S., Thorsgaard, N., Krabbe, S., Andersen, V., Dahlerup, J. F., Kjeldsen, J., Salupere, R., Olsen, J., Nielsen, K. R., Manninen, P., Munkholm, P. (**2014**). **Environmental factors in a population-based inception cohort of inflammatory bowel disease patients in Europe—An ECCO-EpiCom study☆**. *Journal of Crohn's and Colitis*, *8*(7), 607–616. https://doi.org/10.1016/j.crohns.2013.11.021

***Butel, M.-J.**, Waligora-Dupriet, A.-J., & Wydau-Dematteis, S. (**2018**). **The developing gut microbiota and its consequences for health.** *Journal of Developmental Origins of Health and Disease*, *9*(6), 590–597. https://doi.org/10.1017/S2040174418000119

Byun, R., Nadkarni, M. A., Chhour, K.-L., Martin, F. E., Jacques, N. A., & Hunter, N. (**2004**). **Quantitative analysis of diverse Lactobacillus species present in advanced dental caries.** *Journal of Clinical Microbiology*, *42*(7), 3128–3136. https://doi.org/10.1128/JCM.42.7.3128-3136.2004

Caminero, A., Galipeau, H. J., McCarville, J. L., Johnston, C. W., Bernier, S. P., Russell, A. K., Jury, J., Herran, A. R., Casqueiro, J., Tye-Din, J. A., Surette, M. G., Magarvey, N. A., Schuppan, D., & Verdu, E. F. (**2016**). **Duodenal bacteria from patients with celiac disease and healthy subjects distinctly affect gluten breakdown and immunogenicity**. *Gastroenterology*, *151*(4), 670–683. https://doi.org/10.1053/j.gastro.2016.06.041

Cano, P. G., Santacruz, A., Moya, Á., & Sanz, Y. (**2012**). **Bacteroides uniformis CECT 7771 ameliorates metabolic and immunological dysfunction in mice with high-fat-diet induced obesity.** *PLOS ONE*, *7*(7), e41079. https://doi.org/10.1371/journal.pone.0041079

Chaput, N., Lepage, P., Coutzac, C., Soularue, E., Roux, K. L., Monot, C., Boselli, L., Routier, E., Cassard, L., Collins, M., Vaysse, T., Marthey, L., Eggermont, A., Asvatourian, V., Lanoy, E., Mateus, C., Robert, C., & Carbonnel, F. (**2017**). **Baseline gut microbiota predicts clinical response and colitis in metastatic melanoma patients treated with ipilimumab.** *Annals of Oncology*, *28*(6), 1368–1379. https://doi.org/10.1093/annonc/mdx108

Chen, C.-L., Wang, Y., Huang, C.-Y., Zhou, Z.-Q., Zhao, J.-J., Zhang, X.-F., Pan, Q.-Z., Wu, J.-X., Weng, D.-S., Tang, Y., Zhu, Q., Yuan, L.-P., & Xia, J.-C. (**2018**). **IL-17 induces antitumor immunity by promoting beneficial neutrophil recruitment and activation in esophageal squamous cell carcinoma.** *OncoImmunology*, *7*(1), e1373234. https://doi.org/10.1080/2162402X.2017.1373234

***Chen, J.**, Domingue, J. C., & Sears, C. L. (**2017**). **Microbiota dysbiosis in select human cancers: Evidence of association and causality.** *Seminars in Immunology*, *32*, 25–34. https://doi.org/10.1016/j.smim.2017.08.001

***Cheng, H.**, Guan, X., Chen, D., & Ma, W. (**2019**). **The Th17/Treg cell balance: A gut microbiota-modulated story.** *Microorganisms*, *7*(12), 583. https://doi.org/10.3390/microorganisms7120583

***Conteh, A. R.**, & Huang, R. (**2020**). **Targeting the gut microbiota by Asian and Western dietary constituents: A new avenue for diabetes.** *Toxicology Research*, *9*(4), 569–577. https://doi.org/10.1093/toxres/tfaa065

Coutzac, C., Jouniaux, J.-M., Paci, A., Schmidt, J., Mallardo, D., Seck, A., Asvatourian, V., Cassard, L., Saulnier, P., Lacroix, L., Woerther, P.-L., Vozy, A., Naigeon, M., Nebot-Bral, L., Desbois, M., Simeone, E., Mateus, C., Boselli, L., Grivel, J., Chaput, N. (**2020**). **Systemic short chain fatty acids limit antitumor effect of CTLA-4 blockade in hosts with cancer.** *Nature Communications*, *11*(1), 2168. https://doi.org/10.1038/s41467-020-16079-x

***Cresci, G. A., & Bawden, E.** (**2015**). **The gut microbiome: What we do and don't know**. *Nutrition in Clinical Practice : Official Publication of the American Society for Parenteral and Enteral Nutrition*, *30*(6), 734–746. https://doi.org/10.1177/0884533615609899

da Fonseca-Martins, A. M., Ramos, T. D., Pratti, J. E. S., Firmino-Cruz, L., Gomes, D. C. O., Soong, L., Saraiva, E. M., & de Matos Guedes, H. L. (**2019**). **Immunotherapy using anti-PD-1 and anti-PD-L1 in Leishmania amazonensis -infected BALB/c mice reduce parasite load**. *Scientific Reports*, *9*(1), 20275. https://doi.org/10.1038/s41598-019-56336-8

Daillère, R., Vétizou, M., Waldschmitt, N., Yamazaki, T., Isnard, C., Poirier-Colame, V., Duong, C. P. M., Flament, C., Lepage, P., Roberti, M. P., Routy, B., Jacquelot, N., Apetoh, L., Becharef, S., Rusakiewicz, S., Langella, P., Sokol, H., Kroemer, G., Enot, D., Zitvogel, L. (**2016**). **Enterococcus hirae and Barnesiella intestinihominis Facilitate Cyclophosphamide-Induced Therapeutic Immunomodulatory Effects.** *Immunity*, *45*(4), 931–943. https://doi.org/10.1016/j.immuni.2016.09.009

Dashper, S. G., Mitchell, H. L., Lê Cao, K.-A., Carpenter, L., Gussy, M. G., Calache, H., Gladman, S. L., Bulach, D. M., Hoffmann, B., Catmull, D. V., Pruilh, S., Johnson, S., Gibbs, L., Amezdroz, E., Bhatnagar, U., Seemann, T., Mnatzaganian, G., Manton, D. J., & Reynolds, E. C. (**2019**). T**emporal development of the oral microbiome and prediction of early childhood caries.** *Scientific Reports*, *9*(1), 19732. https://doi.org/10.1038/s41598-019-56233-0

Davar, D., Dzutsev, A. K., McCulloch, J. A., Rodrigues, R. R., Chauvin, J.-M., Morrison, R. M., Deblasio, R. N., Menna, C., Ding, Q., Pagliano, O., Zidi, B., Zhang, S., Badger, J. H., Vetizou, M., Cole, A. M., Fernandes, M. R., Prescott, S., Costa, R. G. F., Balaji, A. K., Zarour, H. M. (**2021**). **Fecal microbiota transplant overcomes resistance to anti–PD-1 therapy in melanoma patients.** *Science*, *371*(6529), 595–602. https://doi.org/10.1126/science.abf3363

David, L. A., Maurice, C. F., Carmody, R. N., Gootenberg, D. B., Button, J. E., Wolfe, B. E., Ling, A. V., Devlin, A. S., Varma, Y., Fischbach, M. A., Biddinger, S. B., Dutton, R. J., & Turnbaugh, P. J. (**2014**). **Diet rapidly and reproducibly alters the human gut microbiome.** *Nature*, *505*(7484), 559–563. https://doi.org/10.1038/nature12820

DeFilipp, Z., Bloom, P. P., Torres Soto, M., Mansour, M. K., Sater, M. R. A., Huntley, M. H., Turbett, S., Chung, R. T., Chen, Y.-B., & Hohmann, E. L. (**2019**). **Drug-Resistant E. coli bacteremia transmitted by fecal microbiota transplant.** *The New England Journal of Medicine*, *381*(21), 2043–2050. https://doi.org/10.1056/NEJMoa1910437

***DeNardo, D. G., & Ruffell, B.** (**2019**). **Macrophages as regulators of tumor immunity and immunotherapy.** *Nature Reviews. Immunology*, *19*(6), 369–382. https://doi.org/10.1038/s41577-019-0127-6

Dethlefsen, L., & Relman, D. A. (**2011**). **Incomplete recovery and individualized responses of the human distal gut microbiota to repeated antibiotic perturbation.** *Proceedings of the National Academy of Sciences of the United States of America*, *108*(Suppl 1), 4554–4561. https://doi.org/10.1073/pnas.1000087107

***Ding, Y.-H.**, Qian, L.-Y., Pang, J., Lin, J.-Y., Xu, Q., Wang, L.-H., Huang, D.-S., & Zou, H. (**2017**). **The regulation of immune cells by Lactobacilli: A potential therapeutic target for anti-atherosclerosis therapy**. *Oncotarget*, *8*(35), 59915–59928. https://doi.org/10.18632/oncotarget.18346

Dominguez-Bello, M. G., Costello, E. K., Contreras, M., Magris, M., Hidalgo, G., Fierer, N., & Knight, R. (**2010**). **Delivery mode shapes the acquisition and structure of the initial microbiota across multiple body habitats in newborns**. *Proceedings of the National Academy of Sciences*, *107*(26), 11971–11975. https://doi.org/10.1073/pnas.1002601107

Dong, P., Yang, Y., & Wang, W. (**2010**). **The role of intestinal bifidobacteria on immune system development in young rats.** *Early Human Development*, *86*(1), 51–58. https://doi.org/10.1016/j.earlhumdev.2010.01.002

Duffy, A. G., Ulahannan, S. V., Makorova-Rusher, O., Rahma, O., Wedemeyer, H., Pratt, D., Davis, J. L., Hughes, M. S., Heller, T., ElGindi, M., Uppala, A., Korangy, F., Kleiner, D. E., Figg, W. D., Venzon, D., Steinberg, S. M., Venkatesan, A. M., Krishnasamy, V., Abi-Jaoudeh, N., Greten, T. F. (**2017**). **Tremelimumab in combination with ablation in patients with advanced hepatocellular carcinoma.** *Journal of Hepatology*, *66*(3), 545–551. https://doi.org/10.1016/j.jhep.2016.10.029

***Dunn, G. P.**, Old, L. J., & Schreiber, R. D. (**2004**). **The immunobiology of cancer immunosurveillance and immunoediting.** *Immunity*, *21*(2), 137–148. https://doi.org/10.1016/j.immuni.2004.07.017

Efremova, M., Rieder, D., Klepsch, V., Charoentong, P., Finotello, F., Hackl, H., Hermann-Kleiter, N., Löwer, M., Baier, G., Krogsdam, A., & Trajanoski, Z. (**2018**). **Targeting immune checkpoints potentiates immunoediting and changes the dynamics of tumor evolution.** *Nature Communications*, *9*. https://doi.org/10.1038/s41467-017-02424-0

Espinassous, Q., Garcia-de-Paco, E., Garcia-Verdugo, I., Synguelakis, M., Aulock, S. von, Sallenave, J.-M., McKenzie, A. N. J., & Kanellopoulos, J. (**2009**). **IL-33 enhances lipopolysaccharide-induced inflammatory cytokine production from mouse macrophages by regulating lipopolysaccharide receptor complex.** *The Journal of Immunology*, *183*(2), 1446–1455. https://doi.org/10.4049/jimmunol.0803067

Ewaschuk, J. B., Diaz, H., Meddings, L., Diederichs, B., Dmytrash, A., Backer, J., Looijer-van Langen, M., & Madsen, K. L. (**2008**). **Secreted bioactive factors from Bifidobacterium infantis enhance epithelial cell barrier function.** *American Journal of Physiology. Gastrointestinal and Liver Physiology*, *295*(5), G1025-1034. https://doi.org/10.1152/ajpgi.90227.2008

Eyre, R., Alférez, D. G., Santiago-Gómez, A., Spence, K., McConnell, J. C., Hart, C., Simões, B. M., Lefley, D., Tulotta, C., Storer, J., Gurney, A., Clarke, N., Brown, M., Howell, S. J., Sims, A. H., Farnie, G., Ottewell, P. D., & Clarke, R. B. (**2019**). M**icroenvironmental IL1β promotes breast cancer metastatic colonisation in the bone via activation of Wnt signalling.** *Nature Communications*, *10*(1), 5016. https://doi.org/10.1038/s41467-019-12807-0

***Fearon, E. R., & Vogelstein, B.** (**1990**). **A genetic model for colorectal tumorigenesis**. *Cell*, *61*(5), 759–767. https://doi.org/10.1016/0092-8674(90)90186-i

***Fernández, M. F.**, Reina-Pérez, I., Astorga, J. M., Rodríguez-Carrillo, A., Plaza-Díaz, J., & Fontana, L. (**2018**). **Breast cancer and its relationship with the microbiota.** *International Journal of Environmental Research and Public Health*, *15*(8). https://doi.org/10.3390/ijerph15081747

Filippis, F. D., Pellegrini, N., Vannini, L., Jeffery, I. B., Storia, A. L., Laghi, L., Serrazanetti, D. I., Cagno, R. D., Ferrocino, I., Lazzi, C., Turroni, S., Cocolin, L., Brigidi, P., Neviani, E., Gobbetti, M., O'Toole, P. W., & Ercolini, D. (2016). **High-level adherence to a Mediterranean diet beneficially impacts the gut microbiota and associated metabolome.** *Gut*, *65*(11), 1812–1821. https://doi.org/10.1136/gutjnl-2015-309957

Filippo, C. D., Cavalieri, D., Paola, M. D., Ramazzotti, M., Poullet, J. B., Massart, S., Collini, S., Pieraccini, G., & Lionetti, P. (**2010**). **Impact of diet in shaping gut microbiota revealed by a comparative study in children from Europe and rural Africa**. *Proceedings of the National Academy of Sciences*, *107*(33), 14691–14696. https://doi.org/10.1073/pnas.1005963107

Fu, T., He, Q., & Sharma, P. (**2011**). **The ICOS/ICOSL pathway is required for optimal antitumor responses mediated by anti-CTLA-4 therapy.** *Cancer Research*, *71*(16), 5445–5454. https://doi.org/10.1158/0008-5472.CAN-11-1138

Gao, C. E., Zhang, M., Song, Q., & Dong, J. (**2019**). **PD-1 inhibitors dependent CD8+ T cells inhibit mouse colon cancer cell metastasis.** *OncoTargets and Therapy*, *12*, 6961–6971. https://doi.org/10.2147/OTT.S202941

***García-Castillo, V.**, Sanhueza, E., McNerney, E., Onate, S. A., & García, A. (**2016**). **Microbiota dysbiosis: A new piece in the understanding of the carcinogenesis puzzle.** *Journal of Medical Microbiology*, *65*(12), 1347–1362. https://doi.org/10.1099/jmm.0.000371

Garcia-Diaz, A., Shin, D. S., Moreno, B. H., Saco, J., Escuin-Ordinas, H., Rodriguez, G. A., Zaretsky, J. M., Sun, L., Hugo, W., Wang, X., Parisi, G., Saus, C. P., Torrejon, D. Y., Graeber, T. G., Comin-Anduix, B., Hu-Lieskovan, S., Damoiseaux, R., Lo, R. S., & Ribas, A. **(2017**). I**nterferon receptor signaling pathways regulating PD-L1 and PD-L2 expression.** *Cell Reports*, *19*(6), 1189–1201. https://doi.org/10.1016/j.celrep.2017.04.031

Garon, E. B., Rizvi, N. A., Hui, R., Leighl, N., Balmanoukian, A. S., Eder, J. P., Patnaik, A., Aggarwal, C., Gubens, M., Horn, L., Carcereny, E., Ahn, M.-J., Felip, E., Lee, J.-S., Hellmann, M. D., Hamid, O., Goldman, J. W., Soria, J.-C., Dolled-Filhart, M., Gandhi, L. (**2015**). **Pembrolizumab for the treatment of non–small-cell lung cancer**, *The New England Journal of Medicine*. https://doi.org/10.1056/NEJMoa1501824

Garza, D. R., Taddese, R., Wirbel, J., Zeller, G., Boleij, A., Huynen, M. A., & Dutilh, B. E. (**2020**). **Metabolic models predict bacterial passengers in colorectal cancer.** *Cancer & Metabolism*, *8*(1), 3. https://doi.org/10.1186/s40170-020-0208-9

Geem, D., Medina-Contreras, O., McBride, M., Newberry, R. D., Koni, P. A., & Denning, T. L. (**2014**). **Specific microbiota-induced intestinal Th17 differentiation requires MHC II but not GALT and mesenteric lymph nodes.** *Journal of Immunology (Baltimore, Md. : 1950)*, *193*(1), 431–438. https://doi.org/10.4049/jimmunol.1303167

Gevers, D., Kugathasan, S., Denson, L. A., Vázquez-Baeza, Y., Van Treuren, W., Ren, B., Schwager, E., Knights, D., Song, S. J., Yassour, M., Morgan, X. C., Kostic, A. D., Luo, C., González, A., McDonald, D., Haberman, Y., Walters, T., Baker, S., Rosh, J., Xavier, R. J. (**2014**). **The treatment-naïve microbiome in new-onset Crohn's disease.** *Cell Host & Microbe*, *15*(3), 382–392. https://doi.org/10.1016/j.chom.2014.02.005

***Gilbert, J.**, Blaser, M. J., Caporaso, J. G., Jansson, J., Lynch, S. V., & Knight, R. (**2018**). **Current understanding of the human microbiome.** *Nature Medicine*, *24*(4), 392–400. https://doi.org/10.1038/nm.4517

Goedert, J. J., Jones, G., Hua, X., Xu, X., Yu, G., Flores, R., Falk, R. T., Gail, M. H., Shi, J., Ravel, J., & Feigelson, H. S. (**2015**). **Investigation of the association between the fecal microbiota and breast cancer in postmenopausal women: A population-based case-control pilot study.** *Journal of the National Cancer Institute*, *107*(8). https://doi.org/10.1093/jnci/djv147

Goff, S. L., Dudley, M. E., Citrin, D. E., Somerville, R. P., Wunderlich, J. R., Danforth, D. N., Zlott, D. A., Yang, J. C., Sherry, R. M., Kammula, U. S., Klebanoff, C. A., Hughes, M. S., Restifo, N. P., Langhan, M. M., Shelton, T. E., Lu, L., Kwong, M. L. M., Ilyas, S., Klemen, N. D., Rosenberg, S. A. (**2016**). **Randomized, prospective evaluation comparing intensity of lymphodepletion before adoptive transfer of tumor-infiltrating lymphocytes for patients with metastatic melanoma.** *Journal of Clinical Oncology: Official Journal of the American Society of Clinical Oncology*, *34*(20), 2389–2397. https://doi.org/10.1200/JCO.2016.66.7220

Gopalakrishnan, V., Spencer, C. N., Nezi, L., Reuben, A., Andrews, M. C., Karpinets, T. V., Prieto, P. A., Vicente, D., Hoffman, K., Wei, S. C., Cogdill, A. P., Zhao, L., Hudgens, C. W., Hutchinson, D. S., Manzo, T., Petaccia de Macedo, M., Cotechini, T., Kumar, T., Chen, W. S., Wargo, J. A. (**2018**). **Gut microbiome modulates response to anti-PD-1 immunotherapy in melanoma patients.** *Science*, *359*(6371), 97–103. https://doi.org/10.1126/science.aan4236

Gorska-Ponikowska, M., Ploska, A., Jacewicz, D., Szkatula, M., Barone, G., Lo Bosco, G., Lo Celso, F., Dabrowska, A. M., Kuban-Jankowska, A., Gorzynik-Debicka, M., Knap, N., Chmurzynski, L., Dobrucki, L. W., Kalinowski, L., & Wozniak, M. (**2020**). **Modification of DNA structure by reactive nitrogen species as a result of 2-methoxyestradiol-induced neuronal nitric oxide synthase uncoupling in metastatic osteosarcoma cells.** *Redox Biology*, *32*, 101522. https://doi.org/10.1016/j.redox.2020.101522

***Groom, J. R., & Luster, A. D.** (**2011**). **CXCR3 ligands: Redundant, collaborative and antagonistic functions.** *Immunology & Cell Biology*, *89*(2), 207–215. https://doi.org/10.1038/icb.2010.158

Guo, Y., Zhang, Y., Gerhard, M., Gao, J.-J., Mejias-Luque, R., Zhang, L., Vieth, M., Ma, J.-L., Bajbouj, M., Suchanek, S., Liu, W.-D., Ulm, K., Quante, M., Li, Z.-X., Zhou, T., Schmid, R., Classen, M., Li, W.-Q., You, W.-C., & Pan, K.-F. (2020). **Effect of Helicobacter pylori on gastrointestinal microbiota: A population-based study in Linqu, a high-risk area of gastric cancer.** *Gut*, *69*(9), 1598–1607. https://doi.org/10.1136/gutjnl-2019-319696

Han, Y., Chen, W., Li, P., & Ye, J. (**2015**). **Association between coeliac disease and risk of any malignancy and gastrointestinal malignancy.** *Medicine*, *94*(38). https://doi.org/10.1097/MD.0000000000001612

Haniffa, M., Shin, A., Bigley, V., McGovern, N., Teo, P., See, P., Wasan, P. S., Wang, X.-N., Malinarich, F., Malleret, B., Larbi, A., Tan, P., Zhao, H., Poidinger, M., Pagan, S., Cookson, S., Dickinson, R., Dimmick, I., Jarrett, R. F., Ginhoux, F. (**2012**). **Human tissues contain CD141hi cross-presenting dendritic cells with functional homology to mouse CD103+ nonlymphoid dendritic cells.** *Immunity*, *37*(1), 60–73. https://doi.org/10.1016/j.immuni.2012.04.012

Hasegawa, M., Kamada, N., Jiao, Y., Liu, M. Z., Núñez, G., & Inohara, N. (**2012**). **Protective role of commensals against Clostridium difficile infection via an IL-1β-mediated positive feedback loop.** *Journal of Immunology (Baltimore, Md. : 1950)*, *189*(6), 3085–3091. https://doi.org/10.4049/jimmunol.1200821

He, B., Liu, Y., Hoang, T. K., Tian, X., Taylor, C. M., Luo, M., Tran, D. Q., Tatevian, N., & Rhoads, J. M. (**2019**). **Antibiotic-modulated microbiome suppresses lethal inflammation and prolongs lifespan in Treg-deficient mice.** *Microbiome*, *7*(1), 145. https://doi.org/10.1186/s40168-019-0751-1

He, Z., Gharaibeh, R. Z., Newsome, R. C., Pope, J. L., Dougherty, M. W., Tomkovich, S., Pons, B., Mirey, G., Vignard, J., Hendrixson, D. R., & Jobin, C. (**2019**). C**ampylobacter jejuni promotes colorectal tumorigenesis through the action of cytolethal distending toxin.** *Gut*, *68*(2), 289–300. https://doi.org/10.1136/gutjnl-2018-317200

Huang, X.-Z., Gao, P., Song, Y.-X., Xu, Y., Sun, J.-X., Chen, X.-W., Zhao, J.-H., & Wang, Z.-N. (**2019**). **Antibiotic use and the efficacy of immune checkpoint inhibitors in cancer patients: A pooled analysis of 2740 cancer patients.** *Oncoimmunology*, *8*(12). https://doi.org/10.1080/2162402X.2019.1665973

Iida, N., Dzutsev, A., Stewart, C. A., Smith, L., Bouladoux, N., Weingarten, R. A., Molina, D. A., Salcedo, R., Back, T., Cramer, S., Dai, R.-M., Kiu, H., Cardone, M., Naik, S., Patri, A. K., Wang, E., Marincola, F. M., Frank, K. M., Belkaid, Y., Goldszmid, R. S. (**2013**). C**ommensal bacteria control cancer response to therapy by modulating the tumor microenvironment.** *Science*, *342*(6161), 967–970. https://doi.org/10.1126/science.1240527

Ivanov, I. I., Atarashi, K., Manel, N., Brodie, E. L., Shima, T., Karaoz, U., Wei, D., Goldfarb, K. C., Santee, C. A., Lynch, S. V., Tanoue, T., Imaoka, A., Itoh, K., Takeda, K., Umesaki, Y., Honda, K., & Littman, D. R. (**2009**). **Induction of intestinal Th17 cells by segmented filamentous bacteria**. *Cell*, *139*(3), 485–498. https://doi.org/10.1016/j.cell.2009.09.033

Ivanov, I. I., de Llanos Frutos, R., Manel, N., Yoshinaga, K., Rifkin, D. B., Sartor, R. B., Finlay, B. B., & Littman, D. R. (**2008**). **Specific microbiota direct the differentiation of Th17 cells in the mucosa of the small intestine.** *Cell Host & Microbe*, *4*(4), 337–349. https://doi.org/10.1016/j.chom.2008.09.009

Jablonski, K. A., Amici, S. A., Webb, L. M., Ruiz-Rosado, J. de D., Popovich, P. G., Partida-Sanchez, S., & Guerau-de-Arellano, M. (**2015**). **Novel markers to delineate murine M1 and M2 macrophages.** *PLOS ONE*, *10*(12), e0145342. https://doi.org/10.1371/journal.pone.0145342

Jana, A., Krett, N. L., Guzman, G., Khalid, A., Ozden, O., Staudacher, J. J., Bauer, J., Baik, S. H., Carroll, T., Yazici, C., & Jung, B. (2017). **NFkB is essential for activin-induced colorectal cancer migration via upregulation of PI3K-MDM2 pathway.** *Oncotarget*, *8*(23), 37377–37393. https://doi.org/10.18632/oncotarget.16343

Jang, S.-O., Kim, H.-J., Kim, Y.-J., Kang, M.-J., Kwon, J.-W., Seo, J.-H., Kim, H. Y., Kim, B.-J., Yu, J., & Hong, S.-J. (**2012**). **Asthma prevention by Lactobacillus Rhamnosus in a mouse model is associated with CD4(+)CD25(+)Foxp3(+) T Cells**. *Allergy, Asthma & Immunology Research*, *4*(3), 150–156. https://doi.org/10.4168/aair.2012.4.3.150

Jepson, M. A., Clark, M. A., Simmons, N. L., & Hirst, B. H. (**1993**). **Actin accumulation at sites of attachment of indigenous apathogenic segmented filamentous bacteria to mouse ileal epithelial cells.** *Infection and Immunity*, *61*(9), 4001–4004. https://doi.org/10.1128/IAI.61.9.4001-4004.1993

Jiménez, E., Marín, M. L., Martín, R., Odriozola, J. M., Olivares, M., Xaus, J., Fernández, L., & Rodríguez, J. M. (**2008**). **Is meconium from healthy newborns actually sterile?** *Research in Microbiology*, *159*(3), 187–193. https://doi.org/10.1016/j.resmic.2007.12.007

Jin, Y., Dong, H., Xia, L., Yang, Y., Zhu, Y., Shen, Y., Zheng, H., Yao, C., Wang, Y., & Lu, S. (**2019**). **The diversity of gut microbiome is associated with favorable responses to anti–programmed death 1 immunotherapy in Chinese patients with NSCLC.** *Journal of Thoracic Oncology*, *14*(8), 1378–1389. https://doi.org/10.1016/j.jtho.2019.04.007

Jonsson, H., Hugerth, L. W., Sundh, J., Lundin, E., & Andersson, A. F. (**2020**). **Genome sequence of segmented filamentous bacteria present in the human intestine.** *Communications Biology*, *3*(1), 1–9. https://doi.org/10.1038/s42003-020-01214-7

***Jorgovanovic, D.**, Song, M., Wang, L., & Zhang, Y. (**2020**). **Roles of IFN-γ in tumor progression and regression: A review.** *Biomarker Research*, *8*. https://doi.org/10.1186/s40364-020-00228-x

Juneja, V. R., McGuire, K. A., Manguso, R. T., LaFleur, M. W., Collins, N., Haining, W. N., Freeman, G. J., & Sharpe, A. H. (**2017**). **PD-L1 on tumor cells is sufficient for immune evasion in immunogenic tumors and inhibits CD8 T cell cytotoxicity.** *The Journal of Experimental Medicine*, *214*(4), 895–904. https://doi.org/10.1084/jem.20160801

Kamada, T., Togashi, Y., Tay, C., Ha, D., Sasaki, A., Nakamura, Y., Sato, E., Fukuoka, S., Tada, Y., Tanaka, A., Morikawa, H., Kawazoe, A., Kinoshita, T., Shitara, K., Sakaguchi, S., & Nishikawa, H. (**2019**). **PD-1+ regulatory T cells amplified by PD-1 blockade promote hyperprogression of cancer.** *Proceedings of the National Academy of Sciences*, *116*(20), 9999–10008. https://doi.org/10.1073/pnas.1822001116

Kang, D.-W., Adams, J. B., Coleman, D. M., Pollard, E. L., Maldonado, J., McDonough-Means, S., Caporaso, J. G., & Krajmalnik-Brown, R. (**2019**). **Long-term benefit of microbiota transfer therapy on autism symptoms and gut microbiota.** *Scientific Reports*, *9*. https://doi.org/10.1038/s41598-019-42183-0

Klare, I., Konstabel, C., Werner, G., Huys, G., Vankerckhoven, V., Kahlmeter, G., Hildebrandt, B., Müller-Bertling, S., Witte, W., & Goossens, H. (**2007**). **Antimicrobial susceptibilities of Lactobacillus, Pediococcus and Lactococcus human isolates and cultures intended for probiotic or nutritional use.** *Journal of Antimicrobial Chemotherapy*, *59*(5), 900–912. https://doi.org/10.1093/jac/dkm035

Klimesova, K., Kverka, M., Zakostelska, Z., Hudcovic, T., Hrncir, T., Stepankova, R., Rossmann, P., Ridl, J., Kostovcik, M., Mrazek, J., Kopecny, J., Kobayashi, K. S., & Tlaskalova-Hogenova, H. (**2013**). A**ltered gut microbiota promotes colitis-associated cancer in IL-1 receptor-associated kinase M deficient mice.** *Inflammatory Bowel Diseases*, *19*(6), 1266–1277. https://doi.org/10.1097/MIB.0b013e318281330a

Knoop, K. A., McDonald, K. G., Kulkarni, D. H., & Newberry, R. D. (**2016**). **Antibiotics promote inflammation through the translocation of native commensal colonic bacteria.** *Gut*, *65*(7), 1100–1109. https://doi.org/10.1136/gutjnl-2014-309059

Kong, C., Gao, R., Yan, X., Huang, L., & Qin, H. (**2019**). **Probiotics improve gut microbiota dysbiosis in obese mice fed a high-fat or high-sucrose diet.** *Nutrition (Burbank, Los Angeles County, Calif.)*, *60*, 175–184. https://doi.org/10.1016/j.nut.2018.10.002

***Konstantinidis, T.**, Tsigalou, C., Karvelas, A., Stavropoulou, E., Voidarou, C., & Bezirtzoglou, E. (**2020**). **Effects of Antibiotics upon the Gut Microbiome: A Review of the Literature.** *Biomedicines*, *8*(11). https://doi.org/10.3390/biomedicines8110502

Korn, T., Mitsdoerffer, M., Croxford, A. L., Awasthi, A., Dardalhon, V. A., Galileos, G., Vollmar, P., Stritesky, G. L., Kaplan, M. H., Waisman, A., Kuchroo, V. K., & Oukka, M. (**2008**). **IL-6 controls Th17 immunity in**

vivo by inhibiting the conversion of conventional T cells into Foxp3+ regulatory T cells. *Proceedings of the National Academy of Sciences*, *105*(47), 18460–18465. https://doi.org/10.1073/pnas.0809850105

Korpela, K., Salonen, A., Virta, L. J., Kekkonen, R. A., Forslund, K., Bork, P., & de Vos, W. M. (**2016**). **Intestinal microbiome is related to lifetime antibiotic use in Finnish pre-school children.** *Nature Communications*, *7*. https://doi.org/10.1038/ncomms10410

Kovács, T., Mikó, E., Vida, A., Sebő, É., Toth, J., Csonka, T., Boratkó, A., Ujlaki, G., Lente, G., Kovács, P., Tóth, D., Árkosy, P., Kiss, B., Méhes, G., Goedert, J. J., & Bai, P. (**2019**). **Cadaverine, a metabolite of the microbiome, reduces breast cancer aggressiveness through trace amino acid receptors.** *Scientific Reports*, *9*(1), 1300. https://doi.org/10.1038/s41598-018-37664-7

***Kovaleva, O.** V., Romashin, D., Zborovskaya, I. B., Davydov, M. M., Shogenov, M. S., & Gratchev, A. (**2019**). **Human lung microbiome on the way to cancer.** *Journal of Immunology Research*, *2019*. https://doi.org/10.1155/2019/1394191

Ku, H.-J., & Lee, Y.-T. K. and J.-H. (**2020**). **Microbiome study of initial gut microbiota from newborn infants to children reveals that diet determines its compositional development.** *Journal of Microbiology and Biotechnology 30*(7), 1067–1071. https://doi.org/10.4014/jmb.2002.02042

Kuang, D.-M., Zhao, Q., Wu, Y., Peng, C., Wang, J., Xu, Z., Yin, X.-Y., & Zheng, L. (**2011**). **Peritumoral neutrophils link inflammatory response to disease progression by fostering angiogenesis in hepatocellular carcinoma.** *Journal of Hepatology*, *54*(5), 948–955. https://doi.org/10.1016/j.jhep.2010.08.041

Kulkarni, D. H., Gustafsson, J. K., Knoop, K. A., McDonald, K. G., Bidani, S. S., Davis, J. E., Floyd, A. N., Hogan, S. P., Hsieh, C.-S., & Newberry, R. D. (**2020**). **Goblet cell associated antigen passages support the induction and maintenance of oral tolerance.** *Mucosal Immunology*, *13*(2), 271–282. https://doi.org/10.1038/s41385-019-0240-7

Kumagai, S., Togashi, Y., Kamada, T., Sugiyama, E., Nishinakamura, H., Takeuchi, Y., Vitaly, K., Itahashi, K., Maeda, Y., Matsui, S., Shibahara, T., Yamashita, Y., Irie, T., Tsuge, A., Fukuoka, S., Kawazoe, A., Udagawa, H., Kirita, K., Aokage, K., Nishikawa, H. (**2020**). **The PD-1 expression balance between effector and regulatory T cells predicts the clinical efficacy of PD-1 blockade therapies.** *Nature Immunology*, *21*(11), 1346–1358. https://doi.org/10.1038/s41590-020-0769-3

Kverka, M., Zakostelska, Z., Klimesova, K., Sokol, D., Hudcovic, T., Hrncir, T., Rossmann, P., Mrazek, J., Kopecny, J., Verdu, E. F., & Tlaskalova-Hogenova, H. (**2011**). **Oral administration of Parabacteroides distasonis antigens attenuates experimental murine colitis through modulation of immunity and microbiota composition.** *Clinical and Experimental Immunology*, *163*(2), 250–259. https://doi.org/10.1111/j.1365-2249.2010.04286.x

Lal, D., Keim, P., Delisle, J., Barker, B., Rank, M. A., Chia, N., Schupp, J. M., Gillece, J. D., & Cope, E. K. (**2017**). **Mapping and comparing bacterial microbiota in the sinonasal cavity of healthy, allergic rhinitis, and chronic rhinosinusitis subjects.** *International Forum of Allergy & Rhinology*, *7*(6), 561–569. https://doi.org/10.1002/alr.21934

Lécuyer, E., Rakotobe, S., Lengliné-Garnier, H., Lebreton, C., Picard, M., Juste, C., Fritzen, R., Eberl, G., McCoy, K. D., Macpherson, A. J., Reynaud, C.-A., Cerf-Bensussan, N., & Gaboriau-Routhiau, V. (**2014**). **Segmented filamentous bacterium uses secondary and tertiary lymphoid tissues to induce gut IgA and specific T helper 17 cell responses.** *Immunity*, *40*(4), 608–620. https://doi.org/10.1016/j.immuni.2014.03.009

Lehmann, F. M., von Burg, N., Ivanek, R., Teufel, C., Horvath, E., Peter, A., Turchinovich, G., Staehli, D., Eichlisberger, T., Gomez de Agüero, M., Coto-Llerena, M., Prchal-Murphy, M., Sexl, V., Bentires-Alj, M., Mueller, C., & Finke, D. (**2020**). **Microbiota-induced tissue signals regulate ILC3-mediated antigen presentation.** *Nature Communications*, *11*. https://doi.org/10.1038/s41467-020-15612-2

Li, W., Wang, W., Zuo, R., Liu, C., Shu, Q., Ying, H., & Sun, K. (**2017**). **Induction of pro-inflammatory genes by serum amyloid A1 in human amnion fibroblasts.** *Scientific Reports*, *7*(1), 693. https://doi.org/10.1038/s41598-017-00782-9

***Li, Y.**, Jin, L., & Chen, T. (**2020**). **The effects of secretory IgA in the mucosal immune system.** *BioMed Research International*, *2020*, 2032057. https://doi.org/10.1155/2020/2032057

Liu, R., Li, P., Bi, C. W., Ma, R., Yin, Y., Bi, K., & Li, Q. (**2017**). **Plasma N-acetylputrescine, cadaverine and 1,3-diaminopropane: Potential biomarkers of lung cancer used to evaluate the efficacy of anticancer drugs.** *Oncotarget*, *8*(51), 88575–88585. https://doi.org/10.18632/oncotarget.19304

Liu, T., Peng, L., Yu, P., Zhao, Y., Shi, Y., Mao, X., Chen, W., Cheng, P., Wang, T., Chen, N., Zhang, J., Liu, X., Li, N., Guo, G., Tong, W., Zhuang, Y., & Zou, Q. (**2012**). **Increased circulating Th22 and Th17 cells are associated with tumor progression and patient survival in human gastric cancer.** *Journal of Clinical Immunology*, *32*(6), 1332–1339. https://doi.org/10.1007/s10875-012-9718-8

***Lozupone, C. A.**, Stombaugh, J. I., Gordon, J. I., Jansson, J. K., & Knight, R. (**2012**). **Diversity, stability and resilience of the human gut microbiota.** *Nature*, *489*(7415), 220–230. https://doi.org/10.1038/nature11550

Lugli, G. A., Duranti, S., Milani, C., Mancabelli, L., Turroni, F., Alessandri, G., Longhi, G., Anzalone, R., Viappinai, A., Tarracchini, C., Bernasconi, S., Yonemitsu, C., Bode, L., Goran, M. I., Ossiprandi, M. C., van Sinderen, D., & Ventura, M. (**2020**). I**nvestigating bifidobacteria and human milk oligosaccharide composition of lactating mothers.** *FEMS Microbiology Ecology*, *96*(5). https://doi.org/10.1093/femsec/fiaa049

Lynch, T. J., Bondarenko, I., Luft, A., Serwatowski, P., Barlesi, F., Chacko, R., Sebastian, M., Neal, J., Lu, H., Cuillerot, J.-M., & Reck, M. (**2012**). **Ipilimumab in combination with paclitaxel and carboplatin as first-line treatment in stage IIIB/IV non-small-cell lung cancer: Results from a randomized, double-blind, multicenter phase II study.** *Journal of Clinical Oncology:30*(17), 2046–2054. https://doi.org/10.1200/JCO.2011.38.4032

Ma, C., Han, M., Heinrich, B., Fu, Q., Zhang, Q., Sandhu, M., Agdashian, D., Terabe, M., Berzofsky, J. A., Fako, V., Ritz, T., Longerich, T., Theriot, C. M., McCulloch, J. A., Roy, S., Yuan, W., Thovarai, V., Sen, S. K., Ruchirawat, M., Greten, T. F. (**2018**). **Gut microbiome-mediated bile acid metabolism regulates liver cancer via NKT cells.** *Science (New York, N.Y.)*, *360*(6391). https://doi.org/10.1126/science.aan5931

Ma, J., Li, Z., Zhang, W., Zhang, C., Zhang, Y., Mei, H., Zhuo, N., Wang, H., Wang, L., & Wu, D. (**2020**). **Comparison of gut microbiota in exclusively breast-fed and formula-fed babies: A study of 91 term infants**. *Scientific Reports*, *10*(1), 15792. https://doi.org/10.1038/s41598-020-72635-x

Mager, L. F., Burkhard, R., Pett, N., Cooke, N. C. A., Brown, K., Ramay, H., Paik, S., Stagg, J., Groves, R. A., Gallo, M., Lewis, I. A., Geuking, M. B., & McCoy, K. D. (**2020**). **Microbiome-derived inosine modulates response to checkpoint inhibitor immunotherapy.** *Science*, *369*(6510), 1481–1489. https://doi.org/10.1126/science.abc3421

Matson, V., Fessler, J., Bao, R., Chongsuwat, T., Zha, Y., Alegre, M.-L., Luke, J. J., & Gajewski, T. F. (**2018**). **The commensal microbiome is associated with anti-PD-1 efficacy in metastatic melanoma patients.** *Science (New York, N.Y.)*, *359*(6371), 104–108. https://doi.org/10.1126/science.aao3290

Mazmanian, S. K., Round, J. L., & Kasper, D. L. (**2008**). **A microbial symbiosis factor prevents intestinal inflammatory disease.** *Nature*, *453*(7195), 620–625. https://doi.org/10.1038/nature07008

McAleer, J. P., Nguyen, N. L. H., Chen, K., Kumar, P., Ricks, D. M., Binnie, M., Armentrout, R. A., Pociask, D. A., Hein, A., Yu, A., Vikram, A., Bibby, K., Umesaki, Y., Rivera, A., Sheppard, D., Ouyang, W., Hooper, L. V., & Kolls, J. K. (**2016**). **Pulmonary Th17 anti-fungal immunity is regulated by the gut microbiome.** *Journal of Immunology, 197*(1), 97–107. https://doi.org/10.4049/jimmunol.1502566

Morgan, R. N., Saleh, S. E., Farrag, H. A., & Aboulwafa, M. M. (**2019**). **Prevalence and pathologic effects of colibactin and cytotoxic necrotizing factor-1 (Cnf 1) in Escherichia coli: Experimental and bioinformatics analyses.** *Gut Pathogens*, *11*. https://doi.org/10.1186/s13099-019-0304-y

Münch, N. S., Fang, H.-Y., Ingermann, J., Maurer, H. C., Anand, A., Kellner, V., Sahm, V., Wiethaler, M., Baumeister, T., Wein, F., Einwächter, H., Bolze, F., Klingenspor, M., Haller, D., Kavanagh, M., Lysaght, J., Friedman, R., Dannenberg, A. J., Pollak, M., Quante, M. (**2019**). **High-fat diet accelerates carcinogenesis in a mouse model of Barrett's esophagus via interleukin 8 and alterations to the gut microbiome.** *Gastroenterology*, *157*(2), 492-506.e2. https://doi.org/10.1053/j.gastro.2019.04.013

Nejman, D., Livyatan, I., Fuks, G., Gavert, N., Zwang, Y., Geller, L. T., Rotter-Maskowitz, A., Weiser, R., Mallel, G., Gigi, E., Meltser, A., Douglas, G. M., Kamer, I., Gopalakrishnan, V., Dadosh, T., Levin-Zaidman, S., Avnet, S., Atlan, T., Cooper, Z. A., Straussman, R. (**2020**). **The human tumor microbiome is composed of tumor type–specific intracellular bacteria.** *Science*, *368*(6494), 973–980. https://doi.org/10.1126/science.aay9189

***Neuman, H.**, Forsythe, P., Uzan, A., Avni, O., & Koren, O. (**2018**). **Antibiotics in early life: Dysbiosis and the damage done.** *FEMS Microbiology Reviews*, *42*(4), 489–499. https://doi.org/10.1093/femsre/fuy018

Niu, C., Li, M., Zhu, S., Chen, Y., Zhou, L., Xu, D., Xu, J., Li, Z., Li, W., & Cui, J. (**2020**). **PD-1-positive natural killer cells have a weaker antitumor function than that of PD-1-negative natural killer cells in lung cancer.** *International Journal of Medical Sciences*, *17*(13), 1964–1973. https://doi.org/10.7150/ijms.47701

Nomura, M., Nagatomo, R., Doi, K., Shimizu, J., Baba, K., Saito, T., Matsumoto, S., Inoue, K., & Muto, M. (**2020**). **Association of short-chain fatty acids in the gut microbiome with clinical response to treatment with nivolumab or pembrolizumab in patients with solid cancer tumors.** *JAMA Network Open*, *3*(4). https://doi.org/10.1001/jamanetworkopen.2020.2895

Okada, M., Shimizu, K., Iyoda, T., Ueda, S., Shinga, J., Mochizuki, Y., Watanabe, T., Ohara, O., & Fujii, S. (**2020**). **PD-L1 expression affects neoantigen presentation.** *IScience*, *23*(6). https://doi.org/10.1016/j.isci.2020.101238

Pahl, J. H. W., Koch, J., Götz, J.-J., Arnold, A., Reusch, U., Gantke, T., Rajkovic, E., Treder, M., & Cerwenka, A. **(2018**). **CD16A activation of NK cells promotes NK cell proliferation and memory-like cytotoxicity against cancer cells.** *Cancer Immunology Research*, *6*(5), 517–527. https://doi.org/10.1158/2326-6066.CIR-17-0550

Palleja, A., Mikkelsen, K. H., Forslund, S. K., Kashani, A., Allin, K. H., Nielsen, T., Hansen, T. H., Liang, S., Feng, Q., Zhang, C., Pyl, P. T., Coelho, L. P., Yang, H., Wang, J., Typas, A., Nielsen, M. F., Nielsen, H. B., Bork, P., Wang, J., Pedersen, O. (**2018**). **Recovery of gut microbiota of healthy adults following antibiotic exposure.** *Nature Microbiology*, *3*(11), 1255–1265. https://doi.org/10.1038/s41564-018-0257-9

Paulos, C. M., Wrzesinski, C., Kaiser, A., Hinrichs, C. S., Chieppa, M., Cassard, L., Palmer, D. C., Boni, A., Muranski, P., Yu, Z., Gattinoni, L., Antony, P. A., Rosenberg, S. A., & Restifo, N. P. (**2007**). **Microbial translocation augments the function of adoptively transferred self/tumor-specific CD8+ T cells via TLR4 signaling.** *Journal of Clinical Investigation*, *117*(8), 2197–2204. https://doi.org/10.1172/JCI32205

Pichery, M., Mirey, E., Mercier, P., Lefrancais, E., Dujardin, A., Ortega, N., & Girard, J.-P. (**2012**). **Endogenous IL-33 is highly expressed in mouse epithelial barrier tissues, lymphoid organs, brain, embryos, and inflamed tissues: In situ analysis using a novel Il-33-LacZ gene trap reporter strain.** *Journal of Immunology*, *188*(7), 3488–3495. https://doi.org/10.4049/jimmunol.1101977

***Plottel, C. S., & Blaser, M. J.** (**2011**). **Microbiome and Malignancy**. *Cell Host & Microbe*, *10*(4), 324–335. https://doi.org/10.1016/j.chom.2011.10.003

Proctor, L. M., Creasy, H. H., Fettweis, J. M., Lloyd-Price, J., Mahurkar, A., Zhou, W., Buck, G. A., Snyder, M. P., Strauss, J. F., Weinstock, G. M., White, O., Huttenhower, C. (**2019**). **The integrative human microbiome project.** *Nature*, *569*(7758), 641–648. https://doi.org/10.1038/s41586-019-1238-8

Pushalkar, S., Hundeyin, M., Daley, D., Zambirinis, C. P., Kurz, E., Mishra, A., Mohan, N., Aykut, B., Usyk, M., Torres, L. E., Werba, G., Zhang, K., Guo, Y., Li, Q., Akkad, N., Lall, S., Wadowski, B., Gutierrez, J., Kochen Rossi, J. A., Miller, G. (**2018**). **The pancreatic cancer microbiome promotes oncogenesis by induction of innate and adaptive immune suppression.** *Cancer Discovery*, *8*(4), 403–416. https://doi.org/10.1158/2159-8290.CD-17-1134

Qin, J., Li, R., Raes, J., Arumugam, M., Burgdorf, K. S., Manichanh, C., Nielsen, T., Pons, N., Levenez, F., Yamada, T., Mende, D. R., Li, J., Xu, J., Li, S., Li, D., Cao, J., Wang, B., Liang, H., Zheng, H., Wang, J. (**2010**). **A human gut microbial gene catalogue established by metagenomic sequencing.** *Nature*, *464*(7285), 59–65. https://doi.org/10.1038/nature08821

***Quatrini, L.**, Mariotti, F. R., Munari, E., Tumino, N., Vacca, P., & Moretta, L. (**2020**). **The immune checkpoint PD-1 in natural killer cells: expression, function and targeting in tumour immunotherapy.** *Cancers*, *12*(11). https://doi.org/10.3390/cancers12113285

***Raskov, H.**, Burcharth, J., & Pommergaard, H.-C. (**2017**). **Linking gut microbiota to colorectal cancer.** *Journal of Cancer*, *8*(17), 3378–3395. https://doi.org/10.7150/jca.20497

Reck, M., Rodríguez-Abreu, D., Robinson, A. G., Hui, R., Csőszi, T., Fülöp, A., Gottfried, M., Peled, N., Tafreshi, A., Cuffe, S., O'Brien, M., Rao, S., Hotta, K., Leiby, M. A., Lubiniecki, G. M., Shentu, Y., Rangwala, R., & Brahmer, J. R. (**2016**). **Pembrolizumab versus chemotherapy for PD-L1–positive non–small-cell lung cancer**; *Massachusetts Medical Society*, https://doi.org/10.1056/NEJMoa1606774

Riquelme, E., Zhang, Y., Zhang, L., Montiel, M., Zoltan, M., Dong, W., Quesada, P., Sahin, I., Chandra, V., Lucas, A. S., Scheet, P., Xu, H., Hanash, S. M., Feng, L., Burks, J. K., Do, K.-A., Peterson, C. B., Nejman, D., Tzeng, C.-W. D., McAllister, F. (**2019**). **Tumor microbiome diversity and composition influence pancreatic cancer outcomes.** *Cell*, *178*(4), 795-806.e12. https://doi.org/10.1016/j.cell.2019.07.008

Robert, C., Schachter, J., Long, G. V., Arance, A., Grob, J. J., Mortier, L., Daud, A., Carlino, M. S., McNeil, C., Lotem, M., Larkin, J., Lorigan, P., Neyns, B., Blank, C. U., Hamid, O., Mateus, C., Shapira-Frommer, R., Kosh, M., Zhou, H., Ribas, A. (**2015**). **Pembrolizumab versus Ipilimumab in Advanced Melanoma.** *New England Journal of Medicine*, *372*(26), 2521–2532. https://doi.org/10.1056/NEJMoa1503093

***Rotte, A.** (**2019**). **Combination of CTLA-4 and PD-1 blockers for treatment of cancer.** *Journal of Experimental & Clinical Cancer Research*, *38*(1), 255. https://doi.org/10.1186/s13046-019-1259-z

***Round, J. L., & Mazmanian, S. K.** (**2009**). **The gut microbiome shapes intestinal immune responses during health and disease.** *Nature Reviews. Immunology*, *9*(5), 313–323. https://doi.org/10.1038/nri2515

Routy, B., Chatelier, E. L., Derosa, L., Duong, C. P. M., Alou, M. T., Daillère, R., Fluckiger, A., Messaoudene, M., Rauber, C., Roberti, M. P., Fidelle, M., Flament, C., Poirier-Colame, V., Opolon, P., Klein, C., Iribarren, K., Mondragón, L., Jacquelot, N., Qu, B., Zitvogel, L. (**2018**). **Gut microbiome influences efficacy of PD-1–based immunotherapy against epithelial tumors.** *Science*, *359*(6371), 91–97. https://doi.org/10.1126/science.aan3706

Rubinstein, M. R., Baik, J. E., Lagana, S. M., Han, R. P., Raab, W. J., Sahoo, D., Dalerba, P., Wang, T. C., & Han, Y. W. (**2019**). **Fusobacterium nucleatum promotes colorectal cancer by inducing Wnt/β-catenin modulator Annexin A1.** *EMBO Reports*, *20*(4). https://doi.org/10.15252/embr.201847638

Rutter, M. D., Saunders, B. P., Wilkinson, K. H., Rumbles, S., Schofield, G., Kamm, M. A., Williams, C. B., Price, A. B., Talbot, I. C., & Forbes, A. (**2004**). C**ancer surveillance in longstanding ulcerative colitis:**

endoscopic appearances help predict cancer risk. *Gut*, *53*(12), 1813–1816. https://doi.org/10.1136/gut.2003.038505

Sano, T., Huang, W., Hall, J. A., Yang, Y., Chen, A., Gavzy, S. J., Lee, J.-Y., Ziel, J., Miraldi, E. R., Bonneau, R., & Littman, D. R. (**2015**). **An IL-23R/IL-22 circuit regulates epithelial serum amyloid A to promote local effector Th17 responses.** *Cell*, *163*(2), 381–393. https://doi.org/10.1016/j.cell.2015.08.061

Scandiuzzi, L., Ghosh, K., Hofmeyer, K. A., Abadi, Y. M., Lázár-Molnár, E., Lin, E. Y., Liu, Q., Jeon, H., Almo, S. C., Chen, L., Nathenson, S. G., & Zang, X. (**2014**). **Tissue-expressed B7-H1 critically controls intestinal inflammation.** *Cell Reports*, *6*(4), 625–632. https://doi.org/10.1016/j.celrep.2014.01.020

***Schreiber, R. D**., Old, L. J., & Smyth, M. J. (**2011**). **Cancer Immunoediting: Integrating Immunity's Roles in Cancer Suppression and Promotion.** *Science*, *331*(6024), 1565–1570. https://doi.org/10.1126/science.1203486

Schroeder, B. O., Birchenough, G. M. H., Ståhlman, M., Arike, L., Johansson, M. E. V., Hansson, G. C., & Bäckhed, F. (**2018**). **Bifidobacteria or fiber protects against diet-induced microbiota-mediated colonic mucus deterioration.** *Cell Host & Microbe*, *23*(1), 27-40.e7. https://doi.org/10.1016/j.chom.2017.11.004

***Schwabe, R. F., & Jobin, C.** (**2013**). **The microbiome and cancer.** *Nature Reviews. Cancer*, *13*(11), 800–812. https://doi.org/10.1038/nrc3610

***Seidel, J. A.**, Otsuka, A., & Kabashima, K. (**2018**). **Anti-PD-1 and anti-CTLA-4 therapies in cancer: mechanisms of action, efficacy, and limitations.** *Frontiers in Oncology*, *8*. https://doi.org/10.3389/fonc.2018.00086

Sender, R., Fuchs, S., & Milo, R. (**2016**). **Are we really vastly outnumbered? Revisiting the ratio of bacterial to host cells in humans.** *Cell*, *164*(3), 337–340. https://doi.org/10.1016/j.cell.2016.01.013

Sheng, K.-C., Day, S., Wright, M. D., Stojanovska, L., & Apostolopoulos, V. (**2013**). **Enhanced dendritic cell-mediated antigen-specific CD4+ T cell responses: IFN-gamma aids TLR stimulation.** *Journal of Drug Delivery*, *2013*, e516749. https://doi.org/10.1155/2013/516749

Shi, Y., Zheng, W., Yang, K., Harris, K. G., Ni, K., Xue, L., Lin, W., Chang, E. B., Weichselbaum, R. R., & Fu, Y.-X. (**2020**). **Intratumoral accumulation of gut microbiota facilitates CD47-based immunotherapy via STING signaling.** *Journal of Experimental Medicine*, *217*(e20192282). https://doi.org/10.1084/jem.20192282

Simard, J.-C., Cesaro, A., Chapeton-Montes, J., Tardif, M., Antoine, F., Girard, D., & Tessier, P. A. (**2013**). **S100A8 and S100A9 induce cytokine expression and regulate the NLRP3 inflammasome via ROS-dependent activation of NF-κB1.** *PLOS ONE*, *8*(8), e72138. https://doi.org/10.1371/journal.pone.0072138

Sivan, A., Corrales, L., Hubert, N., Williams, J. B., Aquino-Michaels, K., Earley, Z. M., Benyamin, F. W., Lei, Y. M., Jabri, B., Alegre, M.-L., Chang, E. B., & Gajewski, T. F. (**2015**). **Commensal Bifidobacterium promotes antitumor immunity and facilitates anti–PD-L1 efficacy.** *Science, 350*(6264), 1084–1089. https://doi.org/10.1126/science.aac4255

***Sorbara, M. T.**, & Pamer, E. G. (**2019**). **Interbacterial mechanisms of colonization resistance and the strategies pathogens use to overcome them.** *Mucosal Immunology*, *12*(1), 1–9. https://doi.org/10.1038/s41385-018-0053-0

***Srikrishna, G.** (**2011**). **S100A8 and S100A9: new insights into their roles in malignancy.** *Journal of Innate Immunity*, *4*(1), 31–40. https://doi.org/10.1159/000330095

Stehlikova, Z., Kostovcikova, K., Kverka, M., Rossmann, P., Dvorak, J., Novosadova, I., Kostovcik, M., Coufal, S., Srutkova, D., Prochazkova, P., Hudcovic, T., Kozakova, H., Stepankova, R., Rob, F., Juzlova, K., Hercogova, J., Tlaskalova-Hogenova, H., & Jiraskova Zakostelska, Z. (**2019**). **Crucial role of microbiota in**

experimental psoriasis revealed by a gnotobiotic mouse model. *Frontiers in Microbiology*, *10*. https://doi.org/10.3389/fmicb.2019.00236

Sugita, S., Kawazoe, Y., Imai, A., Yamada, Y., Horie, S., & Mochizuki, M. (**2012**). **Inhibition of Th17 differentiation by anti-TNF-alpha therapy in uveitis patients with Behçet's disease.** *Arthritis Research & Therapy*, *14*(3), R99. https://doi.org/10.1186/ar3824

Suzuki, K., Meek, B., Doi, Y., Muramatsu, M., Chiba, T., Honjo, T., & Fagarasan, S. (**2004**). **Aberrant expansion of segmented filamentous bacteria in IgA-deficient gut.** *Proceedings of the National Academy of Sciences*, *101*(7), 1981–1986. https://doi.org/10.1073/pnas.0307317101

Tan, T. G., Sefik, E., Geva-Zatorsky, N., Kua, L., Naskar, D., Teng, F., Pasman, L., Ortiz-Lopez, A., Jupp, R., Wu, H.-J. J., Kasper, D. L., Benoist, C., & Mathis, D. (**2016**). **Identifying species of symbiont bacteria from the human gut that, alone, can induce intestinal Th17 cells in mice.** *Proceedings of the National Academy of Sciences*, *113*(50), E8141–E8150. https://doi.org/10.1073/pnas.1617460113

Tanoue, T., Morita, S., Plichta, D. R., Skelly, A. N., Suda, W., Sugiura, Y., Narushima, S., Vlamakis, H., Motoo, I., Sugita, K., Shiota, A., Takeshita, K., Yasuma-Mitobe, K., Riethmacher, D., Kaisho, T., Norman, J. M., Mucida, D., Suematsu, M., Yaguchi, T., Honda, K. (**2019**). **A defined commensal consortium elicits CD8 T cells and anti-cancer immunity.** *Nature*, *565*(7741), 600–605. https://doi.org/10.1038/s41586-019-0878-z

Taylor, M. A., Hughes, A. M., Walton, J., Coenen-Stass, A. M. L., Magiera, L., Mooney, L., Bell, S., Staniszewska, A. D., Sandin, L. C., Barry, S. T., Watkins, A., Carnevalli, L. S., & Hardaker, E. L. (**2019**). **Longitudinal immune characterization of syngeneic tumor models to enable model selection for immune oncology drug discovery.** *Journal for ImmunoTherapy of Cancer*, *7*(1), 328. https://doi.org/10.1186/s40425-019-0794-7

Tomayko, M. M., & Reynolds, C. P. (**1989**). **Determination of subcutaneous tumor size in athymic (nude) mice.** *Cancer Chemotherapy and Pharmacology*, *24*(3), 148–154. https://doi.org/10.1007/BF00300234

Topalian, S. L., Hodi, F. S., Brahmer, J. R., Gettinger, S. N., Smith, D. C., McDermott, D. F., Powderly, J. D., Carvajal, R. D., Sosman, J. A., Atkins, M. B., Leming, P. D., Spigel, D. R., Antonia, S. J., Horn, L., Drake, C. G., Pardoll, D. M., Chen, L., Sharfman, W. H., Anders, R. A., Sznol, M. (**2012**). **Safety, activity, and immune correlates of anti–PD-1 antibody in cancer.** *New England Journal of Medicine*, *366*(26), 2443–2454. https://doi.org/10.1056/NEJMoa1200690

Tosolini, M., Kirilovsky, A., Mlecnik, B., Fredriksen, T., Mauger, S., Bindea, G., Berger, A., Bruneval, P., Fridman, W.-H., Pagès, F., & Galon, J. (**2011**). **Clinical impact of different classes of infiltrating T cytotoxic and helper cells (Th1, th2, treg, th17) in patients with colorectal cancer.** *Cancer Research*, *71*(4), 1263–1271. https://doi.org/10.1158/0008-5472.CAN-10-2907

Turnbaugh, P. J., Ley, R. E., Hamady, M., Fraser-Liggett, C. M., Knight, R., & Gordon, J. I. (**2007**). **The Human Microbiome Project.** *Nature*, *449*(7164), 804–810. https://doi.org/10.1038/nature06244

Urbaniak, C., Gloor, G. B., Brackstone, M., Scott, L., Tangney, M., & Reid, G. (**2016**). **The microbiota of breast tissue and its association with breast cancer.** *Applied and Environmental Microbiology*, *82*(16), 5039–5048. https://doi.org/10.1128/AEM.01235-16

***Vangay, P.**, Ward, T., Gerber, J. S., & Knights, D. (**2015**). **Antibiotics, pediatric dysbiosis, and disease.** *Cell Host & Microbe*, *17*(5), 553–564. https://doi.org/10.1016/j.chom.2015.04.006

Vétizou, M., Pitt, J. M., Daillère, R., Lepage, P., Waldschmitt, N., Flament, C., Rusakiewicz, S., Routy, B., Roberti, M. P., Duong, C. P. M., Poirier-Colame, V., Roux, A., Becharef, S., Formenti, S., Golden, E., Cording, S., Eberl, G., Schlitzer, A., Ginhoux, F., Zitvogel, L. (**2015**). **Anticancer immunotherapy by CTLA-4**

blockade relies on the gut microbiota. *Science*, *350*(6264), 1079–1084. https://doi.org/10.1126/science.aad1329

Viaud, S., Saccheri, F., Mignot, G., Yamazaki, T., Daillère, R., Hannani, D., Enot, D. P., Pfirschke, C., Engblom, C., Pittet, M. J., Schlitzer, A., Ginhoux, F., Apetoh, L., Chachaty, E., Woerther, P.-L., Eberl, G., Bérard, M., Ecobichon, C., Clermont, D., Zitvogel, L. (**2013**). **The intestinal microbiota modulates the anticancer immune effects of cyclophosphamide.** *Science*, *342*(6161), 971–976. https://doi.org/10.1126/science.1240537

Vonderheide, R. H., LoRusso, P. M., Khalil, M., Gartner, E. M., Khaira, D., Soulieres, D., Dorazio, P., Trosko, J. A., Rüter, J., Mariani, G. L., Usari, T., & Domchek, S. M. (**2010**). T**remelimumab in combination with exemestane in patients with advanced breast cancer and treatment-associated modulation of inducible costimulator expression on patient T cells.** *Clinical Cancer Research: An Official Journal of the American Association for Cancer Research*, *16*(13), 3485–3494. https://doi.org/10.1158/1078-0432.CCR-10-0505

Wang, G., Yu, G., Wang, D., Guo, S., & Shan, F. (**2017**). **Comparison of the purity and vitality of natural killer cells with different isolation kits.** *Experimental and Therapeutic Medicine*, *13*(5), 1875–1883. https://doi.org/10.3892/etm.2017.4189

Wang, H., Yao, H., Li, C., Liang, L., Zhang, Y., Shi, H., Zhou, C., Chen, Y., Fang, J.-Y., & Xu, J. (2017). **PD-L2 expression in colorectal cancer: Independent prognostic effect and targetability by deglycosylation.** *Oncoimmunology*, *6*(7). https://doi.org/10.1080/2162402X.2017.1327494

Wang, Z., Shaheen, N. J., Whiteman, D. C., Anderson, L. A., Vaughan, T. L., Corley, D. A., El-Serag, H. B., Rubenstein, J. H., & Thrift, A. P. (**2018**). **Helicobacter pylori infection is associated with reduced risk of Barrett's esophagus: An analysis of the Barrett's and Esophageal adenocarcinoma consortium.** *The American Journal of Gastroenterology*, *113*(8), 1148–1155. https://doi.org/10.1038/s41395-018-0070-3

Wolf, A. J., Arruda, A., Reyes, C. N., Kaplan, A. T., Shimada, T., Shimada, K., Arditi, M., Liu, G., & Underhill, D. M. (**2011**). **Phagosomal degradation increases TLR access to bacterial ligands and enhances macrophage sensitivity to bacteria.** *Journal of Immunology*, *187*(11), 6002–6010. https://doi.org/10.4049/jimmunol.1100232

***Wolf, A. J.**, Liu, G. Y., & Underhill, D. M. (**2017**). **Inflammatory properties of antibiotic-treated bacteria.** *Journal of Leukocyte Biology*, *101*(1), 127–134. https://doi.org/10.1189/jlb.4MR0316-153RR

Wu, H.-J., Ivanov, I. I., Darce, J., Hattori, K., Shima, T., Umesaki, Y., Littman, D. R., Benoist, C., & Mathis, D. (**2010**). **Gut-residing segmented filamentous bacteria drive autoimmune arthritis via T helper 17 cells**. *Immunity*, *32*(6), 815–827. https://doi.org/10.1016/j.immuni.2010.06.001

Xie, C., Yi, J., Lu, J., Nie, M., Huang, M., Rong, J., Zhu, Z., Chen, J., Zhou, X., Li, B., Chen, H., Lu, N., & Shu, X. (**2018**). **N-Acetylcysteine reduces ROS-mediated oxidative DNA damage and PI3K/Akt pathway activation induced by helicobacter pylori infection.** *Oxidative Medicine and Cellular Longevity*, *2018*, 1874985. https://doi.org/10.1155/2018/1874985

Xu, S., & Cao, X. (**2010**). **Interleukin-17 and its expanding biological functions.** *Cellular & Molecular Immunology*, *7*(3), 164–174. https://doi.org/10.1038/cmi.2010.21

Xu, X., Lv, J., Guo, F., Li, J., Jia, Y., Jiang, D., Wang, N., Zhang, C., Kong, L., Liu, Y., Zhang, Y., Lv, J., & Li, Z. (**2020**). **Gut microbiome influences the efficacy of PD-1 antibody immunotherapy on MSS-type colorectal cancer via metabolic pathway.** *Frontiers in Microbiology*, *11*. https://doi.org/10.3389/fmicb.2020.00814

Yachida, S., Mizutani, S., Shiroma, H., Shiba, S., Nakajima, T., Sakamoto, T., Watanabe, H., Masuda, K., Nishimoto, Y., Kubo, M., Hosoda, F., Rokutan, H., Matsumoto, M., Takamaru, H., Yamada, M., Matsuda, T.,

Iwasaki, M., Yamaji, T., Yachida, T., Yamada, T. (**2019**). **Metagenomic and metabolomic analyses reveal distinct stage-specific phenotypes of the gut microbiota in colorectal cancer.** *Nature Medicine*, *25*(6), 968–976. https://doi.org/10.1038/s41591-019-0458-7

Yang, Y., Misra, B. B., Liang, L., Bi, D., Weng, W., Wu, W., Cai, S., Qin, H., Goel, A., Li, X., & Ma, Y. (**2019**). **Integrated microbiome and metabolome analysis reveals a novel interplay between commensal bacteria and metabolites in colorectal cancer.** *Theranostics*, *9*(14), 4101–4114. https://doi.org/10.7150/thno.35186

Yang, Y., Torchinsky, M. B., Gobert, M., Xiong, H., Xu, M., Linehan, J. L., Alonzo, F., Ng, C., Chen, A., Lin, X., Sczesnak, A., Liao, J.-J., Torres, V. J., Jenkins, M. K., Lafaille, J. J., & Littman, D. R. (**2014**). **Focused specificity of intestinal Th17 cells towards commensal bacterial antigens.** *Nature*, *510*(7503), 152–156. https://doi.org/10.1038/nature13279

Yu, W., Zheng, Y., Li, H., Lin, H., Chen, Z., Tian, Y., Chen, H., Zhang, P., Xu, X., & Shen, Y. (**2020**). **The Toll-like receptor ligand, CpG oligodeoxynucleotides, regulate proliferation and osteogenic differentiation of osteoblast.** *Journal of Orthopaedic Surgery and Research*, *15*. https://doi.org/10.1186/s13018-020-01844-x

Zákostelská, Z., Málková, J., Klimešová, K., Rossmann, P., Hornová, M., Novosádová, I., Stehlíková, Z., Kostovčík, M., Hudcovic, T., Štepánková, R., Jůzlová, K., Hercogová, J., Tlaskalová-Hogenová, H., & Kverka, M. (**2016**). **Intestinal microbiota promotes psoriasis-like skin inflammation by enhancing Th17 response.** *PLOS ONE*, *11*(7), e0159539. https://doi.org/10.1371/journal.pone.0159539

Zegeye, M. M., Lindkvist, M., Fälker, K., Kumawat, A. K., Paramel, G., Grenegård, M., Sirsjö, A., & Ljungberg, L. U. (**2018**). **Activation of the JAK/STAT3 and PI3K/AKT pathways are crucial for IL-6 trans-signaling-mediated pro-inflammatory response in human vascular endothelial cells.** *Cell Communication and Signaling: CCS*, *16*(1), 55. https://doi.org/10.1186/s12964-018-0268-4

Zhang, J., Xiao, X., Dong, Y., Wu, J., Yao, F., & Zhou, X. (**2015**). **Effect of fermented wheat germ extract with Lactobacillus plantarum dy-1 on HT-29 cell proliferation and apoptosis.** *Journal of Agricultural and Food Chemistry*, *63*(9), 2449–2457. https://doi.org/10.1021/acs.jafc.5b00041

Zhang, Y., Liu, C., Gao, J., Shao, S., Cui, Y., Yin, S., & Pan, B. (**2020**). **IL-22 promotes tumor growth of breast cancer cells in mice.** *Aging*, *12*(13), 13354–13364. https://doi.org/10.18632/aging.103439

***Zhang, Y., & Zheng, J.** (**2020**). **Functions of immune checkpoint molecules beyond immune evasion.** *Advances in Experimental Medicine and Biology*, *1248*, 201–226. https://doi.org/10.1007/978-981-15-3266-5_9

***Zheng, D.**, Liwinski, T., & Elinav, E. (**2020**). **Interaction between microbiota and immunity in health and disease.** *Cell Research*, *30*(6), 492–506. https://doi.org/10.1038/s41422-020-0332-7

Zheng, Y., Sun, L., Jiang, T., Zhang, D., He, D., & Nie, H. (**2014**). **TNFα promotes Th17 cell differentiation through IL-6 and IL-1β produced by monocytes in rheumatoid arthritis.** *Journal of Immunology Research*, *2014*, e385352. https://doi.org/10.1155/2014/385352

10 Supplements

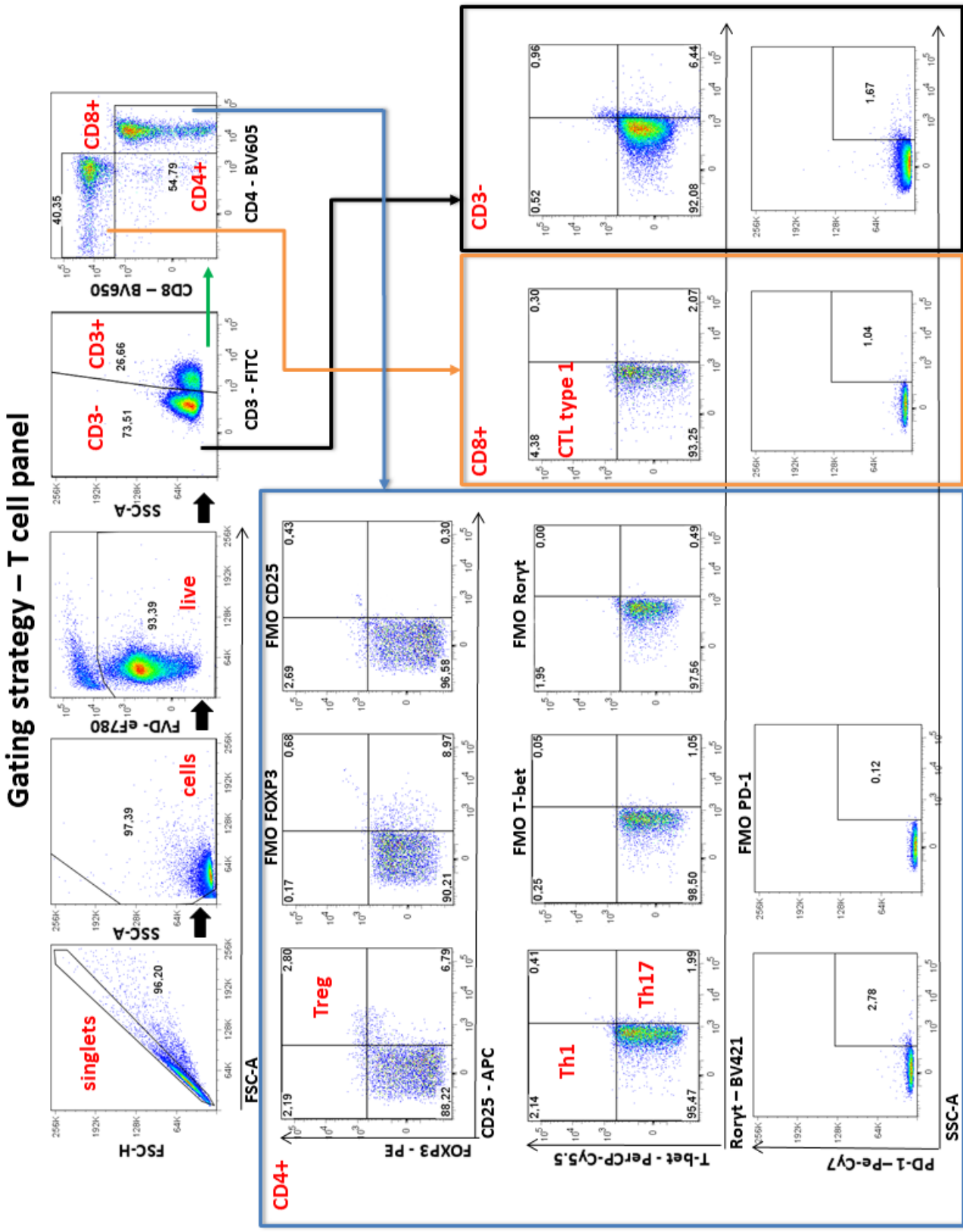

Figure S1 Gating strategy T cell panel: The flow cytometry data were analysed as depicted. FMO = fluorescence minus one, FOXP3 = Forkhead Box P3, FVD = Fixable viability dye, CD = cluster of differentiation, CTL = cytotoxic T cells, PD-1 = programmed cell death protein, RORγt = retinoic-acid-receptor-related orphan receptor gamma T-bet = T-box expressed in T cells, Th = T helper, Treg = regulatory T cells

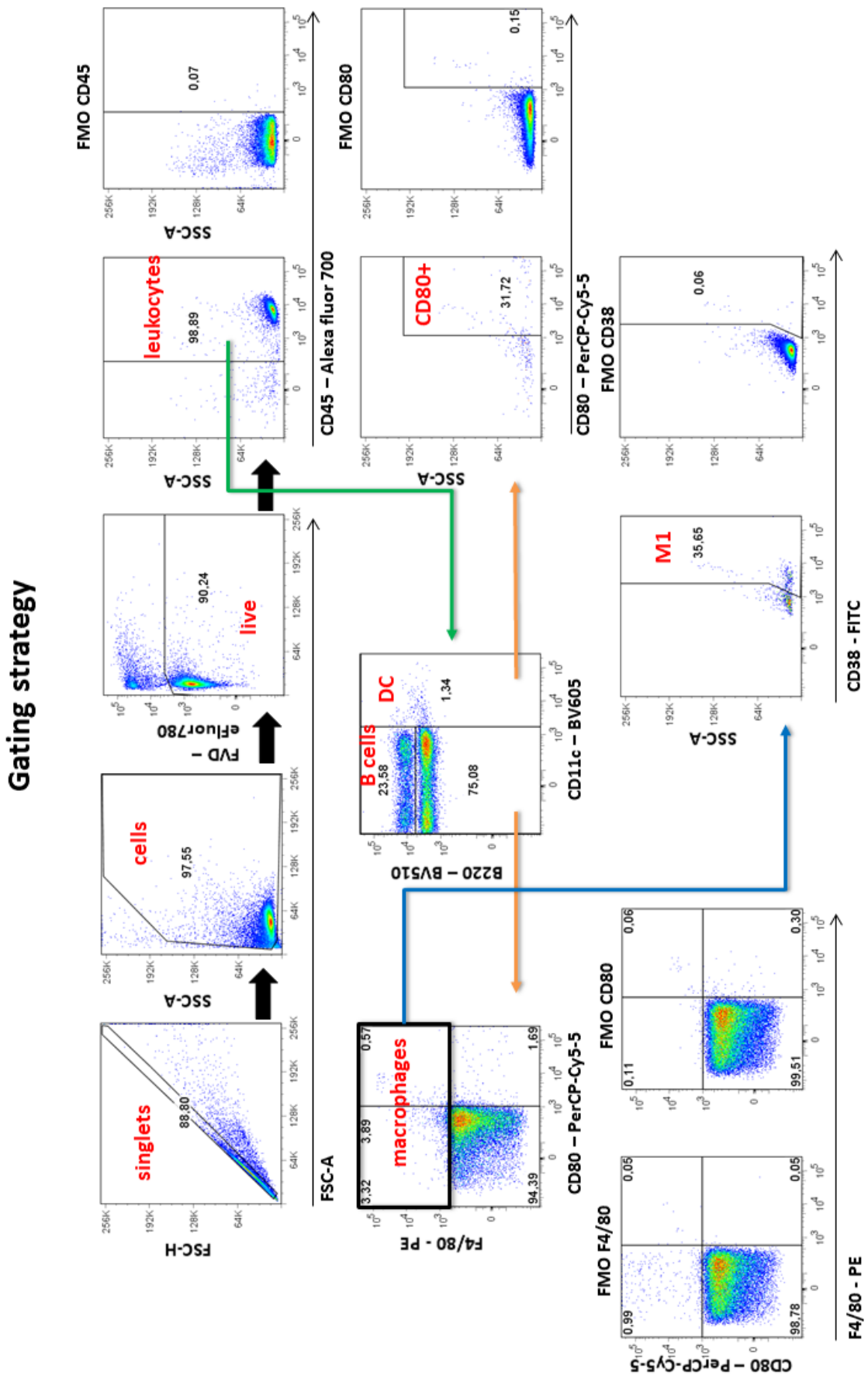

Figure S2 Gating strategy innate cells + B cells: The gating of flow cytometry data was performed as depicted. CD = cluster of differentiation, DC = dendritic cells, FMO = fluorescence minus one, FVD = fixable viability dye, M1 = type one macrophages

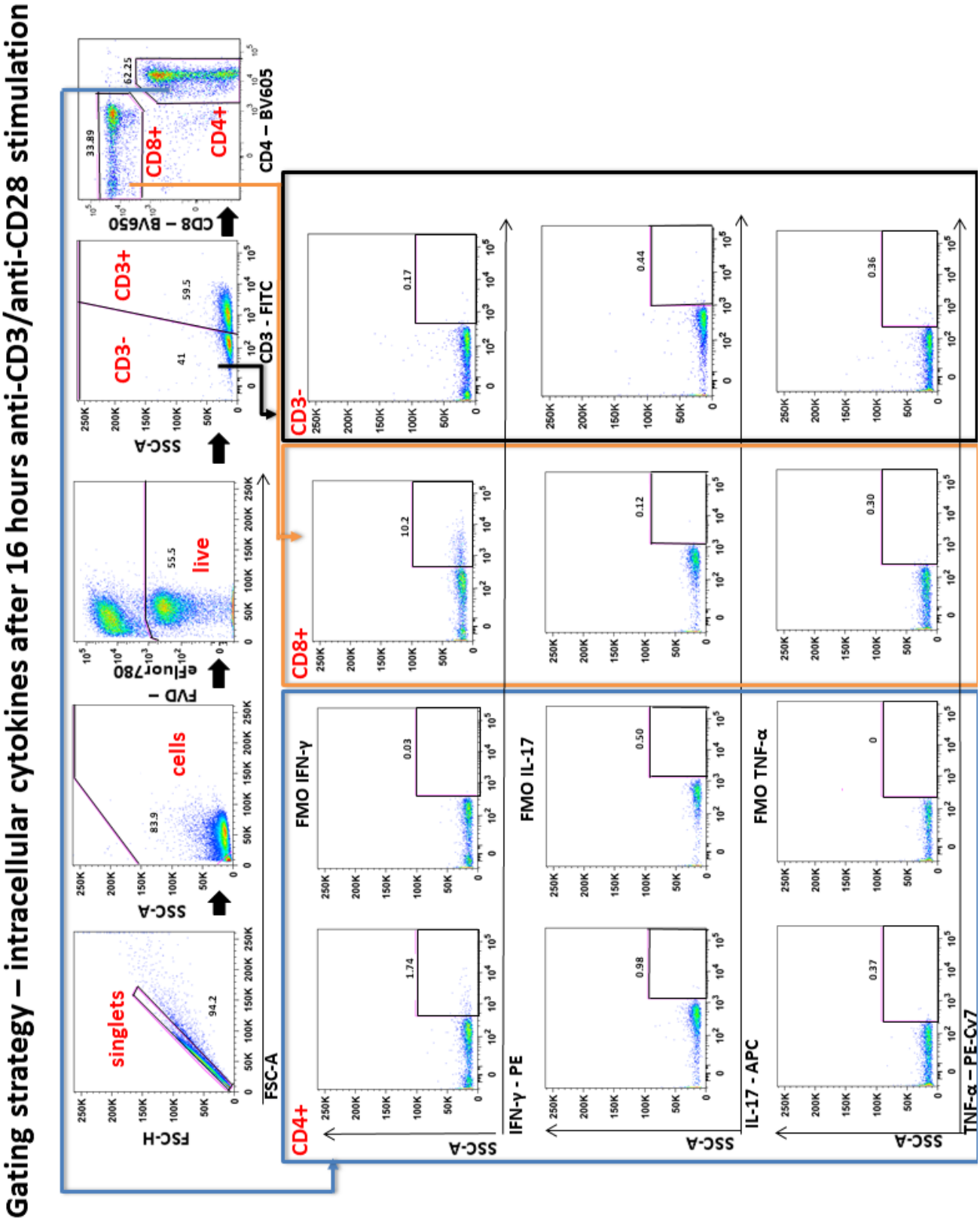

Figure S3 Gating strategy intracellular cytokines after 16 hours anti-CD3/anti-CD28 stimulation: The gating of flow cytometry data data was performed as depicted. CD = cluster of differentiation, FMO = fluorescence minus one, FVD = fixable viability dye, IFN-γ = interferon gamma, IL = interleukin, TNF-α = tumour necrosis factor-alpha

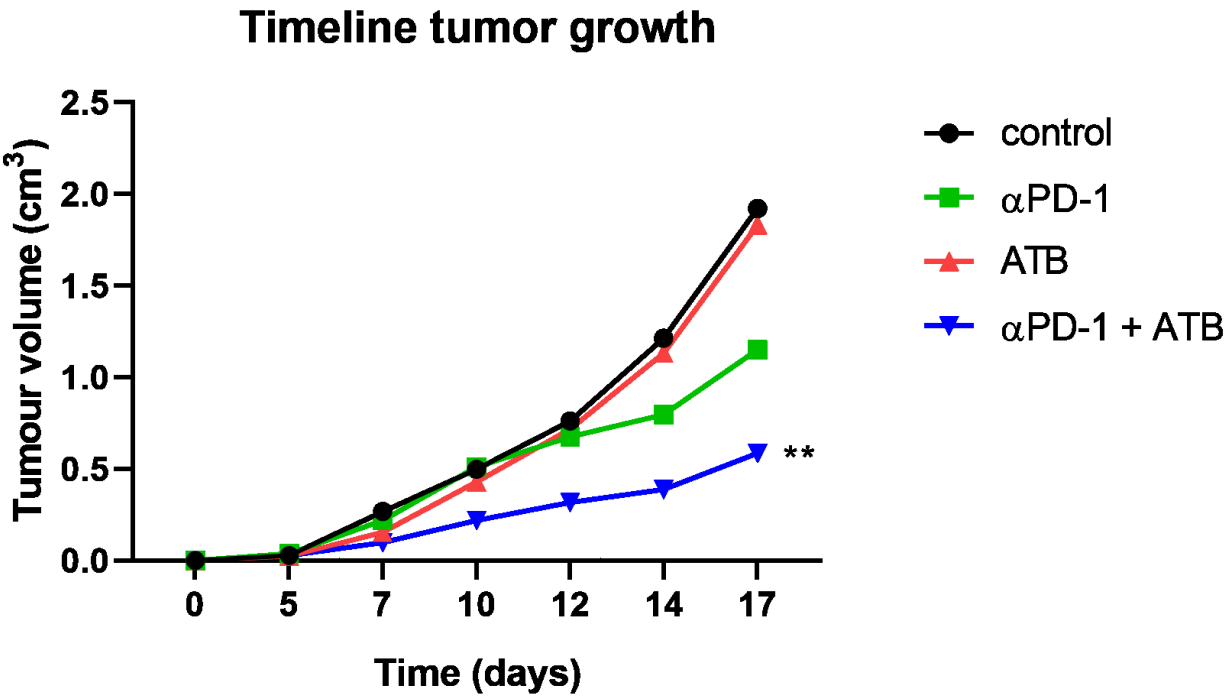

Figure S4: Only αPD-1 + ATB treated group shows considerably reduced tumour growth. The experiment consisted of 4 groups, controls, αPD-1, ATB or αPD-1 + ATB treated mice (n=7 per group). The tumour growth was measured every 2-3 days and analysed by two-way ANOVA with Bonferroni post hoc test. Experiment was performed by Anietie Udoumoh DVM., PhD. SD is omitted for clarity. **p < 0.01, αPD-1 = anti-programmed cell death protein 1, ATB = antibiotics